THE RHEOLOGICAL PROPERTIES AND BOILING VISUALISATION OF HARD-TO-BOIL MASSECUITES

Nirvana Naidu

213516946

In fulfilment of the degree of Master of Science in Mechanical Engineering at the School of Mechanical Engineering, University of KwaZulu-Natal.

June 2022

As the candidate's supervisor, I agree to the submission of this thesis.

Supervisor: Dr R.C. Loubser

DECLARATION 1 – PLAGIARISM

I, Nirvana Naidu, declare that

1. The research reported in this thesis, except where otherwise indicated, is my original research.

2. This thesis has not been submitted for any degree or examination at any other university.

3. This thesis does not contain other persons' data, pictures, graphs or other information, unless specifically acknowledged as being sourced from other persons.

4. This thesis does not contain other persons' writing, unless specifically acknowledged as being sourced from other researchers. Where other written sources have been quoted, then:
    a. Their words have been re-written but the general information attributed to them has been referenced;
    b. Where their exact words have been used, then their writing has been placed in italics and inside quotation marks and referenced.

5. This thesis does not contain text, graphics or tables copied and pasted from the Internet, unless specifically acknowledged, and the source being detailed in the thesis and in the References sections.

Signed:

…………………………………………………………………………………

DECLARATION 2 - PUBLICATIONS

DETAILS OF CONTRIBUTION TO PUBLICATIONS that form part and/or include research presented in this thesis (include publications in preparation, submitted, *in press* and published and give details of the contributions of each author to the experimental work and writing of each publication)

Publication 1- Poster Presentation at SASTA Congress

"A view into the boiling behaviour of synthetic massecuite in a pan tube"

N. Naidu and R. Loubser, South African Sugar Technologists Association Conference (SASTA), page 61, August 2018, Durban ICC, South Africa

Signed:

………………………………………………………………………………

ACKNOWLEDGMENTS

"Sometimes to get to where you want to be, you need to keep taking one step after another (no matter how small)"

I would like to thank my parents, Ujen and Dhaya, who always taught me to never give up and supported me throughout my education. A special acknowledgement goes to my mother who inspired me and gave me my love for sciences and to this day has never stopped teaching me.

I would like to thank Professor Sarp Adali without whom, I would have never finished this topic. His knowledge and guidance was invaluable to this work.

I would like to thank Gareth Oregan Hoskins, for inspiring me every single day and never giving up on me. For always being my biggest supporter and pushing me to be my best through emotional and moral support. I can't wait to marry you.

Abstract

In the sugar milling industry, sugar cane is crushed and the juice obtained is processed, to first yield a syrup, and further to produce massecuite. Massecuite is a combination of sugar crystals and mother liquor and when separated from the massecuite is known as molasses. Massecuite is boiled to reduce the water percentage of the total mixture, to promote the growth of sugar crystals. Once boiled, it is then transferred to a centrifuge where the molasses and sugar crystals are completely separated.

During bad weather conditions, the harvesting process of sugar cane is delayed. Due to these delays, bacterial infections occur within the cane that causes a deterioration effect on the juice extracted. The massecuite produced from this cane is known as Hard-To-Boil (HTB) massecuites. The absolute mechanism behind HTB massecuites is still unknown.

When exposed to the standard boiling process, HTB massecuites require lengthily boiling periods and yield lower levels of sugar, when compared to good massecuites. Once the mixture has completed the boiling period, a thick, viscous solution remains inside the boiling chamber. HTB massecuites produce an elastic and stringy product that is difficult to remove from a boiling pan. Specific cases, in certain mills, produced an extremely high tensile material that could be stretched as if it were a rubber band. The mentioned scenarios have resulted in the clogging of industrial machinery, as well as a less efficient process of producing sugar.

A hypothesis was formulated to describe the relationship between the viscoelasticity of the HTB massecuite, and the boiling properties. A comparative study between standard and HTB massecuites was performed, to test the hypothesis. A single tube vacuum pan, with open front face to view boiling and bubbling, as well as evaporation rates were noted for both good and HTB samples. The nature of HTB samples was determined purely based on what factories and industries considered ‘’difficult to boil’’, and tests were run, thereafter, to determine true differences in the boiling behaviour of good and HTB samples.

Samples were tested using NIRS to determine the basic chemical properties. To determine the rheological differences between samples, tests were run using an Anton Paar rheometer to determine the viscous and elastic properties. Graphs were produced to illustrate these results.

Using the information obtained, apparent characteristic differences were observed between the different sample types. There were observable differences between HTB and good samples that coincide with the hypothesis. However, the errors with testing were also analysed. This impacted the success of the results. While an absolute result was not extracted, the results from the research may be used for future work, to find a real solution and mitigate the effect of HTB massecuites.

Acronyms

HTB	Hard-to-boil
HTCD	Harvest to crush delay
MISG	Mathematics in Industry Study Group
HTC	Heat transfer Coefficient
CFD	Computational Fluid Dynamics
BPE	Boiling point elevation
LVER	Linear Viscoelastic Range
TPD	Target Purity Difference

Contents

Table of Figures

List of Tables

Chapter 1

Introduction

1.1 Background Information

It is without a doubt that one would be able to find sugar anywhere in the world. In every household, almost every food product contains sugar in some form. The sugar manufacturing industry of South Africa is one of the 15 largest in the world (South African Sugar Association, 2020). In South Africa, sugar cane is harvested from the eastern regions of the country, where it is grown in abundance. Sugar cane is submitted to a crushing process, where the cane fibres are separated from the juice. This juice is boiled down to form a two-phase syrup made up of a combination of mother liquor and sugar particles. The overall substance is known as massecuite.

Due to bad weather conditions, the harvesting of sugar cane can be delayed. The massecuite produced from cane that experienced a delay in harvesting, is substantially different to the standard harvested cane. In the sugar milling industry, there occurs a natural phenomenon known as hard-to-boil (HTB) massecuites that is said to arise during the wet seasons where rain is abundant. The effect of HTB on manufacturing is undeniably harmful as it slows production rate by increasing boiling periods and reducing sugar yield. The effect is linked to deterioration of the cane, caused by microbial infection causing the gum polysaccharide levels within the massecuite to increase. These gums produce the altered properties experienced. The most common experience is that this massecuite requires a much longer boiling period with increased viscoelasticity. The overall yield of sugar from this massecuite is substantially lower. There are currently some solutions in place to aid the boiling; however, the causative mechanism is still unknown.

Aside from the lower yield and lengthy boiling times, HTB samples are extremely difficult to remove from the boiling chambers. The reduced substance has an extremely high viscoelasticity. In extreme industrial cases, this substance simulates sticky ropes that yields less product and makes the cleaning process laborious. It is this reason that HTB samples are a harm to industrial efficiency and general processes.

The massecuites that contains these high levels of polysaccharides with problematic boiling are referred to as HTB massecuites. For the remainder of this dissertation, these massecuites will simply be referred to as HTB samples.

1.2 Topic Description

To remedy the effects of HTB massecuites, factories have solutions that are commonly used to alleviate such effects. While these solutions may aid factories, they do not provide a fulltime resolution capable of combatting the problem. This is due to the lack of understanding of the causative mechanism that disrupts the standard boiling of massecuite. If the mechanism is better understood, it is possible that factories will be better equipped to handle the problems created by this phenomenon.

It is known that the deteriorative effects are linked to microbial decay resulting in the formation of polysaccharides known collectively as gums (Nel, 2018). Gums are commonly used, especially in the food industry as thickening agents capable of increasing the viscoelasticity of a liquid. The effect of these gums are dependent on the type and concentration used. The effects observed in HTB massecuites are said to be caused by a combined effect of different gums and depending on the infection occurring that caused deterioration. While this topic does not delve into the study of these gums, it focuses on the **effects** they will have during processing as a result of the **mechanism** inhibiting boiling.

This research topic looked at the hypothesis put forward by the Mathematics in Industry Study Group (MISG) in the paper titled "*Hard-to-boil Massecuites*" (Fowkes *et al.*, 2017). This paper put forward the theory of suppression of water vapour bubble formation and growth, during the boiling of HTB massecuites in vacuum pans due to the presence of property altering gums. These gums alter the viscoelastic properties that then retards the boiling process when in high concentrations at the final boiling process under vacuum. With boiling being characterised by the formation of bubbles occurring owing to phase change, the theory puts forward an idea that difficulties in boiling stems from the reduction of bubble size and growth. Bubbles in boiling require adequate energy from phase change to escape the surface and overcome the viscoelastic properties of the liquid. This suggests that the bubble suppression theory is a vital factor in the phenomenon of boiling HTB samples.

In order to test this theory, equipment capable of visualising boiling and testing the flow properties are required. In 2017, the student's final year project was aimed at the design and manufacturing of a test rig capable of visually monitoring massecuite boiling. This led to the design and manufacturing of a single tube vacuum pan, with clear front face, able to investigate the boiling occurring within vacuum pans. The apparatus is a to-scale, being a single tube vacuum pan, with the front face having a glass pane, capable of letting researchers watch the boiling of massecuite. The observation of the effects, due to increased concentration of polysaccharides and other components, were investigated. This involved visual monitoring of the boiling of the mixture, documenting controllable factors and correlating these results with the rheological properties of the mixture before and after boiling.

Rheological testing involves the testing of flow properties of substances. In this study, the rheology of the HTB samples are to be compared to the standard massecuite samples. This will aid in describing how the presence of polysaccharides alters the samples characteristics. This was done using the Anton Paar MCR 320 Rheometer in conjunction with the bubble suppression theory to create the experimental method used in this study.

For the purpose of the experimentation within this dissertation, it was decided that a sugar mill's processed molasses, will be used as a standard sample. For the HTB sample, a naturally occurring HTB final molasses was used, and the determination of the HTB nature was based on what factories characterised as HTB. This was generally characterised by long boiling periods and increased viscoelasticity. The choice of this experimental method came as a result of working through many different samples and testing conditions to refine the process. The choices are further elaborated through the thesis.

It is imperative that a hypothesis, based on the following research, must be formulated, in order to constrain the bounds of the project scope. This hypothesis will be based on the research obtained through past experience.

1.3 Hypothesis & Research Questions

In order to investigate the statements of the hypothesis put forward by Fowkes (2017), the experimentation must be modelled to adequately represent these ideas. For the purpose of this dissertation, the hypothesis was evolved into the following statement:

Boiling of Hard-to-boil massecuite will lead to an increased viscoelasticity. This viscoelasticity property will result in changes in the boiling properties of massecuite.

The focus of this research is to determine the accuracy of this hypothesis. The hypothesis will be further elaborated on during the methodology design. Refer to chapter 3 for an expansion of the hypothesis proposed.

The topic of this study raised the following key questions: **Is it possible to visually monitor the boiling of massecuites occurring within vacuum pans, and compare the observations made between normal and HTB samples to determine the mechanism of HTB?** Similarly: **Can the rheological properties of each sample type be determined and compared to support the observations made in the vacuum pan?**

Further investigation led to the following set of sub-questions:

- Is the vacuum pan testing rig adequate in providing the required conditions to mimic factory pan boiling as well as mimicking the boiling assumptions put forward by the modelling completed by MISG?

- Is the vacuum pan testing rig able to provide good visual monitoring in order to compare sample types for research purposes?
- Is the testing system capable of handling the high viscosity and other effects noted in HTB samples, where properties have changed and are known to cause problems for equipment?
- Are there measurable differences in the rheometric properties and NIRS readings of normal and HTB massecuites?
- How does the rheological changes in massecuites impact the boiling and bubbling regime experienced within vacuum pans?
- What are the limitations with regards to both pieces of equipment used for testing?

The answers to these questions could provide invaluable information to the sugar manufacturing industry with regards to the mechanism causing the HTB problem. This study will aim to provide the information obtained from this testing as well as the various experimental iterations that are required to get to the results.

1.4 Aims & Objectives

This research was aimed to determine the characteristic changes between the boiling of standard and HTB samples, to better understand the mechanism that causes the boiling difficulties, experienced in industry. This was done by visually monitoring the differences in the samples under the same boiling conditions. Once these results were achieved, it was required that the notable differences be linked to the characteristic properties of each sample type, to draw conclusions between the differences of the two samples.

To answer this aim, the following objectives were to be completed:

- Research and determine the current theories surrounding the causes and mechanisms of hardto-boil
- Adapt the vacuum pan to ensure complete boiling
    - Add a sample port to allow for sample taking and Brix monitoring
    - Add a secondary sight glass to monitor the upper portion of the pan
    - Add a condenser for steam side
    - Alter the stirrer for better circulation using a more powerful motor
- Determine if the test rig is adequate in performing the experimental method required for this research topic
- Use the vacuum pan testing rig to identify the key changes in boiling characteristics between normal and HTB samples

- Photograph the boiling occurring
- Take note of the properties and conditions of the boiling
- Visualise the boiling behaviour of massecuite and correlate this with the rheological properties
- Use the rheometer at the Sugar Milling Research Institute NPC (SMRI) to identify the rheological properties of normal and HTB massecuites to obtain properties. These properties must be linked to the vacuum pan boiling characteristics, to support the hypothesis put forward
- Measure the rheological properties of normal and HTB samples, including viscosity, viscoelasticity, the effects of crystals on viscosity and the effect of polysaccharides on flow properties.

1.5 Project Limitations and Assumptions

The project used equipment designed to visually and graphically model the characteristic differences between standard and HTB massecuites. For visual modelling, the rig consists of a single tube, an experimental vacuum pan, with a clear front pan that allows viewing into the front boiling tube. For graphic modelling of flow properties, the rheometer is used. These equipment pieces focus solely on the modelling of the flow and boiling properties, to create a link between the two to find the mechanisms that cause HTB.

In the initial phases of the research, the hypothesis was tested by using a lab-made, synthetic massecuite that was doped with a known polysaccharide. However, due to challenges in creating a synthetic massecuite with rheological properties representative of a real HTB massecuite, and on the advice of a food manufacturing expert (pers. Comm. S.Weyer, 2018), a natural HTB sample was used. It was decided that the focus of the experimentation lies in naturally occurring HTB. The HTB phenomenon generally only occurs once or twice a year, due to excessive rain and is generally found during October and November. During this research, it was only possible to receive samples that were able to provide the results required, once or twice a year. This caused the study to have difficulties in obtaining a steady supply of samples.

1.6 Dissertation Chapter Overviews

This section details a short overview of each chapter in this dissertation, summarising what each chapter entails.

1.6.1 Literature Review

Research was done to learn more about the focal areas with respect to the hypothesis. The mechanisms and theories surrounding HTB were investigated to determine other areas in which experimentation will be focused. The current solutions and research topics regarding chemical changes and rheological changes are also analysed. Vacuum pan boiling modelling, done previously by other research topics was investigated, and the effects of HTB on this process was also discussed.

1.6.2 Methodology & Experimental Design

This section lays the foundation on which the research will be built. Here, the topic looks at the hypothesis framework and a diagrammatic approach to experimentation was developed with regards to the theory and how work will be modelled to support the theory. This section introduces the vacuum pan testing rig and calibration for pressure and temperature. Analytical instrumentation was also discussed, followed up by the experimental framework used to test on each of the apparatuses.

1.6.3 Experimental Testing & Troubleshooting

This section looks at the topic evolution and how it progressed to deal with rising limitations of the testing rig and experimental procedures. The two testing substances chosen prior to the final tests using final molasses are discussed and the testing completed with these liquids. This was done first using a polysaccharide dosed white sugar syrup made to mimic a massecuite before moving onto a true massecuite. The experimental method was discussed, and limitations of using each substance were analysed to remark why final molasses was used ultimately.

1.6.4 Vacuum Boiling Results

This chapter covers the results obtained from the vacuum pan. Various experiments were performed and compared between 2 main samples: Good/standard massecuite, and HTB massecuite. The first set of results investigated the relationship between the Brix levels and the increase in the temperature of the fluid. The second set analysed the relationship of the mass of the condensate formed as the fluid boils. The last set of data investigates the bubble formation in either sample. This was done by photographing the fluids as they boiled and noticing distinct differences.

1.6.5 NIRS & Rheology Results

The results of the rheological and NIRS tests are in this chapter. The experimental method proposed was used to gain the results found here. The importance of the findings within the results are discussed and links were made to the effects seen in the vacuum boiling stage. The relationships between boiling and rheology and NIRS are compared to the theory put forward in the theoretical framework, as well as the proposed hypothesis.

1.6.6 Discussion & Validations

Discussions of the aims and objectives and how they were achieved. The research questions were then reviewed and were answered based on the experimental findings. Using the experimental results and validations, the hypothesis was reviewed, tested and concluded.

1.6.7 Conclusion

For the discussion, the work done in relation to the research was critically analysed to determine that all objectives were met. The individual questions that are proposed at the start of the experimentation are discussed with respect to the study as a whole. The basis of the study is analysed and the effectiveness scrutinised.

Chapter 2

Literature Review

2.1 Introduction

Research into this topic of the rheological properties of HTB massecuite can first be linked to the following topics:

- the HTB phenomenon
- knowledge into the boiling within calandria tubes
- theories behind the occurrence of the phenomenon and influencing factors

The link between the sections comes about in showing how this important phenomenon affects the processing and manufacturing of sugar. Assessment of the problems of HTB to determine the causative mechanics linked to HTB symptoms and short-term solutions for dealing with altered properties affecting the boiling was required. Theories and models created by other research work will be discussed in order to lay the foundation of support for the thesis. The mechanisms that create the problems experienced within factories will be further elaborated on in order to answer the research question: "**How does the rheological changes in massecuites impact the boiling and bubbling regime experienced within vacuum pans?".** This section looks at these different topics to establish the link between them.

2.2 HTB Phenomenon

Under normal circumstances, the general flow of manufacturing occurs, as seen in figure 2.1. Briefly discussed; cane is usually burnt to remove outer leaves before going to the factory where it is billeted, crushed and washed to remove juice before heating, clarifying and filtering to remove impurities and mud. This clear juice undergoes evaporation through a series of multi-effect evaporators, to bring the juices dissolved solid content, better known as the Brix content, up from 11% to approximately 65%, where it is now known as syrup (Meade and Chen, 1977; Rein, 2007).

This dissolved content within the boiling syrup is made up of sucrose and other impurities. These impurities consist of fructose, glucose, inorganic ash constituents such as calcium, potassium and sodium with other organic impurities, for example, starch and dextran (Sahadeo, 1998).

Once evaporation is completed, the syrup is sent to a machine called a vacuum pan where it is boiled under vacuum to increase the Brix levels, by removing excess water and promote crystal growth. In the vacuum pan, the syrup becomes a two-phase mixture known as massecuite, made up of sugar crystals and molasses. When this reaches the required Brix levels, and adequate water is evaporated, the massecuite is sent to a crystalliser to cool the massecuite and promote crystal growth.

Massecuite must then be centrifuged to separate it into sugar and molasses. Once separated, sugar is dried and refined to remove colour while molasses is boiled again to recover any sucrose that was not crystallised in the first run through. The process is shown below in a series of steps showing the flow between each process from cane harvesting until final sucrose refining.

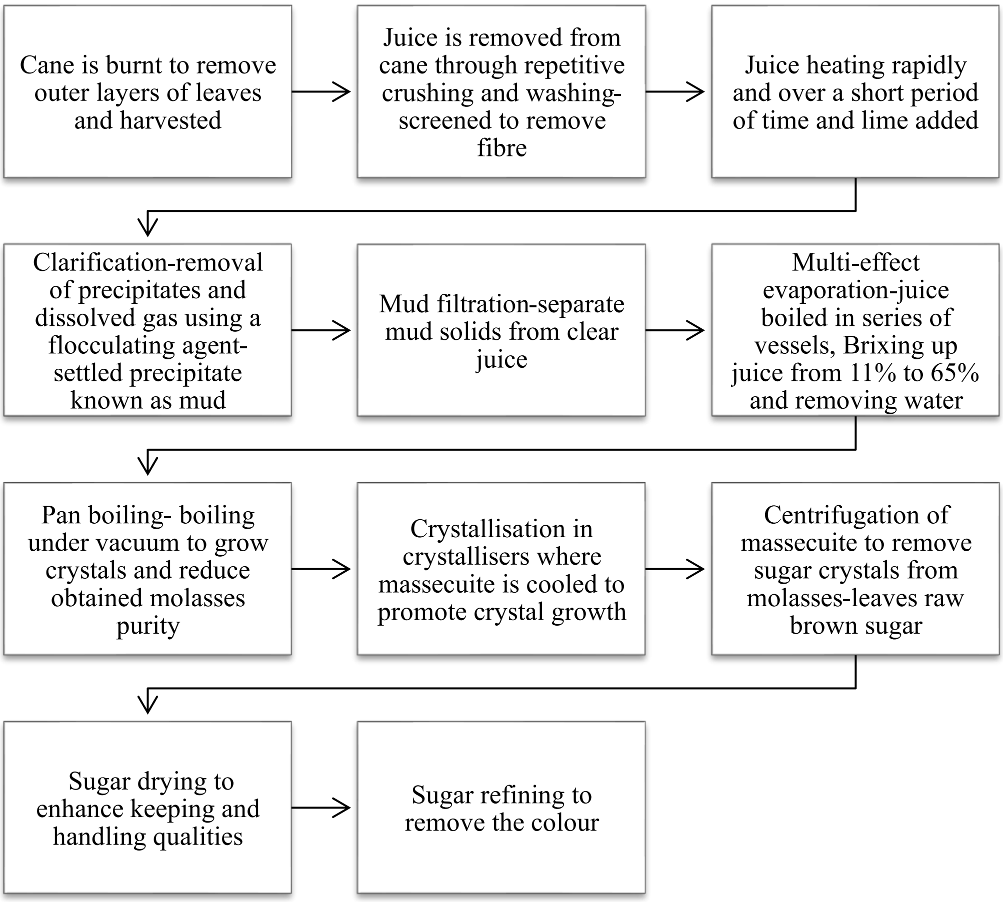

Figure 2.1: Sugar Manufacturing Process

At the end of the season, when weather is unfavourable, for extended periods contributing to burn to crush delays, there occurs a phenomenon known as HTB. During the vacuum boiling stage, factories experience problems with reduced rates of crystal sugar formation and what was seen to be a change in rheological properties of massecuites (Shah, 2017; Nel, 2018). This phenomenon is generally noted in the vacuum pan boiling stage and associated massecuites are given the title “Hard-to-boil massecuites” (HTB).

HTB and its associated effects are linked to impurity presence due to post-harvest deterioration as a product of enzymic, bacterial or microbial activity (Martin, 2008; Shah, 2017). Deterioration of cane occurs as a result of harvest-to-crush-delays, ambient temperature and harvesting practices, sugar cane injury, cane variety, storage conditions and is promoted by bacterial and fungal attack causing longchain polysaccharide formation (Eggleston, Morel du Boil and Walford, 2008; Martin, 2008). In figure 2.2, the processing steps show the points at which sugar manufacturing is altered because of hard-toboil with altered steps depicted in red.

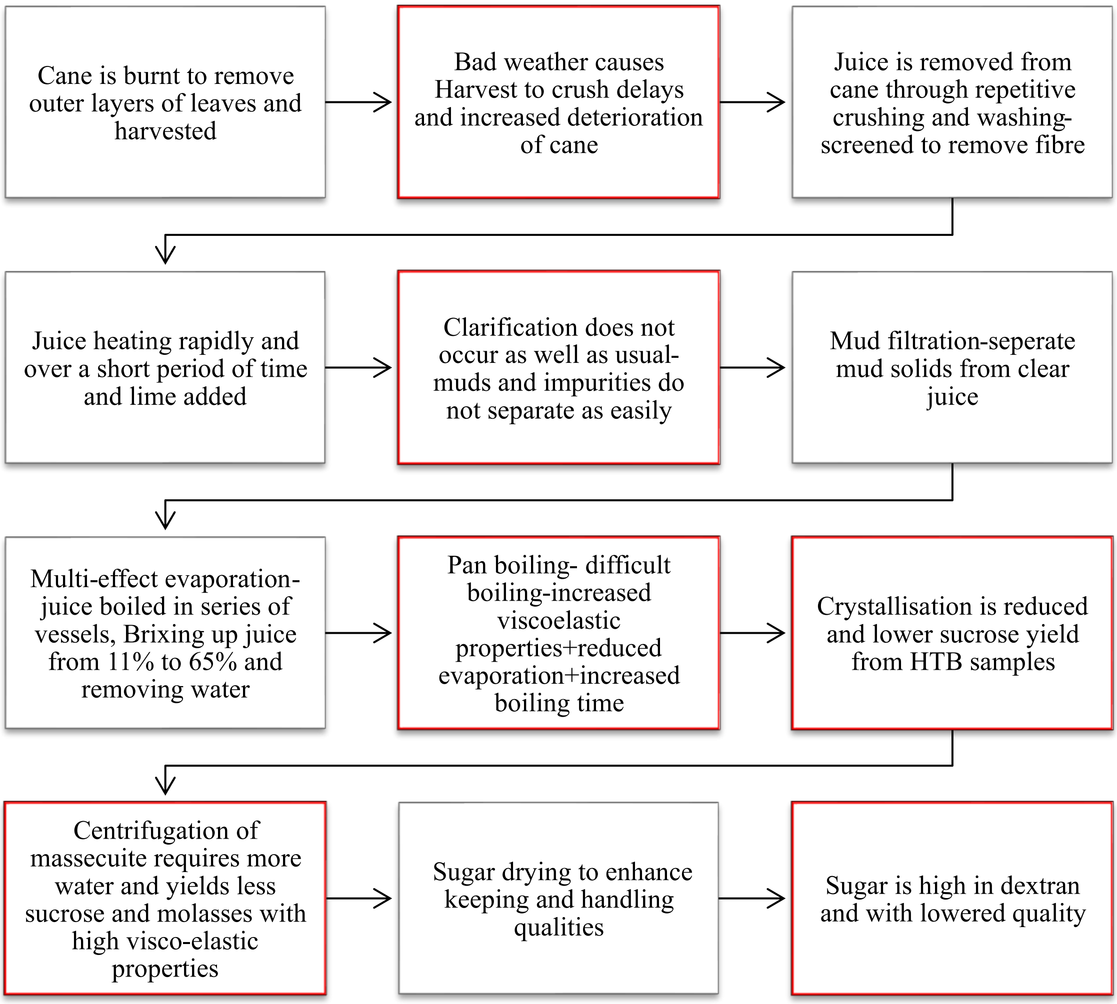

Figure 2.2: How Sugar Manufacturing Process is affected

2.2.1 Characteristics of HTB

Like all plant matter, cane can mature past optimal conditions, become injured due to bad weather and experience insect or microbial decay. This deterioration is further influenced by environmental conditions and natural presence of microbes. This impacts the sugar manufacturing process with problematic side effects on yield percentage and quality. The severity of deterioration has found to depend on several factors, namely ambient temperature, harvest to crush delay (HTCD) and harvesting practices.

Harvesting procedure, burning, freezing or cutting and delays between transportation and processing all contribute to deterioration. The burning of cane removes the outer protective layers of leaves, introducing points of entry for contaminant micro-organisms, increasing the rate and extent of deterioration (Martin, 2008).

Should unfavourable weather conditions follow the period of burning, the likelihood of HTB increases. In South Africa, the main period during which HTB has been noted, lies between October and November of every year, when rain is excessive (Koster *et al.*, 1992). This is seen to occur as a result of harvest-to-crush delays where harvesting and transportation is delayed due to heavy rains. In countries, like Australia, harvesting and transportation to processing is kept to below 24 hours while South Africa can have delays of up to 68 hours due to lack of mechanical harvesting (Lionnet and Reid, 1993).

Bacterial and fungal attacks alter cane carbohydrates to produce polysaccharides that, in larger doses, alter downstream cane processes through changes of rheological properties. Warm and wet weather further promotes micro-organism action, and high humidity and temperatures can result in the formation of viscous gluco-polysaccharides (Du Clou and Walford, 2012; Morel Du Boil, 2020). These microbes alter the cane at the microscopic level, creating long-chain polysaccharides that are best known under the blanket term of "gums". Micro-organisms leave behind deterioration by-products such as mannitol, ethanol and lactic acids (Nel, 2018).

Gums naturally occur in cane irrespective of deterioration through the metabolism of plants and general ageing of cane; however, under deterioration conditions, the total percentage of these impurities can increase significantly. While there are several naturally occurring polysaccharides, of great interest is the polysaccharide dextran, that has been linked to the notable rheological property changes of massecuites. Dextrans come about due to the metabolic activities of micro-organisms, specifically *Leuconostoc mesenteroides* (Nel, 2018).

While it remains uncertain if dextran is the only causative impurity to the effect or if the total impurities create a combined effect that results in these altered properties, it was deemed a key component since the HTB effect is noted when the relative percentage of dextran-like polysaccharides begins to increase to undesirable heights. Due to the uncertainty, the general causative products are labelled under the term gums or related to dextran-like impurities.

The presence of dextran-like polysaccharides in sugar manufacturing has been researched by many in the field. Of note, it has been associated with the change in sugar stream rheological properties that occur due to the HTB phenomenon. The definition of HTB massecuite is quite vast and varies between mills and regions of the world, the term is used to describe several key characteristics. Common factors seen to describe the behaviour are noted below, as well as summarised in figure 2.3 (Du Clou *et al.*, 2015; Shah, 2017; Morel Du Boil, 2020):

- Extremely long periods of boiling

- Slow crystallisation and growth
- High concentrations of gums and impurities
- Reduced evaporation rates-inability to remove excess water
- Reduced heat transfer coefficient
- Production of small bubbles throughout massecuite interfering with heat transfer
- Decreased circulation with massecuite and molasses not moving easily
- Poor clarification and high colour
- High molasses purity-purity deals with the sucrose that was not recovered during the boiling process and remains dissolved in the molasses
- Affected refining efficiency and reduced quality of sugar
- Extreme elongation of crystals
- Viscosities of massecuite and molasses increased to unmanageable levels o Final molasses requiring dilution to be removed from rigs
    - o Tripping of stirrers under the increased viscoelastic effect with C-massecuites having "toffee-like" consistency that wrapped around crystalliser stirrer

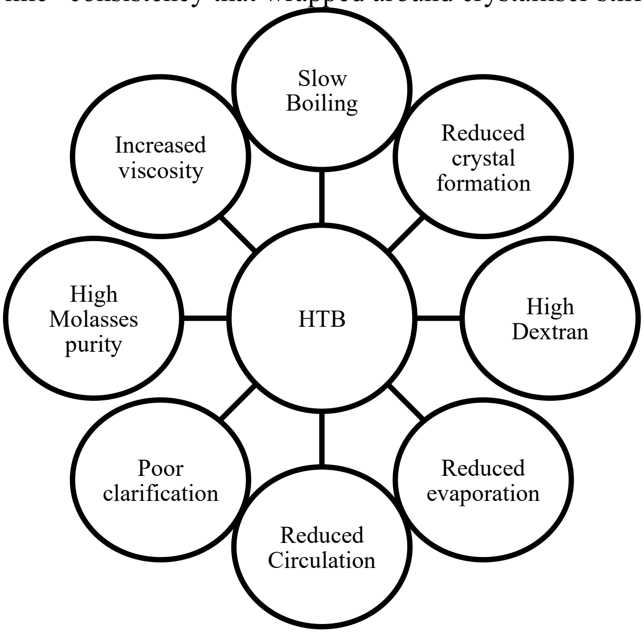

Figure 2.3: Noted changes experienced in HTB

Hard-to-boil is noted in factories as the "increased viscosity" of massecuite that leads to decreased sugar crystallisation. Increased viscosity effects yielded reduced boiling in the form of reduced evaporation and reduced circulation during the vacuum boiling stage. Due to this decreased removal of water crystallisation does not readily occur and if it does, will result in low yields. Consequently, pan boiling length increases. Other effects such as stirrer tripping and ceasing of boiling, causing the factory to strike pans before they have reached the desired sugar yield.

Depending on the severity of the problem, factories can be unaffected in processing or completely shut down as a result. With a notable increased viscoelasticity, damage to pumps and stirrers is possible and may cause malfunctions requiring factory shutdowns (Eggleston, Côté and Santee, 2011). Loss of product and damage to equipment are major issues as a result of HTB.

2.2.2 Chemical Nature & Effect on Processing

To ensure that the maximum yield of sucrose is obtained from each syrup batch, molasses is boiled down twice more to remove as much sugar as possible. The grading of massecuite is determined by the purity and processing step, with A-massecuite having highest purity of extractable sugars after the first boil down, and C- or final massecuite having lowest purity after final boil down.

Through this operation, the concentration of reducing sugars and other impurities increase, thus yielding a C-massecuite with the lowest purity and highest viscosity (Shah, 2017). An increase in concentration of impurities leads to changes in massecuite properties, depending on constituents.

As mentioned before, an increase in polysaccharides is responsible for the formation of HTB samples. The presences of these harmful, long-chain, molecules have been noted for decades, with papers discussing the importance of investigation into the impurity effects on the processing stream. While research has investigated gums in general, there is still a lack of understanding with regards to the effects linked to these substances. However, dextran-like substances produced from the infection of *Leuconostoc* bacteria, raises various points of interest. (Nel, 2018).

“Dextran”, better grouped under the blanket term of dextran-like molecules, have been used as the defining term that is linked to HTB samples and its associated effects. Standard samples are found at approximately 200mg/kg Brix, whereas in deteriorated/HTB samples, were noted to be concentrated at above 10 000 mg/kg Brix (Ravno and Purchase, 2005). While it has been seen in many cases to be a present factor during periods of HTB, there was also seen to be a variety of types of dextran as well as other deterioration by-products formed (Nel, 2014). The levels of each type of are linked to weather patterns, cane variety and cane handling methods (Nel, 2018). In a paper by Duffaut and Godshall (2004), there was a prominent increase in pH, calcium, lactic acid and ash levels compared to other samples. These were seen to be as a result of the metabolic activity of infiltrating microbes. Common chemical characteristics that are noted when HTB samples were tested (Saska, 2003; Eggleston, Morel du Boil and Walford, 2008; Nel, 2014):

- Higher lactate and acetate levels

- High calcium levels that form soluble salts when clarified
- Polysaccharides
- Increased ethanol
- Mannitol
- Presence of oligosaccharides
- High calcium levels
- Increase in Dextran and dextran-like gums
- High pH
- Low phosphate and invert sugar ratio
- Increased Target Purity Difference (TPD) of molasses

These characteristics are important to remember with regards to the way factories may characterise HTB samples. Constituents were observed to be an important marker for early warning indicators for factories and could be overall contributors to HTB effects.

2.2.3 Rheological Properties

Rheological properties describe the flow properties of a liquid and the study of these properties (Mezger, 2006). Rheology shows the flow behaviour as well as deformation behaviour of fluids (Mezger, 2006). Knowledge of rheology is important in being able to design equipment and choose pumps in order to handle the worst possible properties (Broadfoot, Miller and McLaughlin, 1998; Shah, Lokhat and Peacock, 2017).

Gummy massecuite, used to describe massecuites that have been affected by the HTB phenomenon, are generally very viscous during periods of bad weather, which adversely affects circulation in the pans (boiling is not as vigorous), especially within the C-pans. Viscous massecuites are difficult to cure in the centrifuges and require extra water which adversely affects crystal size and requires evaporation of excess water (Madho, 2009; Eggleston, Côté and Santee, 2011).

Liquids can be classified as having one of the following properties:

- Shear thinning or pseudoplastic: under increasing shear stress there is reduced viscosity
- Newtonian or ideal-viscous liquid: under increasing shear stress there is no increase or decrease in viscosity
- Shear thickening or plastisol dispersion: under increasing shear stress there is increasing viscosity
- Thixotropic or time-dependent: under increasing shear, there is decreasing viscosity however once shearing has stopped and sample has been left to rest, the viscosity is seen to increase

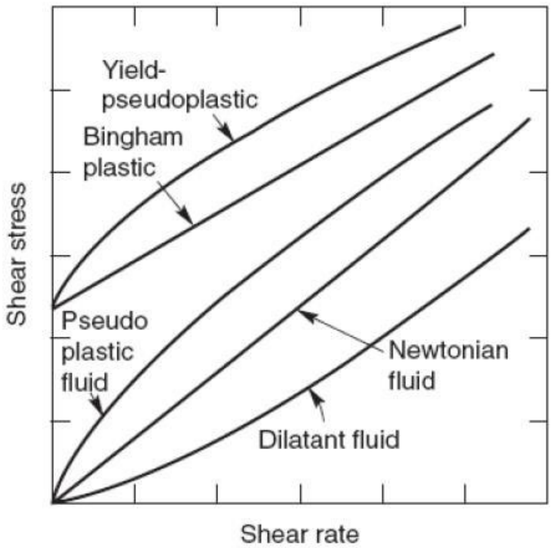

Figure 2.4: Rheological properties of liquids (Chhabra and Richardson, 2008)

All real liquids can be described as viscoelastic, experiencing a deformation and flow behaviour, containing partial liquid and solid properties. Massecuites are reported as shear thinning, nonNewtonian liquid made up of a two-phase mixture of solid sucrose crystals and viscoelastic mother liquor (Shah, 2017). In figure 2.4, standard massecuite does not meet the required conditions to be deemed a Newtonian fluid. Under normal conditions, massecuite flow properties tend to be temperature-dependent and may be altered through evaporation and caramelisation that burns the mixture. The viscosity of the different phases and types of massecuites and molasses are seen below in figure 2.5.

Figure 2.5 shows the various massecuites and molasses and how the viscosities differ based on temperature. From A-massecuites, with the lowest brix, to C-massecuite, with the highest Brix, there are clearly defined differences, such an increased viscosity, with increasing temperature as a result of water removal. The brix content defines the grade of massecuite used. As per the definition of Brix, the HTB samples have a higher Brix content, therefor, C-massecuite would represent HTB samples more closely as opposed to the A-massecuite grade.

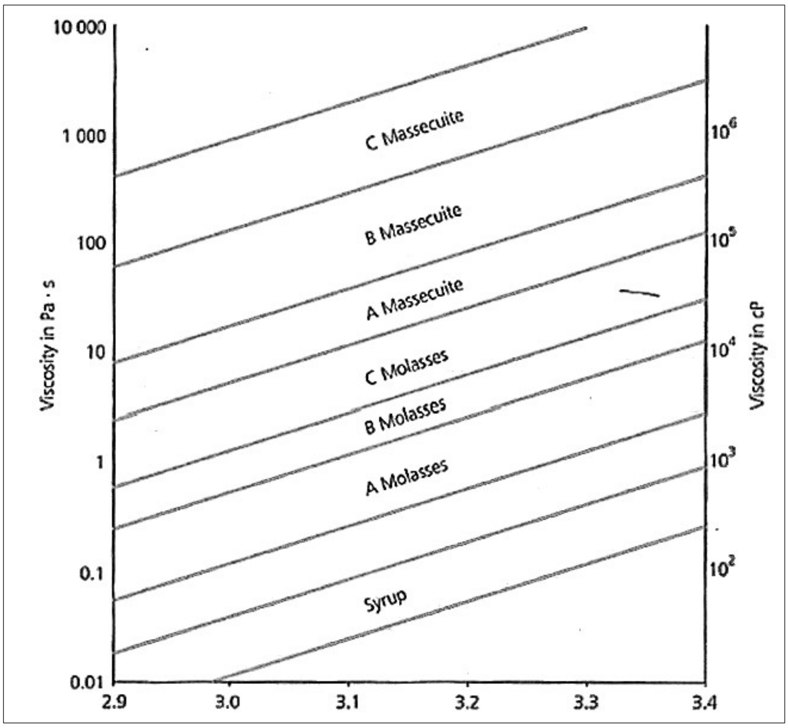

Figure 2.5: Massecuite viscosity as a function of temperature (Shah, Lokhat and Peacock, 2017)

Under the influence of gums, factories have described a notable increase in massecuite "viscosity" during the boiling period. This effect is thought to prevent boiling by reducing the heat transfer and bubble growth occurring within the liquid and reduces the rate of evaporation. Changes in rheological properties are responsible for this effect, as well as the decrease in concentration of water. Exhaustion of molasses is limited by viscoelastic effect produced by HTB samples (MacGillivray and Matic, 1970). Molasses viscosity is temperature sensitive with lower grade molasses showing high viscosity.

Figure 2.6 depicts a HTB molasses sample shown by a factory worker. The quick test for determining if a sample is HTB or not is using the "string proof test" depicted in the picture. A normal sample would flow easily as it is dropped, the molasses would drip from the height and there would be continuity as it flowed. HTB samples form ropes of viscoelastic liquid that pull and stretch as they fall. These samples may form ropes at high Brix levels.

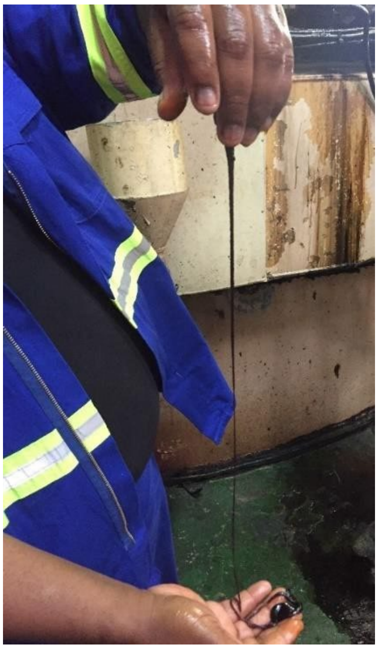

Figure 2.6: Rope-like Hard-to-boil sample tested using string proof test done by Noodsberg factory workers

As concentration of non-sucrose solids increases during the pan boiling, the characteristics they produce become more prominent. Under the effects of polysaccharides, factories have experienced extreme cases of “stretchy” massecuite that could be pulled into rope-like strands with increased elasticity, when cooled, and increased viscosity during boiling (Shah, Lokhat and Peacock, 2017). This leads to problems during processing where boiling is suppressed. Stirrers can trip and not operate accordingly, due to the high electrical current required to overcome the viscosity change. To pump this massecuite through the system, a total system redesign may be required, as piping dimensions and pump sizes are designed for maximum flow rates that does not include these altered properties.

Viscoelasticity affects the time required for the final molasses to reach maximum sucrose exhaustion, as it reduces the boiling ability of molasses. Effects seen, due to increased viscous and kinetic effect due to gums, causes a decrease in sucrose exhaustion. While processing allows for partial removal of gums in the clarification step, there is still a significant increase in gums as the water is removed through the boiling process (Schoonees and Pillay, 2004).

2.2.4 Factory Solutions to HTB effects

Factories identify HTB for various reasons, but mainly due to an increase in dextran-like polysaccharides within sugar. This is identified during the processing of the massecuite, which show an increase in viscoelasticity.

It has been discussed by various papers that the first step in dealing with HTB massecuites are early indicators, starting from the harvesting stage. Factories introduced a penalty to farmers for the total dextran content, calculated through an acceptable percentage (Eggleston, Morel du Boil and Walford, 2008). The use of a deterioration quality parameter in the pay-out process, based on sugar quality, would encourage better cane management and the receival of the best product. This penalty, however, is not used in South Africa (Eggleston, Morel du Boil and Walford, 2008). Currently the payment formula in South Africa is based of Recoverable Value (RV) Cane Payments system. This payment works on an average cane revenue, calculated from the total amount of sugar recovered, taking into account the percentage of non-sucrose and fibre obtained from the cane (Kadwa, 2018). The cane payment method does not consider the nature of the non-sucrose present, and rather looks at it as a whole, over an acceptable range (Mafunga, 2014). Cane growers are not penalised for harvesting delays or problems occurring as result of these delays.

Deteriorative microbes come into the sugarcane from the field and outside environment. Should these infecting micro-organisms survive within the factory environment, it is necessary to ensure the sanitation of areas where cane was stored. For general sanitation of mills, chemical microbicide is used, however, it is often ineffective as they do not adequately target microbes based off the employed chemicals (Nel, 2014). Continuous use of these biocides produces resistant bacteria that are unable to be removed effectively using biocides (Nel, 2014).

Certain factories were seen to employ the use of dextranase enzymes in order to reduce the dextran content of HTB samples. The use of dextranase assumes that dextran is the major fraction of total gums present and is therefore not an official solution for gum-related issues. Problems also deal with the selection of dextranase depending on the type of dextran and specifically the type of gum (Nel, 2014).

With HTB characteristics, factories have maintained quick-term solutions that are targeted at alleviating viscoelastic properties. The use of chemical additives has been listed by many sources as temporary solutions that factories may employ depending on what common practice is in these areas. Here are some of the solutions possibly employed (Saska, 2003; Duffaut and Godshall, 2004; Nel, 2018):

- Reduction of heat transfer coefficient is handled by pan boilers usually increasing the massecuite temperature by increasing the absolute pressure. By increasing atmospheric (inversely reducing the vacuum pressure), boiling occurs at a higher temperature., requiring increased heating to the calandria
- Increasing the inlet of steam to the system to force boiling or sparging with steamto force ebullition within massecuites and thereby force circulation of the calandria.
- Pan boilers add small quantities of sodium hydrosulphite to the massecuite to improve massecuite circulation in the pan. Sodium hydrosulphite is a strong bleaching and reducing agent that may affect the total impurities of the solution

- Reducing the final Brix of the syrup by boiling – this will reduce the total sucrose yield from a batch and may have an adverse effect on pan exhaustion however was seen to help reduce the viscosity of the massecuite.

- The wash water is increased in the centrifuges to improve the curing of the massecuite however, it causes crystal dissolution

- Use of hydrochloric acid or hydrogen peroxide within the pan was to reduce viscosity of the mixture by altering rheological properties

- Increased use of surfactants, lubricants and defoamers that are known viscosity modifiers

- Use of cooking oil to increase the boiling ability of the mixture by altering viscosity and allowing for better boiling

While these solutions may be commonly known to have an effect on the HTB problems experienced, if the severity of the problem is great, some of these solutions may have very little to no effect. Previous work where there was altered viscosity and heat transfer capability, the use of the surfactants, lubricants and soda ash had little to no effect in improving the problems being experienced (Saska, 2003). An inverse problem where a solution works too well and causes problems is the use of chemicals to reduce viscosity that causes destruction of crystal structure and reduces the size of crystals.

As previously mentioned, there is a change in many chemical properties between normal and HTB samples. These properties could possibly be used for early warning indicators of HTB however current systems in place do not use these methods of analysis for early warning indication.

2.3 Theories Surrounding HTB

Articles such as “Microbial diversity profiling in sugarcane processing: what, why and how?” have been able to identify the causative constituents within massecuites that brings about the known HTB effect, however, the exploration into the mechanisms that create the known effect are limited. A paper put forward by the Mathematics in Industry Study Group (MISG) discusses the hypothesis of bubble suppression upon which this study is based. This section will explore the work put forward by this paper by Fowkes et al. titled “Hard-to-boil Massecuites”.

2.3.1 Vacuum Pan Boiling & Effects of Bubbles

For the manufacturing of sugar, vacuum pans become increasingly important. Boiling occurs within the bundles of tubes, called calandria, where excess water is removed through heat addition. Within the vacuum pan, the bundled tubes are submerged within a pool of massecuite and heated from the outside by steam. Figure 2.7 shows the typical setup for a batch vacuum pan.

General boiling is defined when the vapour pressure of the fluid matches the pressure of the surrounding atmosphere causing condensate removal. Under vacuum, the atmospheric pressure is now redefined based off the applied vacuum thus altering the boiling temperature. For sugar manufacturing, it is important to prevent the caramelisation of the sugar as this would require excessive bleaching and refining to remove sugar colour. By boiling under vacuum at a reduced temperature, this can be prevented.

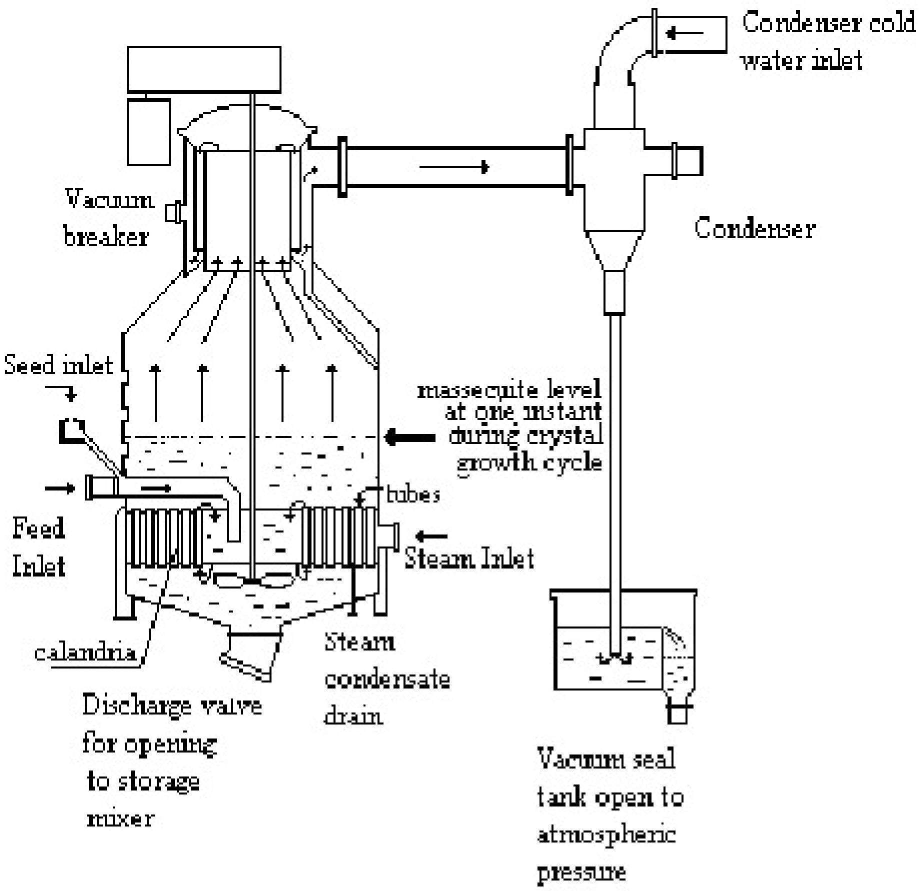

Figure 2.7: Standard schematic of a vacuum pan (Boyer, 2001)

Natural convection comes about through the formation and movement of bubbles in the massecuite, caused by the differences in temperature between the heated calandria tube and the cooler downtake Bubbles occurring due to phase change, form at the heated calandria walls and move up the calandria tubes as a result of density, causing heat to be transferred, and promoting circulation within the tubes in the form of convective currents. The circulation is further facilitated by a stirrer at the base of the pan. Crystal sugar growth is controlled carefully through addition of water and seed crystals, to ensure steady growth, and uniformly sized crystals.

Circulation is an important factor affecting heat and momentum transfer between liquid and bubbles through phase change (Eccheverri, Rein and Acharya, 2007). Through circulation, the pan can produce even heating of the boiling contents, ensure crystallisation and prevent burning and fouling on heating surfaces. Circulation is a result of a hydrostatic head between the two phases in the boiling tube, as vapour flows up through the calandria, through liquid syrup, and the single phase unheated massecuite moving down the down take (Rouillard, 1985a). This movement through the liquid is affected by the fluid flow resistance as a result of pan dimensions, liquid properties and vapour formation.

The hydrostatic head experienced within a pan is determined by the "void fraction" of the mixture (Rouillard, 1985a). This term describes the percentage of vapour that is found in the boiling tube that aerates the space and adds to filled height but does not actually contribute to the total volume of liquid. Void fraction and therefore hydrostatic head are affected by the boiling factors, namely liquid properties such as: Pressure, temperature and filled volume. Hydrostatic head is seen to decrease with increased vapour formation (Rouillard, 1985b).

Figure 2.8 below depicts the boiling in vacuum pans as a result of void fraction and heated temperature (Rouillard, 1985b). Heating of the syrup occurs through convection where heat is passed through the liquid from the heating wall. At the heating surface, i.e., the wall of the heated calandria, a vapour layer forms as liquid closest to the surface begins to heat and phase change occurs. This boundary layer prevents sticking and burning of syrup and is the site of bubble formation (Eccheverri and Rein, 2005).

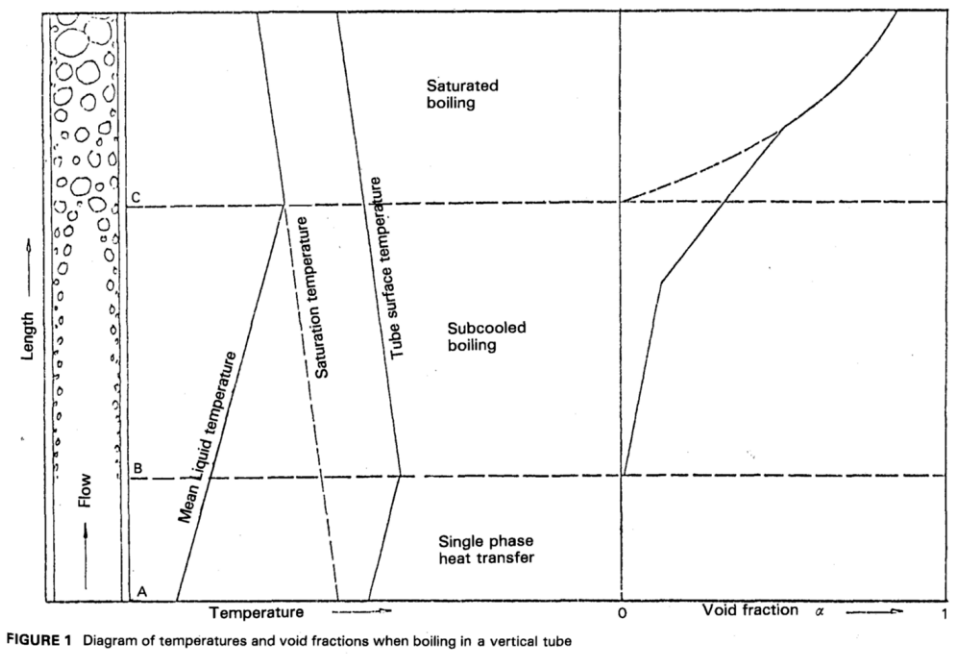

Figure 2.8: Heating phases across the boiling calandria of a vacuum pan (Rouillard, 1985b)

Syrup enters the system being subcooled and is heated by single phase forced convection. As syrup begins to heat it reaches point B where bubbling begins as boiling temperature is reached however the bulk of the fluid is still subcooled. As vapour bubbles grow between zones B and C, vapour bubbles grow through heating and reduced weight of the hydrostatic head causing decompression as it flows upward in the tube and bulk of the liquid begins to heat as bubbles transfer heat through the tube.

2.3.2 The Theories Surrounding HTB

While the chemical aspect of HTB is not the subject of this work, it is a key characteristic that factories use to describe and identify HTB samples. Papers had theorised that the HTB effect was unrelated to any one dextran or starch variety (Saska, 2002; Duffaut and Godshall, 2004). One cause was linked to a precipitation of a complex macromolecule with calcium ions at higher Brix onto heating surfaces that would break down at lowered pH (Duffaut and Godshall, 2004). Others looked rather at a combined effect of all deterioration products that act together to alter rheology (Nel, 2014, 2018; Fowkes *et al.*, 2017).

Theories pertaining to altered rheology have looked at (Saska, 2003; Fowkes *et al.*, 2017):

- the idea of surface fouling due to precipitate formation creating HTB effect
- surface fouling as a result of increased viscosity resulting in burning at tube wall.
- ebullition changes due to rheological properties affecting the crystallisation through decreased evaporation of excess water
- Polysaccharides create strong intermolecular forces that hold onto the water increasing the boiling point elevation (BPE).

This thesis focuses on the idea of an altered BPE as well as a change of bubble formation and size.

2.3.3 Bubbling Theory

Massecuite boiling has been modelled mathematically and experimentally in order to mimic conditions within vacuum pans. Standard viewing of this boiling is extremely limited as there is no way to visually monitor the calandria tubes, and monitoring devices previously used could not withstand the harsh conditions within the pan.

Other researchers, like Eccheverri (2007) and Saska (2002), have used computational fluid dynamics (CFD) and differing forms of pilot pans and tubes with synthetic substances mimicking massecuites, in order to model the flow. The team from MISG mathematically computed the boiling effects under an altered flow property. Research into the boiling within the calandria of vacuum pans have determined the **key factors affecting the boiling** being linked to **bubble growth, circulation, convection and evaporation**.

2.3.3.1 Ebullition within the calandria

Bubbling occurs within the pan tube when syrup nearest to the heating wall reaches boiling temperature. This temperature is determined as a result of the Brix levels of the massecuite. Bubbles, forming as a result of the phase change nearest to the wall, circulate heat through convection and heat the tube. Eccheverri (2005) looked at the bubbling regime within the pan and noted, using a clear boiling tube, the boiling zones. These zones, found in figure 2.9, were distinct, based off the bubble type, number of bubbles and heat:

- Bottom of tube: convective and subcooled boiling
- Middle of tube: saturated and forced convective heat transfer
- Top of tube-: liquid deficient area due to high void fraction and convective heat transfer as vapour is removed from liquid.

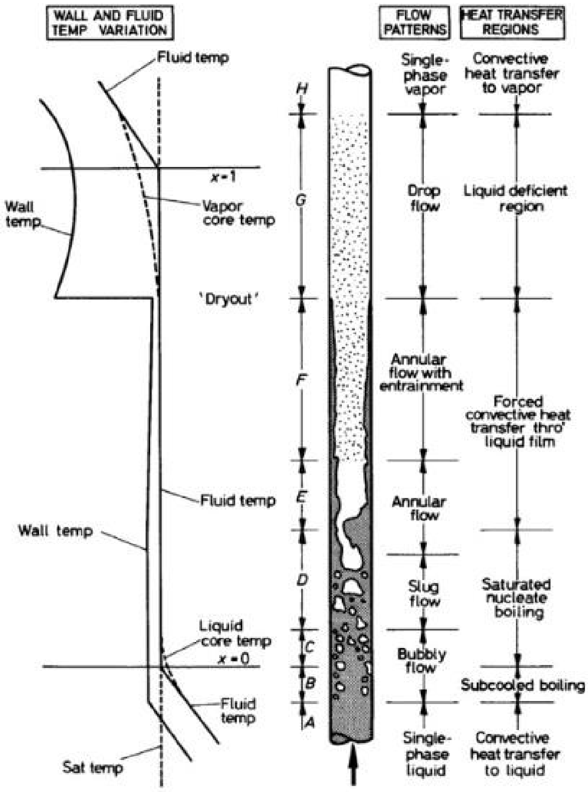

Figure 2.9: Bubbling phases within calandria (Eccheverri, Rein and Acharya, 2007)

The appearance of the bubbles during boiling are dependent on the drag and temperature at the particular height (Eccheverri, Rein and Acharya, 2007). With increased viscosity of the mixture and reduced temperature, bubbling was dominated by slug regime as bubbles struggled to move through the calandria (Eccheverri, Rein and Acharya, 2007).

The Fowkes et. al (2017) model showed that, under increased viscoelastic conditions, bubble growth would be limited, and evaporation and crystallisation would be reduced (Fowkes *et al.*, 2017). Under the drag of friction and viscous effects reducing bubble movement and growth, heat transfer through the liquid would also be limited accounting for the longer boiling periods noted, when dealing with HTB samples.

Bubble suppression describes the reduction in size or complete removal of bubbling within a boiling substance. Bubbles formed during boiling remove excess water and spread heat through the syrup. In the scenario of HTB, the viscoelastic behaviour of the HTB massecuite reduces bubble formation and bubble release and therefore, vapour removal. This is depicted in figure 2.10.

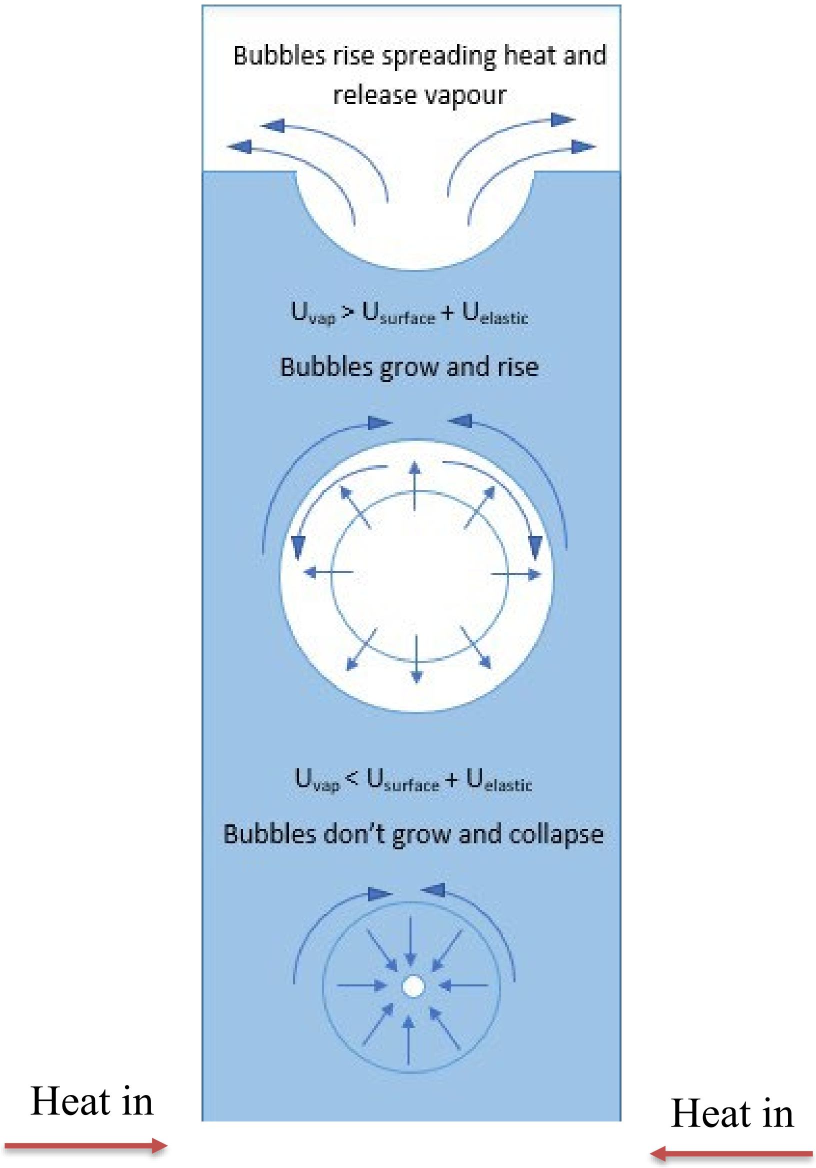

Figure 2.10: Ebullition in Massecuite (Fowkes *et al.*, 2017)

For bubbles to form, the energy of vapour change must be large enough that it overcomes the surface effects of the liquid combined with the elasticity formed due to gum presence. The energy in the above diagram is referred to as the heat of the system and is denoted by the symbol "U". If the vapour formation energy (Uvap) is less than the combination of surface (Usurface) and elastic energy (Uelastic), bubbles will not grow and may collapse on themselves. Only bubbles with enough energy to grow will be able to escape the mixture due to buoyancy effects. Thus evaporation, convection and circulation are reduced.

Since circulation within calandria is dictated by buoyancy driven forces in the form of ebullition, with an increased viscosity and increased density, ebullition will be reduced, and growth of bubbles will be stunted. Inversely, with a lack of ebullition, the density of the mixture increases while a fully bubbling and boiling mixture will have a reduced density as void-fraction increases. This effect is due to high viscoelastic properties that increase the required energy and internal pressure for bubbles to be able to grow and overcome the gumminess of the mixture. For bubbles to grow, it is necessary that the energy formed due to phase change must be large enough to overcome the combined surface tension effects and elastic property increase that occurs due to gum presence (Fowkes *et al.*, 2017). Increased pressure due to the surrounding liquid will cause vapour to condense and bubbles to collapse.

Under the worst-cases of deterioration, gumminess was seen to decrease robustness of boiling normally experienced in pan boiling (Eggleston, Côté and Santee, 2011; Fowkes *et al.*, 2017). Volatility of the boiling syrup is determined by the circulation and growth of bubbles that remove vapour over the boiling period (Fowkes *et al.*, 2017).

To understand the effect, it is important to compare the standard boiling noted within calandria and the mechanism altering boiling properties. A crucial aspect of this study is the combined **theories of bubble suppression and an apparent boiling point elevation being affected**, due to the presence of HTB substances presented by the Mathematics in Industry Study Group (MISG) (2017).

Upon heat addition to the system, boiling begins as bubble nucleation at the heating surface of the calandria, where a vapour film forms and decreases viscosity at the walls. Vapour film acts as a lubricant to facilitate liquid movement. This layer also acts to insulate the syrup from the highly heated pipe surfaces where the sucrose could melt and burn onto the surface.

The state-change due to required heat input causes bubble nuclei formation that forms a bubble layer on the wall heating surface. These bubbles grow with increased heat input to overcome viscous effects within the mother liquor. Bubble buoyancy stimulates convection and heat is spread through the liquid, reducing viscosity. Upon reaching top liquid surface, bubbles will burst and with excess water removed in the process.

Under ideal conditions, ebullition and flow is maintained easily, with convection promoting circulation and water being removed as temperature increases. However, under high apparent viscosity conditions, bubble growth is decreased, as the energy required to overcome surface tension of the massecuite surface around the bubble is higher. It can be assumed that under these conditions, bubbles that do form are few and smaller in size and boiling needs to be increased through increasing steam pressure to increase temperature.

Vacuum pans rely on adequate heat transfer to remove water and increase the concentration of sugar solution, in order to promote sugar crystal growth. The heat transfer coefficient (HTC) was seen to decrease in the presence of problematic gums (Saska, 2005). When it comes to understanding the boiling of massecuite, it is crucial to understand the factors that contribute to the effects noted by various studies. Massecuite under general boiling conditions and chemical properties is affected by (Saska, 2003; Fowkes *et al.*, 2017):

- Brix
- Temperature
- Available crystal surface area
- Nature and concentration of impurities
- Syrup rheology
- Hydrostatic head and tube length
- Vacuum pressure
- Circulation
- Calandria material

2.3.3.2"Hard-to-boil Massecuites" by Fowkes (2017)

The paper by Fowkes et al. (2018) titled "*Hard-to-boil Massecuites*" mathematically modelled the flow properties of massecuite accounting for the rheology, heat transfer coefficients and other boiling parameters(Fowkes *et al.*, 2017). This paper hypothesized that **due to increased viscoelastic properties, there would be an effect on heat transfer, resulting in reduced bubble size**.

HTB samples exhibit viscoelastic rheology due to presence of intermolecular gel-like networks formed by long chain polysaccharides as well as reduced thermal conductivity and heat transfer coefficients. Polysaccharide networks determine the energetic requirements for the nucleation and growth of vapor bubbles. Under theories of the effect of HTB on boiling, it is said that the mixture will appear as if it is not boiling due to the entrapment of bubbles within the polysaccharide matrix (Fowkes *et al.*, 2017). Reduced ebullition and evaporation would be noted as a result.

Bubbling in vacuum pans is an indicator of boiling and evaporation. Through bubble growth and escape, vapor that has formed through phase change of water in the syrup will be removed. Bubble movement carries heat and vapor through the mixture, influencing circulation, convection and evaporation. However, the movement and escape of bubbles is determined by the rheology of the mixture.

For ebullition and successful bubble formation, bubbles need to have adequate energy to grow past their critical size. Bubble nucleation requires additional elastic energy to compress the viscoelastic massecuite as a result of phase change. Critical radius is the minimum radius below which bubble growth will not occur and therefore determines the required energy for bubbles to form and grow. A larger minimum bubble radius is required when a larger massecuite viscosity is present. This results in a need for a larger energy change. The effective critical bubble size models describe the formation and growth of bubbles within any given liquid. For bubbles to form, they require the phase change energy that formed them to be large enough to overcome surface and viscoelastic energy. In the paper by Fowkes et al. (2017), the energy requirement equation is as follows:

$$\Delta E = -U_{vap} + U_{surf} + U_e$$

$$= -\left[\frac{4}{3}\pi R_i^3 \rho_f L_v\right] + 4\pi R^2 \gamma_{lv} + 4\pi \int_R^\infty \left[\frac{1}{2}\lambda (e_{kk})^2 + \mu e_{ij} e_{ij}\right] r^2 dr$$

Where: U_{vap},U_{surf}, U_e =Vaporisation, surface and elastic energies

L_v =latent heat of vaporisation

γ_{lv}=surface tension of the fluid vapour-interface

λ=lame constant

μ=shear modulus

ρ_f, ρ_v=fluid and vapour density respectively

This equation represents the energy required for bubble growth beyond a critical radius. All the mentioned values are affected by the Brix, water percentage and impurities within the massecuite. Under the effects of HTB, bubbles may still form as heat addition to the system will cause phase change. However, these bubbles may not grow large enough to reach critical size and gain buoyancy to move through and leave the liquid.

The assumptions being made by the system in order to fulfill this derivation are as follows (Fowkes *et al.*, 2017):

- Heat flow from walls provide a latent heat that extracts water vapour implying a uniform temperature profile except for the formed vapour layer at the heating wall across which heat is passed
- Flat velocity profile under turbulent two phase flow conditions

- Bubbles and liquid move at the same velocity such that movement within the calandria can be considered single phase flow having varying density due to bubbling • Viscous drag is negligible due to vapour film at heated surface
- Quasi-steady flow assumed.

Due to the temperature of liquid, within the calandria, being unevenly distributed, with heat concentrated at the tube walls, where heat transfer occurs, the growth, density and shape of bubbles should differ across the tube length. The change in ebullition predicts the heat transfer through the tubes and determines the degree of evaporation occurring within the calandria.

The movement of bubbles distributes heat throughout the cross section of the calandria. This heating effect is determined by the heat transfer coefficient of the liquid that is in turn determined by the properties of the massecuite. HTB samples have been characterized by a reduced thermal conductivity and a higher specific heat capacity, resulting in samples that are harder to heat.

The effect of a higher specific heat capacity of the fluid, noted by factories, requires an increase in steam addition to the pans when HTB is experienced. This is related to the apparent boiling point elevation (BPE). When the Brix content of the sample is increased, the BPE requires additional pressure and steam input to achieve a higher temperature. Using the Brix, vacuum pressure and hydrostatic head, it is possible to calculate the temperature at which boiling occurs and this table of calculated properties can be found in Appendix B.1. These results were calculated using a toolbox made by the SMRI. With an increase of Brix there is a need to increase the heat input to induce boiling. This is noted in factory recounts of solutions to dealing with the effects of HTB.

With a decrease in evaporation of water, water vapor bubbles flowing through the liquid decreases and will not adequately transfer heat to anything more than the outer edge closest to tube walls. Heat transfer and state change processes will be confined to a thin layer at the tube surface. Inadequate rate of phase change and bubble growth will result in increased drag at the heating surface. Normally phase change that lubricates and insulates syrup will now decrease and burning and caramelization of sucrose may occur. This scale formation due to burning at the heating surface impedes heat transfer and reduces boiling rate, also affecting the taste of sucrose and can ruin batches. Fouling onto the heat transfer surfaces increase the boiling time and reduce heat transfer into the system. External convective current that normally feeds the tube will halt under HTB conditions and there will be no external forces pushing massecuite through the pipes.

This leads to the determination that the energy required to cause phase change to the water, and for the water vapor to leave the viscous substance, within a HTB sample, is higher than the energy requirement for good boiling samples. This is validated by one of the factory solutions for handling HTB being linked to an increasing heat input to the system. The following expression is derived:

$$U_{boil,HTB} > U_{boil,good}$$

In accordance with the Bubbling Theory, the excess energy is required to further reduce the strength of the molecular bonds within the mother liquid, to overcome the resistance for the bubbles to escape the substance.

2.3.4 Saturation, Boiling & BPE

The control of vacuum pans is a difficult feat and requires one to pay careful attention to manipulation of specific factors to gain as high a yield as possible. Factors affecting vacuum pan boiling include (Eccheverri, Rein and Acharya, 2007; Shah, 2017):

- Absolute pressure
- Crystal content
- Supersaturation
- Inlet feed
- Steam
- Convection
- Circulation
- Water flow rates
- Apparent BPE

In the simplest definition, the saturation point of sugar is defined as the point where the liquid has reached the maximum concentration that can be dissolved while remaining stable (Eccheverri, Rein and Acharya, 2007). Once that maximum concentration is exceeded, the mixture becomes super-saturated where the syrup will begin to crystallise. This supersaturation point is reached through boiling by removing water and thereby increasing the overall brix.

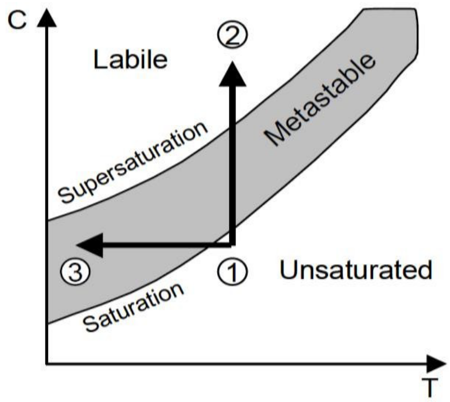

Figure 2.11 : Graph of Concentration vs Temperature and the effect on saturation (Eccheverri, Rein and Acharya, 2007)

The ability of a syrup to dissolve solids is highly dependent on the temperature and concentration of the solids. Figure 2.11 shows the factors affecting saturation with concentration on the y-axis and temperature on the x-axis. As temperature increases, the ability of the liquid to dissolve solids increases.

Degree of saturation can be separated into four phases, namely (Meade and Chen, 1977; Eccheverri and Rein, 2005):

- Unsaturated zone where no new crystals form or grow and crystals in the liquid begin to dissolve
- Metastable phase where existing crystals grow while no new crystals form
- Supersaturated zone where crystals grow, and new crystals may form
- Labile zone where crystals form spontaneously without the introduction of seed crystal

Pans are seeded in the metastable zone and as boiling occurs, crystals will grow. During the boiling period, the boiling must be maintained within this zone in order to prevent formation of false grains and dissolution of grains already formed.

The vacuum pump works together with the condenser to maintain the vacuum pressure at approximately 80-85 kPa vacuum, 15kPa absolute (Rouillard, 1985a). The massecuite temperature is maintained in a range between 70-80ºC. Water may be added (called movement water) to facilitate massecuite circulation and to prevent spontaneous crystallisation.

The pressure within a vacuum pan is determined by the vacuum pump pressure combined with the condensation rate of the boiling side condenser. The rate of heating on the steam side determines the generation of vapour on the boiling side calandria. The phase change that occurs when vapour is converted to liquid creates a vacuum within the condenser. This vacuum pressure combined with the vacuum from the pump can increase overall vacuum, as water evaporates. At the end of the boiling cycle however, rate of evaporation decreases, and vacuum requires adjustment to maintain pressure, making the pressure quite unstable (Rein, Acharya and Echeverri, 2004).

Boiling point elevation (BPE), sometimes called boiling point rise (bpr), is the difference between the temperature of a boiling solution and the boiling point of pure water at the same pressure. BPE will decrease as pressure decreases and increases as purity decreases (Meade and Chen, 1977; Hugot, 1986). BPE within vacuum pans determines the temperature of the system required to reach boiling. As previously noted, the use of vacuum pressure is such that the contents of the vacuum pan be able to reach boiling while preventing caramelisation, production of invert sugars and excessive colouration.

Under normal boiling, the effect of dissolved components in water alters the boiling temperature at operating pressure. However, under vacuum pressure, this temperature may be reduced as the vacuum pressure increases (i.e. decreasing absolute pressure allows for a decreased boiling temperature). BPE is determined by the hydrostatic head, the heat input and the brix content.

Hydrostatic head will determine the boiling temperature where a higher head will require a higher temperature to reach boiling under the same vacuum pressure. This will dictate the design of calandria tubes and determine the size and height of tubes as well as the height fill within pans.

The use of BPE in sugar manufacturing remains a simple and inexpensive means of monitoring supersaturation for a range massecuite purities (Saska, 2002). With an increasing dissolved solids concentration, there is a notable increase in saturated vapour temperature with an increase in pressure (Hugot, 1986; Eccheverri, Rein and Acharya, 2007). This elevation in boiling temperature occurs as a result of liquid property changes as concentration increases.

With boiling reducing the water content and increasing the concentration of the syrup or molasses, there occurs a need to increase in the heat driving force for the same pressure such that crystallisation may occur. The steam temperature (the driving force) is increased to maintain boiling. This temperature is determined by dissolved solid content, vacuum pressure, hydrostatic head and rate of heating. Figure 2.12 graphs the relationships between temperature, pressure and hydrostatic head.

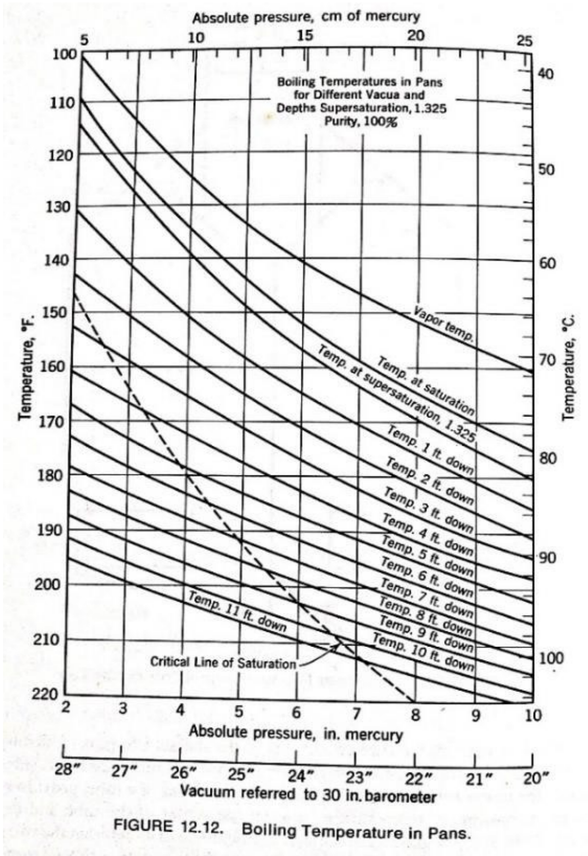

Figure 2.12: Boiling point of massecuite and how it changes based off boiling properties (Meade and Chen, 1977) (Rein, 2007)

The change in properties of massecuite affects the heat transfer occurring within the system by affecting the conductive and convective coefficients. Heating remains limited to the surface of the tube causing uneven distribution of heat. This leads to caramelisation and fouling at the heating surface thus reducing rate of heat transfer.

Pan productivity is determined by boiling time required to achieve a higher yield that in turn depends on the evaporation and crystallisation rates. Concentration of mother liquor, crystal content and viscosity are three distinct yet interwoven factors affecting the boiling of massecuites.

Studies of the effect of HTB on heat transfer have concluded that with increasing impurity and solids content, there is a steady decrease in heat transfer coefficient (Saska, 2003; Eggleston, Côté and Santee, 2011). Surface fouling was assumed in order to explain the reduced heat transfer from the heating surface to the liquid but when contents of pan was drained, no surface fouling was evident (Saska, 2003).

2.4 Conclusion

This chapter analysed the effect of the HTB phenomenon on the sugar manufacturing process. A study was made to investigate the characteristics that define a HTB substance. These characteristics included the chemical nature, as well as the effects on the rheology of the substance. An investigation on how factories have provided solutions to dealing with HTB samples. While these solutions are viable, they do not provide a text book answer to the issue at hand. The effects of bubbling as well as the Bubbling Theory was studied, in order to characterise a relationship between bubbling and various rheological properties. Sections of note that will be further expanded upon in the theoretical framework, are the rheological changes occurring under deteriorative effect and the mechanics of HTB within vacuum pans that alter boiling abilities.

Chapter 3

Methodology & Experimental Design

3.1 Introduction

This section details the methodology chosen in order to complete the research of this topic. The hypothesis developed, for the purpose of this project, needs to be analysed further, to develop a further framework. Here the apparatus and instrumentation used for this research topic is discussed, along with the experimental strategies chosen to generate the results required. The overall experimental objective is to **visualise and document boiling changes, occurring between standard and HTB massecuite samples, linking these to characteristic changes in rheological properties.**

3.2 Hypothesis Framework

The work required to test the theories presented in the literature section needed to investigate two aspects, namely massecuite rheology and boiling within a vacuum pan calandria. A sample with known HTB characteristics, either from a factory or manually dosed, was to be boiled within the vacuum pan test rig, where visual monitoring of boiling would occur and compared to a standard sample. During these tests, samples collected over a chosen interval and tested to monitor Brix changes during boiling would then need to be tested chemically. The rheology of the samples was required these were determined using NIRS and rheometers respectively, to determine the characteristic differences and changes.

In order to investigate the statements of the hypothesis put forward by Fowkes et. al, the experimentation must be modelled to adequately represent these ideas. For the purpose of this dissertation, as stated in chapter 1, the hypothesis was evolved into the following statement:

Boiling of Hard-to-boil massecuite will lead to an increased viscoelasticity. This viscoelasticity property will result in change in the boiling properties of massecuite. Due to the effect mentioned, the following results will be noted:

- Bubbling will differ between standard and HTB samples. HTB samples will have smaller bubbles that will not grow, and have decreased movement and size, being unable to escape the mother liquor due to viscoelastic properties
- The apparent boiling point will differ between sample types where HTB samples will have difficulties removing excess water, as vapour bubbles will require a greater energy

to overcome surface effects. Under steady state condition, HTB samples will have a reduced rate of condensate formation

The hypothesis notes three characteristic changes that will be tested: viscoelasticity, ebullition and evaporation. Under the hypothesis, it was stated that:

- Polysaccharides formed from increased deterioration was the **cause** of the HTB phenomenon
- The **mechanism** was said to be changes in viscoelastic properties of the massecuite, that inhibited boiling, resulting in bubble suppression
- The **effect** was noted by a decreased evaporation rate as vapour was unable to escape the mixture under altered rheological properties
- **Results** in a noted change in bubble growth and pattern, as well as decreased amount of collected condensate in a HTB sample, as opposed to a standard sample

In figure 3.1, a flow chart describes the order and relationship of the hypothesis.

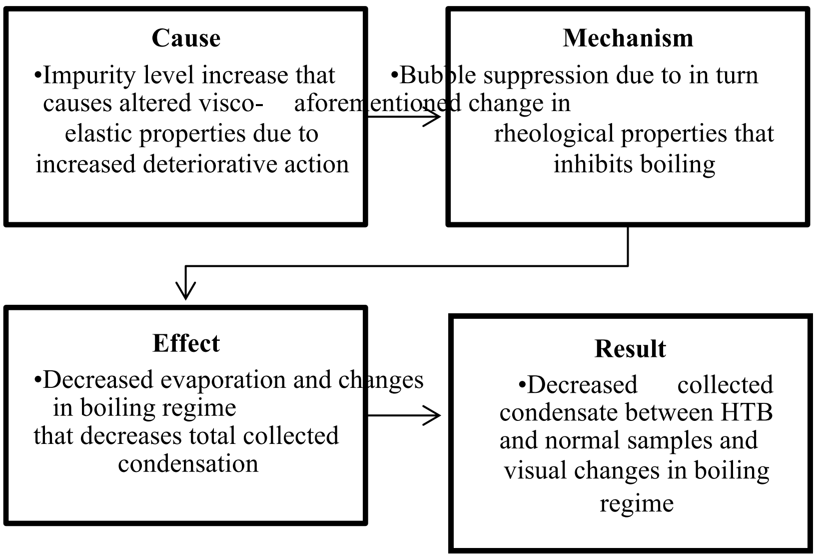

Figure 3.1: Hypothesis flow chart

To test this theory, it is required that vacuum pan boiling was to be replicated, with a steam input and vacuum pressure conditions maintained at one set value, for the entirety of the boiling process. Without increasing these values, the boiling will reach a final point noted by the ending of evaporation. This will be noted by no increase of condensates collected between data collection intervals. For a HTB sample, this point will be reached at a lower collected condensate mass.

The work required for the hypothesis to be tested, in order to accurately display these statements, considering the affecting factors. For this work, three pieces of testing equipment were essential. Namely: the **vacuum pan testing rig**, a **rheometer** and a **Near-Infrared spectrometer (NIRS)**.

The vacuum pan testing rig allows for visual monitoring of vacuum pan boiling. Control of the vacuum pan is manual and allows for the operator to adjust and control the boiling occurring within the system. The rheometer is capable of testing rheological properties of substances using shear force applied through a rotating or oscillating disc plate. Using the equipment mentioned, the work was separated into two sections covering the vacuum pan boiling portion of testing and testing of rheological properties of the samples. Experimental planning will be described in the experimental framework.

Using the vacuum pan testing rig, boiling conditions were to be controlled, such that all samples were tested under steady state conditions that were maintained manually. The vacuum pan testing rig was used for visual monitoring of the calandria boiling activity and was monitored, using the primary and secondary sight glasses on the rig

NIRS is used for quick and accurate analysis of samples, to calculate the total percentage of dissolved solids, as well as other possibly important contents that may be of use in comparing the results. A rheometer was used to measure various rheological properties, to accurately link different sample types with corresponding Brixes. In figure 3.2, the relationship between the mentioned pieces of equipment is described in conjunction with the hypothesis.

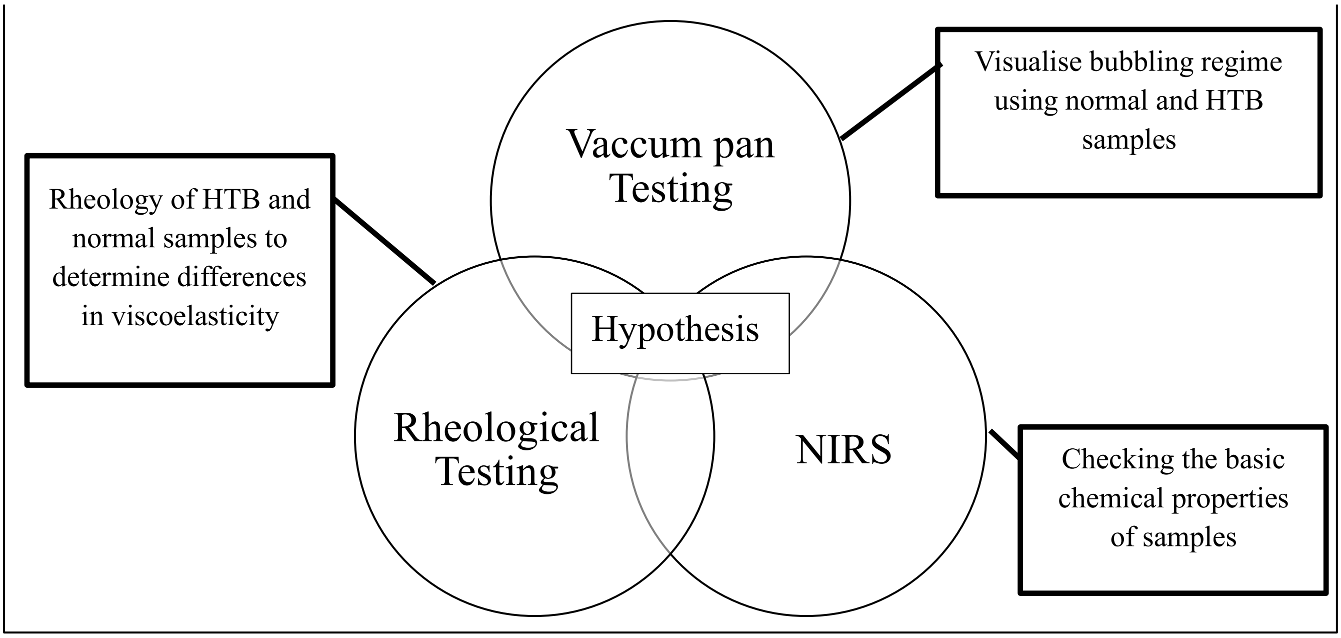

Figure 3.2: Equipment usage schematic

3.3 Vacuum Testing Rig

This testing rig was designed in 2017, for the Sugar Milling Research Institute NPS (SMRI), by UKZN, for the final year project titled "Massecuite Boiling Visualisation". It was used as a test rig capable of monitoring and studying boiling processes, occurring within pan tubes, to solve the HTB phenomenon (Naidu *et al.*, 2017). The rig was made up of one single tube vacuum pan, 3 condensers and a condensate collection tank, with two scales. Figures 3.3 and 3.4 show the rig realistically and schematically.

The purpose of this testing rig was to observe and document boiling properties, as well as the bubbling habits of standard massecuite and compare it to HTB massecuite. This can be achieved on this rig, using the vacuum pan, equipped with a glass panel that allows for viewing of the boiling process within the calandria. The test rig's dimensions are significantly smaller than that of an industrial vacuum pan, however, the dimensions are the same as standard vacuum pans. This allows the experimental process to simulate an industrial process on a smaller scale, using smaller batch quantities.

Figure 3.3: Vacuum Pan Rig Setup

Massecuite boiling occurs in the calandria of the vacuum pan, surrounded by steam, with assisted circulation from a motorised stirrer system within the sump, to promote upward movement. Within the designed rig, heat is transferred from the condensed steam to the tested substance (massecuite or molasses), through the side wall of the tube. Circulation comes about as a combination of convection, due to the temperature gradient formed from the heated front tube and mechanical stirring. Water vapour, in the form of bubbles due to boiling, is released at the head space of the rig and condensed within the primary and secondary condensers. This vapor forms a condensate that is pulled into the storage tank, where its mass is weighed over time. A schematic representation for clear viewing of rig setup is seen in figure 3.4.

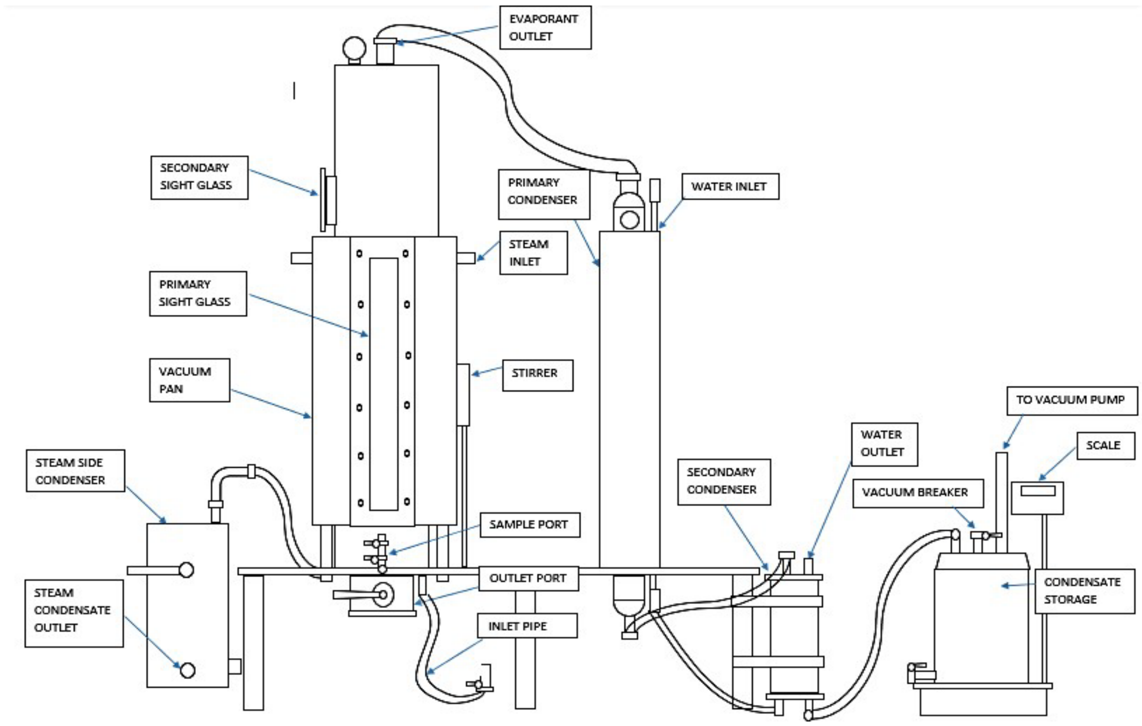

Figure 3.4: Vacuum Pan Schematic

The heat circulation, represented in figure 3.5, shows the heated front pipe (depicted as a red arrow) that rises as it boils to the disengagement space above the baffle plate, before entering the cooler downtake (shown by the blue arrow).

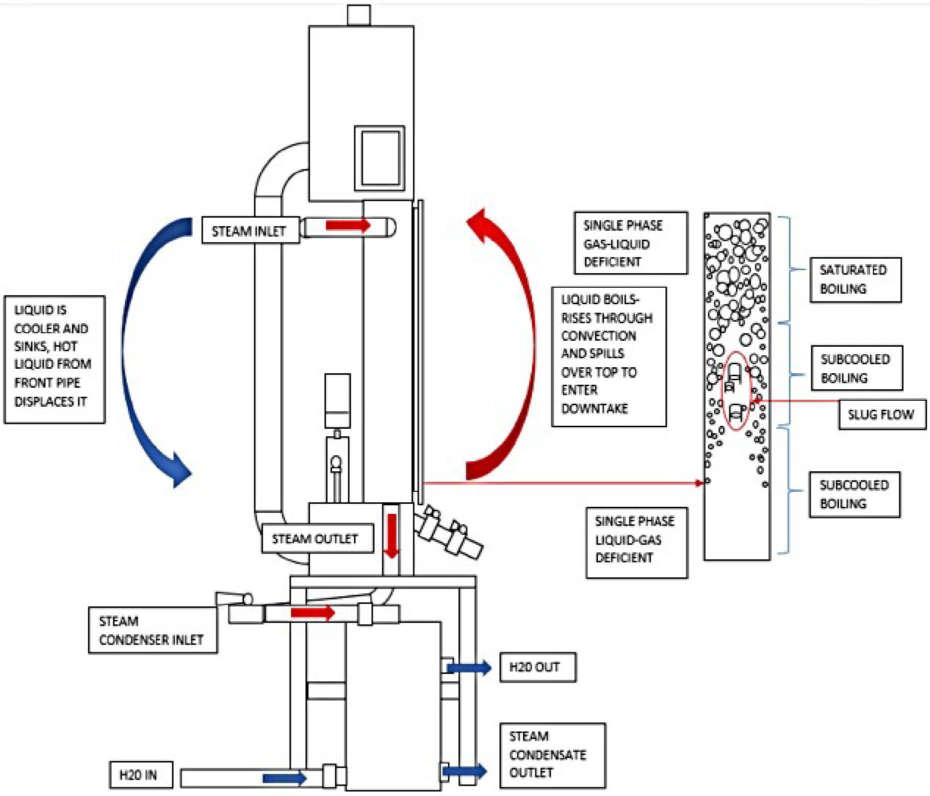

Figure 3.5: Natural convection pattern due to temperature gradient

This vessel, normally used for crystallisation, does not allow for seed injection, to promote crystal growth. Tests are run while trying to prevent crystallisation and removing crystal content, therefore making this unnecessary.

The testing rig was designed using the dimensions of a full-scale vacuum pan calandria, with a 100mm diameter, converted to a square cross-section, with a single face enclosed, with glass, allowing visualisation of the vacuum pan tube boiling. The total length of the tube was also kept to standard practice, at 1m, and encased on three sides by a steam heated jacket. With this clear front pane modification, the boiling behaviour of sugar substances, under vacuum conditions, become observable and can be documented, as shown in figure 3.6. Using applied vacuum pressure and steam supplied by vacuum pump and boiler, samples may be drawn into the rig and boiled under controlled conditions.

Figure 3.6: Boiling in Vacuum Pan Rig

The vacuum pressure used for boiling is achieved using a liquid ring vacuum pump, provided by the SMRI. This pump could theoretically provide up to 100 kPa vacuum (0 kPa absolute) and works by forming a liquid ring through using centrifugal force. As the pump rotor rotates, the vane rings line up such that the space between the two parts expands past the inlet, drawing air in before reducing and compressing the air that is discharged to the outlet (Rein, 2007). The vacuum is connected through the condensate collection tank, where vapour is stored and weighed over time, to run through the system of condensers to the calandria. Figure 3.7 shows the condensers and their connections to other parts of the rig. Figure 3.8 depicts the connection ports of each vessel in the rig, where the arrow colours depict the movement of cool (blue), warm (orange) and hot (red) liquid or vapour through the testing rig.

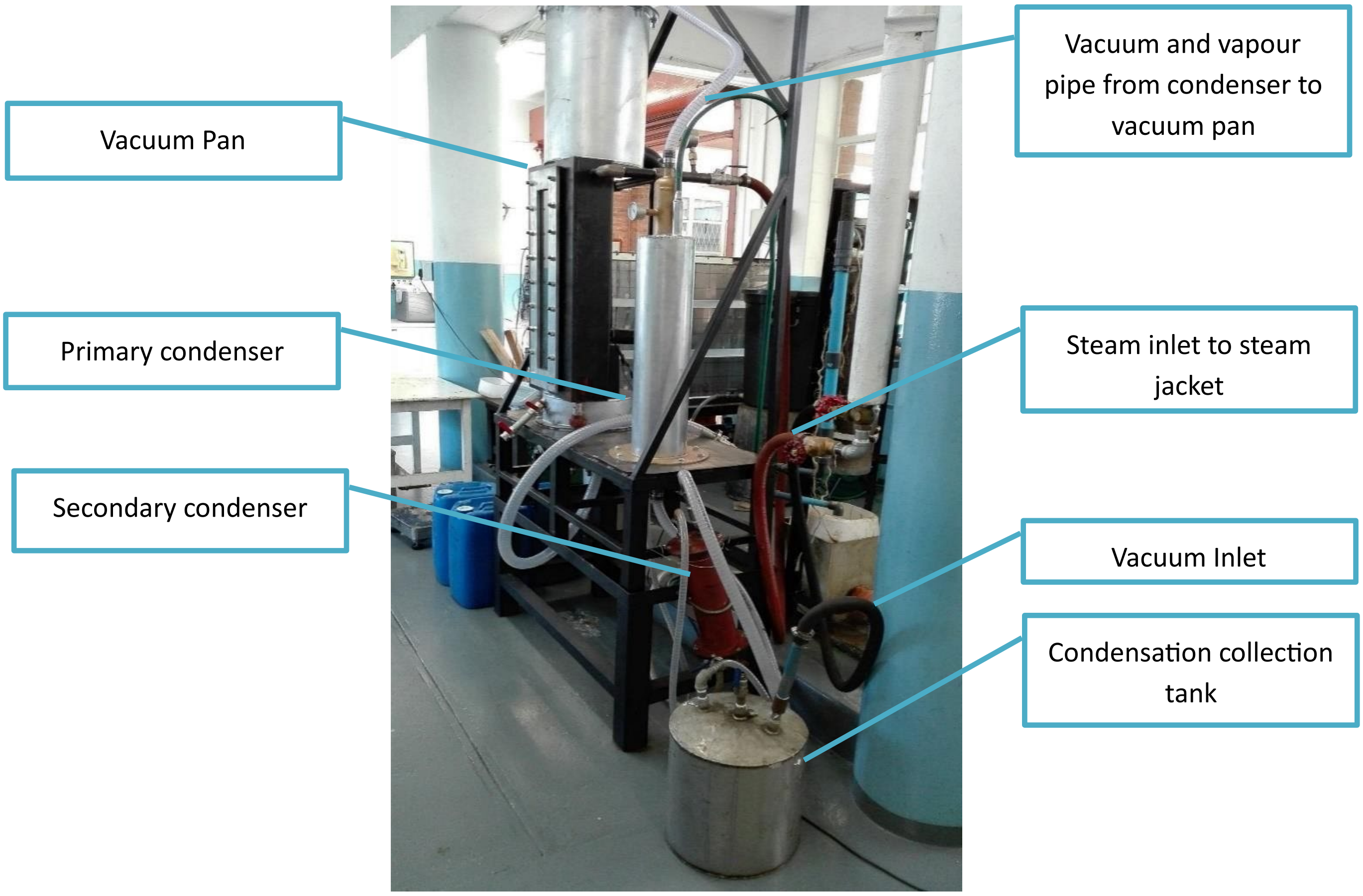

Figure 3.7: Condenser system of rig setup

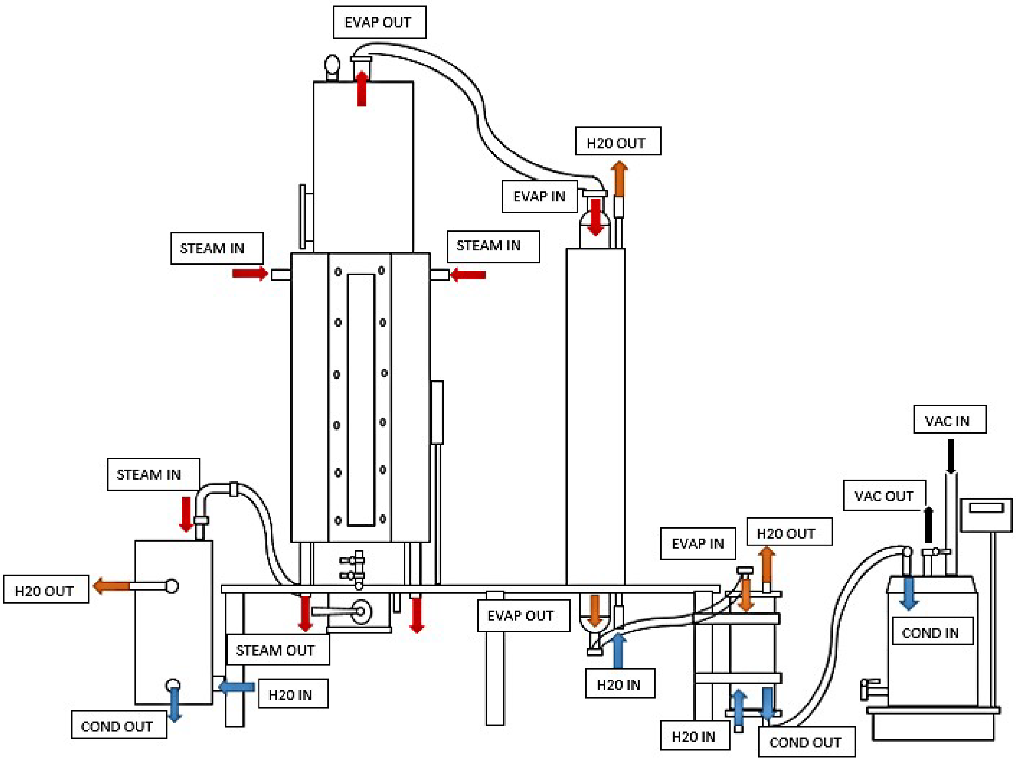

Figure 3.8: Heated and cooled vapour movement through the testing rig

In this vacuum pan's disengagement space, which is required for increasing hydrostatic pressure and increasing the boiling temperature, was made to be 0,5 meters due to the small volume of sample. The vacuum outlet was connected at the top of the disengagement space such that vapour was easily removed as evaporation occurs.

It was deemed necessary to measure total amount of steam being used over the cycle of a test. A condenser was fitted on steam outlet for this purpose. This condenser converts the steam to water, which is to be collected and weighed over time. Steam bleeds into the condenser after passing through the jacket. Figure 3.9 below shows the condenser attached to steam outlet.

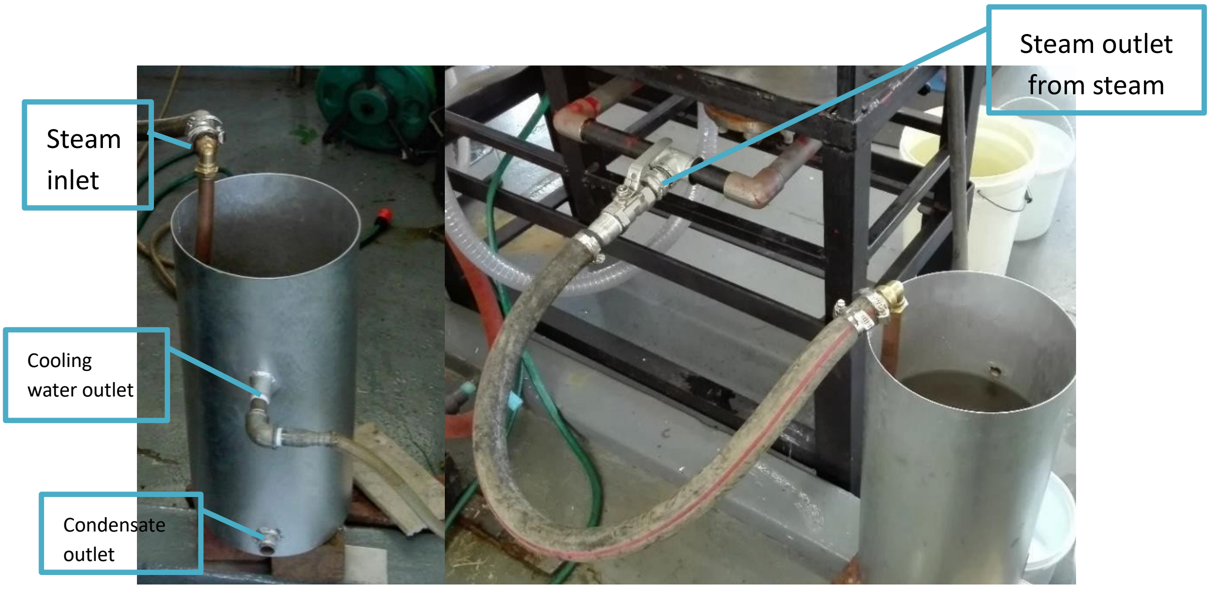

Figure 3.9: Steam side condenser

From the initial calibration of the equipment, it was noted that the condensers on the steam and vapour side worked at different capacities, where the steam side condenser collected a much greater amount of water than the syrup side. This condenser measures the total steam passing through the system and not just the steam condensed by the boiling process. This could be an inefficiency in the syrup side condenser or linked to heat losses to the environment. To ensure vapour side condensate is not lost to the vacuum, a secondary condenser was installed in series with the primary condenser. Secondary condenser works by having condensate entering on the shell side with water entering on the tube side. Once condensed, the liquid moves to storage tank where it is weighed over time.

For the intake and removal of the testing material, there is a valve suction inlet hose allowing for controlled intake to the system, and a large butterfly valve at the base of the pan allowing striking of the pan once boiling is completed. Specific information about the vacuum pan is listed in the table 3.1.

Table 3.1: Table of vacuum pan properties

Vacuum pan information	Values
Vacuum Pan calandria size	850mm×100mm×100mm (l×w×w)
Downcomer pipe	65mm diameter. Length 850mm
Disengagement dimensions	300mm ID, 10mm thick walls, 500mm height
Sump Dimensions	300mm ID, 10mm thick walls, 100mm height
Visualisation pane	180mm×800mm, 10mm thick reinforced, tempered glass
Total volume of system	Approximately 30 litres
Max Vacuum Pressure	85-100kPa
Max Temperature requirements	70-100ºC depending on Brix
Starting Brix of samples	70%
Sample mass taken per period	120g

3.3.1 Vacuum Pan Pressure Calibration

When dealing with the boiling properties of massecuite, it was very important to be able to control the factors that can alter these properties. The research hypothesis is governed by the factors that affect boiling of massecuite and hard-to-boil massecuite.

$$\textbf{Massecuite boiling} \propto \left[\begin{array}{c}\textbf{Vacuum pressure}\\ \text{Boiling temperature}\\ \text{Change in rheological and chemical properties}\end{array}\right]$$

With vacuum pressure being an important factor, that dictates the results of the boiling research, it is important that the readings be as accurate as possible. During a standard run in a factory, massecuite would be maintained at a vacuum pressure of 80-85kPa over the period of boiling. Under the hypothesis of the thesis, it was necessary to ensure complete and total control of vacuum pressure over the boiling period.

Due to the limitations of the testing apparatus and the evolution of the experimentation corresponding to the hypothesis, it was required that the boiling be maintained at the highest vacuum that the system can maintain at the corresponding temperature.

For the pressure measurement portion of the data, the readings were taken from the two main pressure gauges attached to the rig. These pressure gauges are located at the top of the disengagement space on the vacuum pan as well as the top of the primary condenser. During a procedural test, it was noted that the gauges run at different vacuum pressures. This could be problematic for result validity and repeatability, therefore gauges needed to be tested against a control. This was done using a calibrated mercury manometer and testing against the two gauges using the setup seen in figure 3.10 and 3.11.

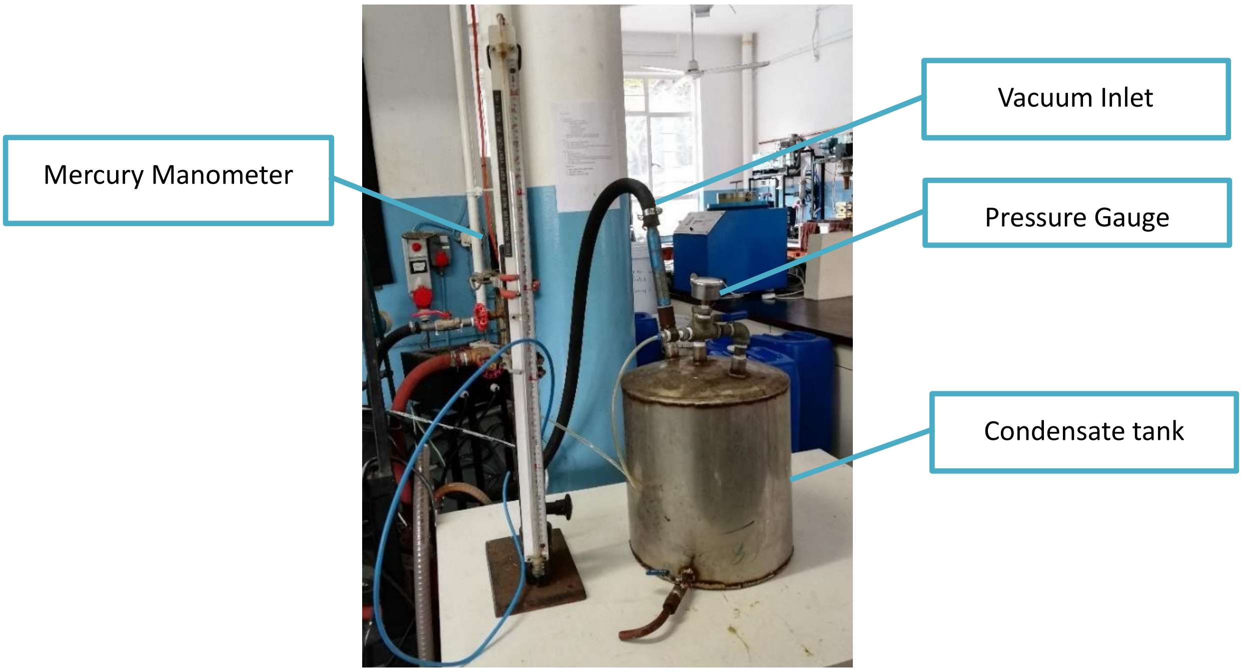

Figure 3.10: Pressure gauge test setup with manometer

Figure 3.11: Manometer (L) and pressure gauge (R)

The gauge and manometer were attached to the condensate collection tank to be able to run both instruments on the same vacuum line through an airtight and sealed system. The tank was disconnected and sealed from the rest of the rig before testing began. Using the bleed valve, pressure was adjusted and controlled to determine the variation between manometer and gauge.

The two gauges were calibrated using the testing setup, however only one gauge yielded results. The gauge used at the top of the vacuum pan was noted to be working incorrectly and all results received using this gauge were unusable. The second gauge on the primary condenser worked efficiently and was used for all tests thereafter.

By altering the gauge pressure using the bleed valve on the condensate tank and noting the manometer and gauge pressure, the graph of calibrated pressure versus gauge pressure was created. While the gauge reads in kPa, the manometer reads millimetres of mercury (mmHg), therefor the units were converted from kPa to mmHg, to create graph in figure 3.12. This graph was made using multiple points, tested in triplicates and can give a more precise representation of the pressure readings to be used for the final results.

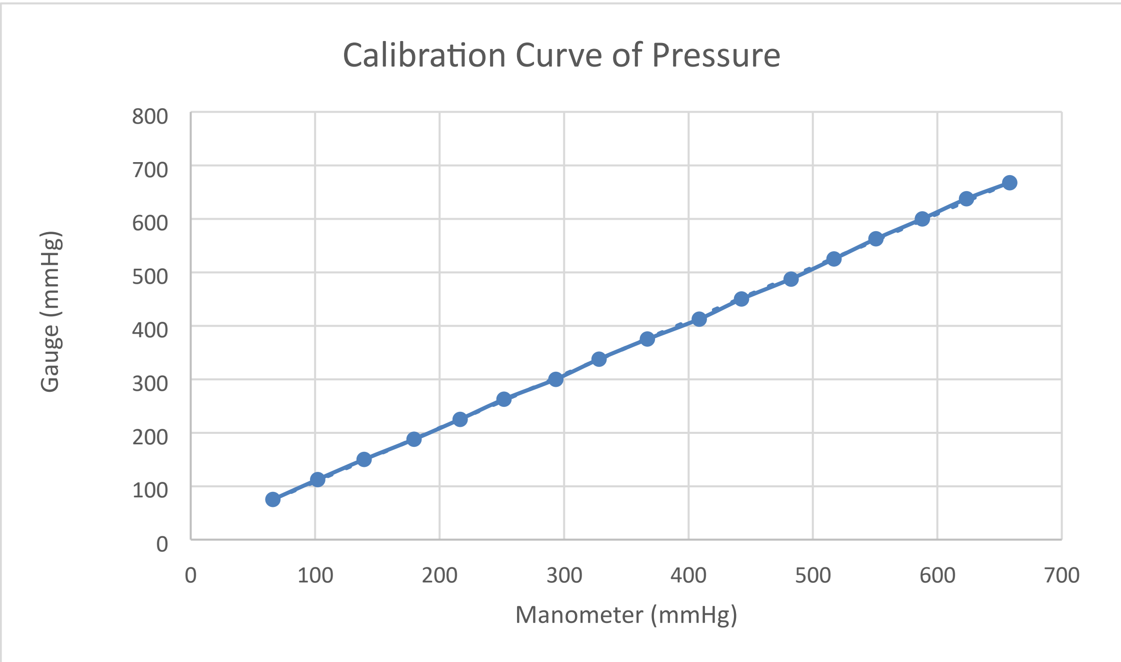

Figure 3.12: Graph of pressure measured by gauge vs pressure measured by manometer

The graph in figure 3.12 allows for the user to determine the percentage error between the true pressure and the readable gauge pressure. The standard deviation was determined for each value run in triplicate and averaged to get the standard deviation of 2.39mmHg. This means that the data points are closer to the mean

After looking at the graph's linear form, the error in the readings deviates by 5-10mmHg (0.7-1.3kPa) at any given point for pressures below approximately 480mmHg (approximately 65kPa). For values above this, there was a greater difference in the values ranging anywhere between 8-14mmHg. This implies that for higher values there is an error from 1.07-1.87kPa.

The line of best fit for the graph is represented by the dotted line found on figure 3.12 above. Using the line of best fit, the relationship between the gauge pressure and manometer readings was found to be the following:

$$P_{gauge} = P_{manometer} + 9{,}006$$

A gradient of 1 proves absolute proportionality across the readings. The pressure gauge at the top of the pan would no longer be used for any tests and the condenser gauge would provide all results.

3.3.2 Vacuum Pan Temperature Calibration

Massecuite boiling and pressure operate in proportion, as the vacuum pressure of the system determines the temperature at which boiling is reached. With regards to the theory of boiling, under negative pressure, massecuite can reach boiling at a reduced temperature. By doing so, the syrup will readily crystallise as water is removed over the boiling period as well as preventing burning.

$$\textbf{Massecuite boiling} \propto \left[\begin{array}{c}\text{Vacuum pressure}\\ \textbf{Boiling temperature}\\ \text{Rheological and chemical properties}\end{array}\right]$$

Massecuite boiling is governed by the boiling pressure which determines the boiling point of the syrup. For the measurement of temperature, the system was equipped with a temperature probe (thermocouple) located at the back in the sump of the vacuum pan. This probe measures the temperature of the liquid in the sump and down-comer pipe due to circulation. While this adequately measures these areas, it does not accurately represent the boiling temperature, a highly important factor in the hypothesis.

The temperature of the front tube where boiling was located would need to be measured as part of the experimental data. Due to the experimental conditions, system design and limited budget and time, permanent alterations were not possible to insert a probe into the calandria however the sample port allowed for alterations to the pipe components to insert a temperature probe capable of reaching into the centre of the pipe.

The chosen probe was a long J-type thermocouple that works by being immersed into the substance it was measuring. Temperature calibration for the thermocouple was done by testing the probe against one that was certified in the SMRI analytical lab using boiling water to determine temperature differences before installing into system as seen in figure 3.13. When tested, the certified probe read the same as the thermocouple used for testing validating the results received. The thermocouple inserted is able to reach into the bottom and centre-front of the boiling pipe.

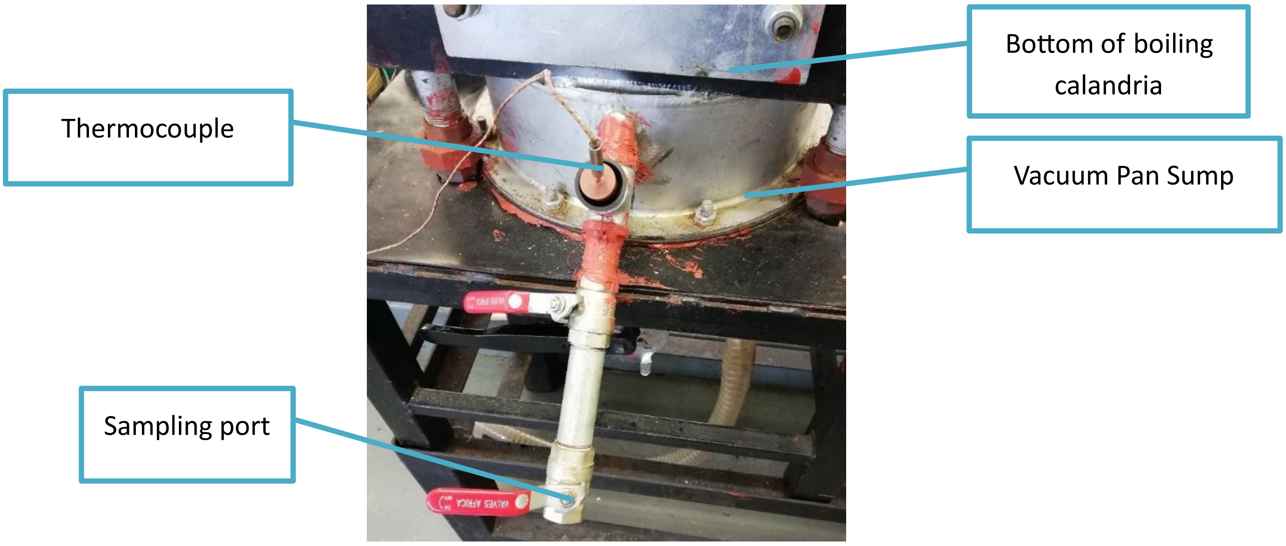

Figure 3.13: Sample port and temperature probe setup

When it came to taking temperature probe readings, it was necessary to allow a few seconds of stabilisation as temperature fluctuated at a given time. This was probably due to the passing of bubbles within the boiling calandria. This is important to note with any future data recording using the probe.

When looking at the sump and probe temperature, a graph was plotted to determine a relationship and yielded figure 3.14. While unnecessary, it was interesting to note the temperature difference between the two pipe areas.

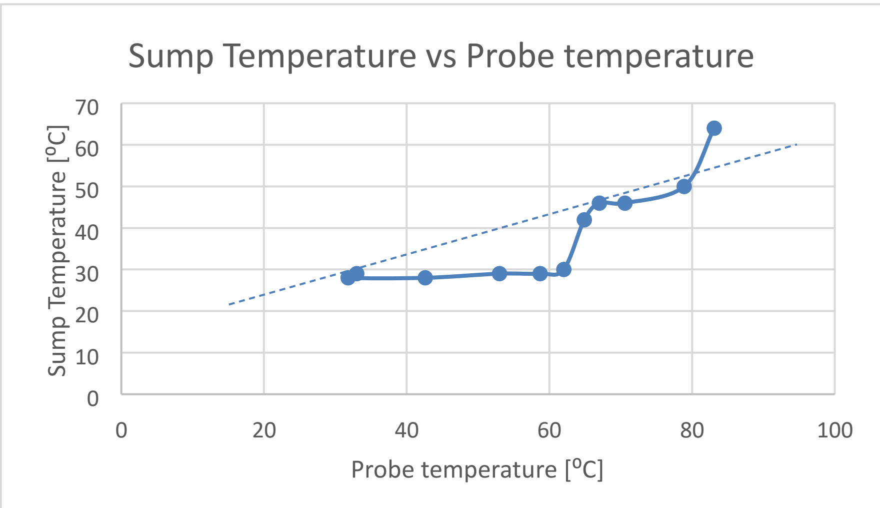

Figure 3.14: Graph of sump temperature probe vs front boiling pipe probe

The downcomer and sump temperature is dependent on the boiling and circulation occuring due to the heating of the calandria (front boiling tube). This relationship however showed that while the front continues to boil, the sump tends to remain at a given temperature for a period before increasing and then stabilising again. The stabilisation period decreases over the time and eventually steps up over shorter periods of time. This could indicate the circulation of the pan and tell the operator how well the pan syrup is circulating over the boiling period. It can be assumed that over the boiling period, as system reaches the conditions for boiling, the circulation will increase until eventaully the temperature will be the same throughout.

Use of the two temperature measuring devices inserted directly into the pan was deemed adequate in measuring the range of temperatures experienced duirng boiling. The results obtained from these devices were in the final results

3.3.3 Pressure and Steam leakage testing

Pressure within a vacuum pan is an important factor affecting pan boiling behaviour. This pressurised system needs to be checked for air pressure leakages as a safety precaution. Air bubbles in the boiling calandria could also interfere with normal boiling regime. Testing was done under standard boiling conditions that the system can reach (namely 50-60kPa, 80-90ºC) and vacuum pipes, steam pipes, vacuum pan joints and valves were checked to pinpoint areas of leakage.

When it comes to working with pressurised equipment, all areas that may be disassembled require adequate sealing to prevent loss of pressure during the run of the equipment. Leaks along steam side is a safety risk to any persons running the apparatus. Upon running the test rig, a number of different leakages were found that required further dissassembly and the addition of a sealing material to keep it from disrupting the pressure readings.

Areas of concern for air leaks found during runs prior to this research topic were:

- Massecuite inlet pipe valve
- Stirrer inlet to bottom area of vacuum pan
- Steam outlet pipes

All joints of issue were sealed with either gasket maker, thread tape or a combination of heat resistant, rubber gaskets that were sealed down with gasket maker. Air leakages on massecuite inlet pipe valve was handled by immersing pipe into a bucket filled with cold water to seal any leaks when tests are to be run. All noted air leakages that could be sealed, were appropriately sealed.

Steam heating condition properties are important to noting boiling behaviour. To determine the rate of evaporation can be done through determination of steam flow rate. To do this, a condenser was built and attached to the steam outlet to see if theory is consistent with reality and to determine if the condenser on the syrup side is working correctly and condensing all the vapour being evaporated.

Assuming heating is steady state, the total condensate formed on the syrup side should equal the total condensate formed on the steam side to show heat transfer being constant and equal. However, during the run it was noted that unequal quantities of condensate was formed in each condenser.

The amount of steam formed from the steam side was sometimes double, almost triple the amount of condensate formed on the syrup side. This uneven heating could be due to several reasons, namely:

- Heat losses to the surrounding environment as temperature between steam and massecuite is too small while environmental temperature difference is larger
- Condenser on syrup side may not entirely condense vapour and vapour is removed by vacuum pump

While a correlation could not be determined between the two condensate measurements, it was still noted due to the importance of the values. Using the steam condensate, the user can determine the consistency of the flow through the system, not the steam condensed to drive the evaporation. The differences found between the steam condensate and the vapour condensate indicates that not all the steam is consumed by the evaporation process. It is not a deviation from the one-to-one evaporation rule of thumb. Both of which are fundamentally important for the research hypothesis.

3.4 Analytical Instrumentation

The use of the NIRS and rheometer will be used alongside the vacuum pan, to produce an accurate reading of the chemical properties of the samples. These samples readings will be compared to locate the differences in HTB and standard samples. The equipment required calibration specific to the NIRS and rheometer.

3.4.1 Near Infra-Red Spectroscopy (NIRS)

Near Infra-Red Spectroscopy (NIRS) in the field of sugar manufacturing was developed for rapid routine analyses of factory products, to monitor sugar processes more effectively, while still maintain accuracy of the results (Gounden and Walthew, 2018). With there being great limitations in testing, using common technologies that are often time consuming, operator-dependent and requiring hazardous reagents, the move to using more precise and reliable systems for determining substance properties have become more important.

The NIRS testing system works using visible and near-infrared spectroscopy to measure sugar content in many applications apart from sugar production. Infrared light is passed through the diluted sample where there is partial absorption of light and reflectance or absorption is measured (Jaywant, Singh and

Arif, 2022). This method of testing is done within a darkly coloured box as it requires light sealing in order to prevent the interactance of light that can create problems with measurement.

NIRS testing methods have been developed by the SMRI such that important properties in juices, syrups, molasses and massecuites. NIRS can determine the Pol, Brix, Dry solids, Sucrose, Glucose, Fructose, Colour and pH levels of these substances.

For the testing with NIRS, final molasses samples are first diluted to a 10% ratio, based off the calculations used within the system. This diluted sample is then injected into the optical transmission cell, called a cuvette that is inserted into the system. Infrared light waves are passed through the transmission cell to a detector on the opposite side. The detector relays the level of absorption of the infrared waves through the sample, to the Toolbox, where properties are calculated according to predetermined equations and absorption properties. This process is described in figure 3.15.

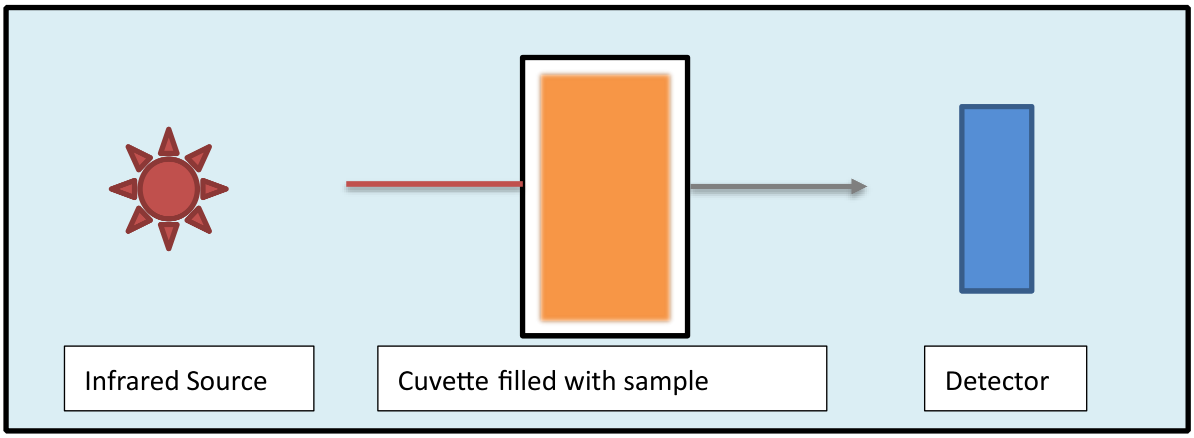

Figure 3.15: How NIRS works using transmission

The reliability of using a NIRS versus refractometric testers can be determined based on experimental accuracy and reliability. Brixmeters, a form of portable refractometers, are used to quickly test °Brix by measuring the refractive index (RI) of the liquid where RI is a ratio of the speed of light in a vacuum to the speed of light within the medium being tested (Jaywant, Singh and Arif, 2022). The brixmeter being used to check the samples retrieved during boiling was an Atago 3810 (PAL-3) capable of measuring 0-93% Brix, with a ±0.1% accuracy (Atago, 2022). This brixmeter however had errors forming as a result of surrounding light sources affecting the measurements or not measuring accurately at higher °Brix thereby not accurately capturing dry solid content.

NIR methods use visible and NIR range of the electromagnetic spectrum within a box preventing foreign light interactance, along with uniformity in sample testing through accurate dilution allowing for less error in results. The NIRS tool used at the SMRI is a Bruker FT NIR spectrometer that has been refined and tested to yield an excellent accuracy. The disadvantages of NIRS comes as a result of requiring new calibration models and equations depending on what is being tested. As the NIR spectrometer being used was specifically programmed with equations and calibrations based off sugar testing, the error margin lies within a 0.01% region. The work completed by the SMRI has managed to yield approved methods of testing for A,B,C massecuite, A, B, C molasses and clear juice samples for testing with a standard error prediction of ± 0.17 for testing brix of C-massecuites which are of particular interest to this study(Simpson and Naidoo, 2010).

3.4.2 Rheometer

Rheometers use a rotating or oscillating spindle piece to determine the rheological properties of a substance, through applied forces. The spindle type and movement determine the test being run and can determine various properties of a substance. For the testing in this dissertation, an AntonPaar MCR 302Modular Compact Rheometer will be used.

The MCR 302 rheometer works by using a low-friction air bearing and electronically commutated (EC) motor with integrated normal force sensors and high-resolution optical encoder, making up the main controls of the system (Anton-Paar, 2020). Figure 3.16 below shows the system. The system is able to take accurate and precise measurements using the TruRate and TruStrain functions for rotation and oscillation testing (Anton-Paar, 2020). This adaptive controller uses TruRate function for rotation and step strain to obtain fast accurate strain control under real time conditions. TruStrain function used for oscillation, guarantees precise measurement at low torque (Anton-Paar, 2020). Figure 3.16 and 3.17 shows the rheometer setup.

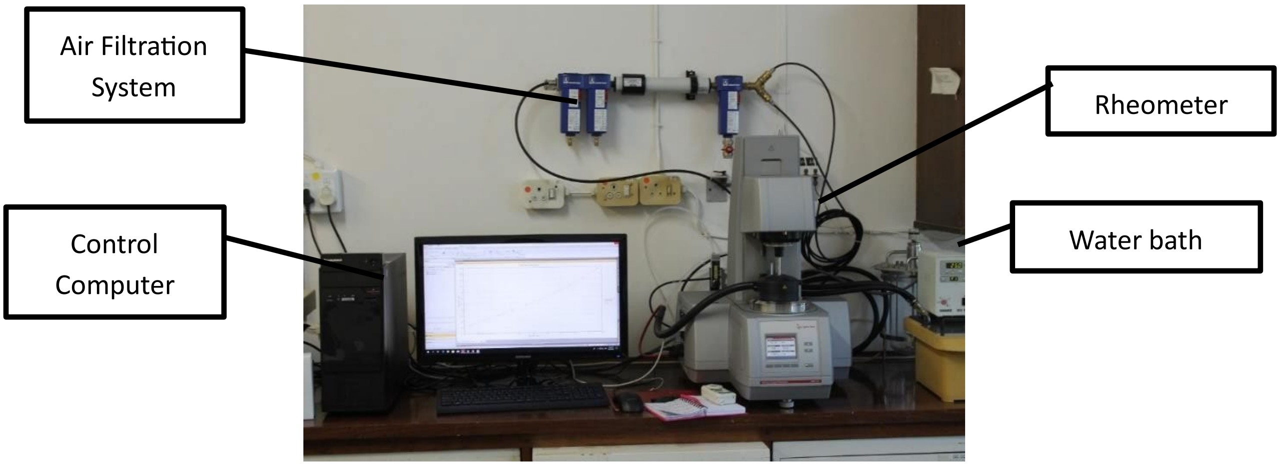

Figure 3.16: Rheometer Setup

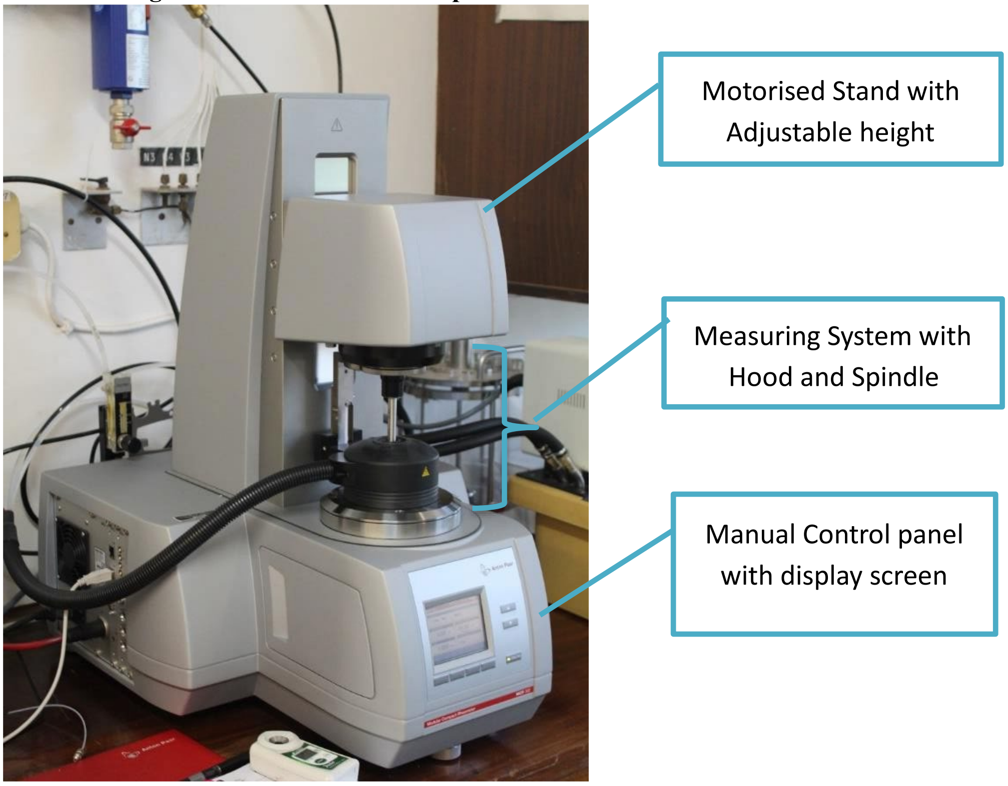

Figure 3.17: AntonPaar MCR 302 Rheometer

With regards to this research topic, the rheometer is an important apparatus that is capable of distinguishing viscoelastic properties between the different samples at their given Brixes. It is known that HTB massecuite has a key characteristic dealing with the viscoelastic changes due to polysaccharide intermolecular forces. The rheometer allows for testing of these samples, using the appropriate predetermined programmes, to determine rheological properties of said samples.

Rheometers work by applying a shear force, using a spindle, to the sample being tested in the form of rotational or oscillatory movements. Depending on the type of test selected, the spindle will begin rotating or oscillating at its final position, where it applies a shear force to the sample. Using derivative formulae of shear stress, deformation behaviour and rheological parameters, the machine can calculate viscoelastic properties.

Standard tests are based off a two-plate model where sample is sheared while sandwiched between two plates, with a moving upper plate and stationary lower plate (Anton-Paar, 2020). With known spindle geometry the rheometer can determine the rate of shear experienced by a sample. As the spindle plate moves in a “shearing” motion against a sample loaded onto the lower plate, the system begins to measure the movement and deformation of the substance under the spindle to determine properties such as viscosity and elasticity. The shape and size of the spindle affects the rate of movement and deformation. Figure 3.18 describes this model.

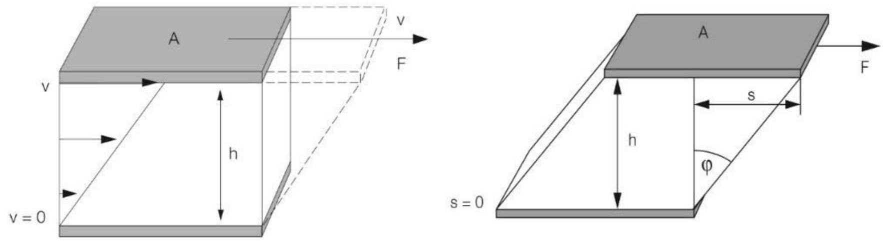

Figure 3.18: Cross section of a uniform area beneath the spindle showing movement under shear (Anton Paar, 2020)

Conical spindles are angled creating a large shear area. This is commonly used for low viscosity samples i.e., samples that flow easily such as oils, lotions, sauces etc. Higher viscosity samples are tested on plates with smaller areas and flat surface areas. Parallel plate measuring systems can be used for various samples, namely: low-viscosity liquids, polymeric samples, viscoelastic materials and paste like samples. Parallel plates can apply a smaller even shear with large gap size making it suitable for many different sample viscosities. Samples are deformed homogeneously throughout the entire shear gap which is better for stiff and particulate substances (massecuites being both).

With regards to HTB substances, a small diameter, parallel plate was used. Parallel plates are used to test varieties of different samples and can test a wide range of viscosities. The small plate diameter uses less sample even with increased gap size. Using the parallel plate for all samples will ensure same conditions across tests and is able to be used for large variety of viscoelastic properties that would be noted under HTB samples.

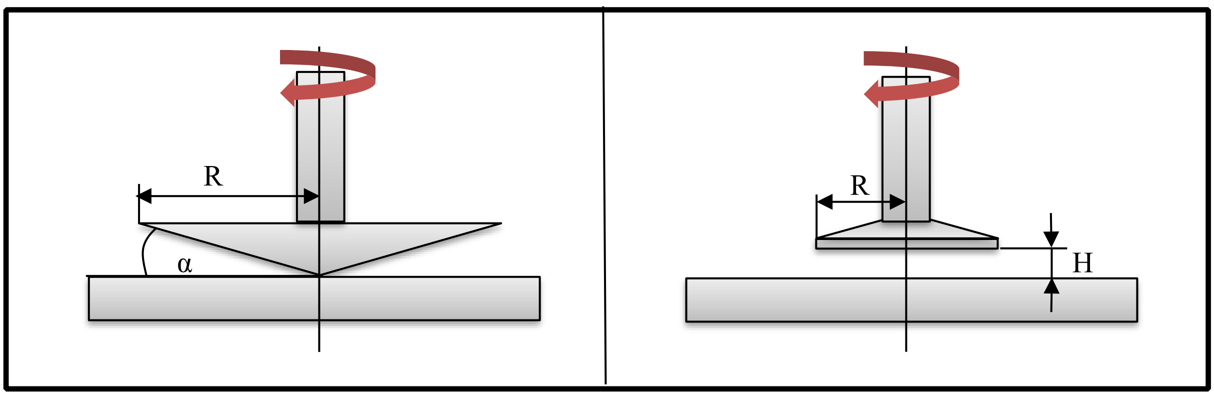

Figure 3.19: Different spindle types used for rheology

Depending on the type of test applied, different sample characteristics can be determined. Rotational tests apply a single direction movement of the spindle and are used to determine the viscosity of samples. Rotational tests create uniformity across samples and are used to simulate force-dependent applications and yield results in the form of flow curves or viscosity curves.

Oscillatory tests perform frequency scans, run by rapid backward and forward motions used to determine viscoelastic properties that are more distinct under:

1. Faster movements and higher oscillation frequency implying higher deformation rate or shear rate
2. Lower temperatures where molecular network will be stiffer and less flexible(Anton Paar, 2020)

Oscillatory tests and rotational tests work under the same theory of the two-plate model. However oscillatory tests are pre-set in the form of a sine curve and is determined by amplitude of movement (Mezger, 2006; Anton Paar, 2020).

The tests that can be run using the rheometer are stored in the application called RheoCompass. This programme allows users to select from a wide variety of tests that are alterable to suit the testing requirements. This rheometer is capable of heating and cooling of samples using liquid and Peltier temperature control systems (AntonPaar, 2020b). Liquid temperature control maintains constant heating and ensures uniform temperature distribution by drawing water into the system to heat and cool the testing plate quickly. Peltier temperature control creates ideal testing conditions using a temperaturecontrolled hood that prevents evaporation by maintaining saturated atmosphere within the hood minimizing gas flow. This reduces temperature gradient, blocks environmental influence and improves temperature distribution.

Figure 3.20: Spindle of Rheometer in loading position (L) and loaded position with hood (R)

3.4.2.1 Rheometer Controls

Rheological properties of massecuite due to the increased levels of causative polysaccharides was one of the main factors affecting the boiling within vacuum pans. Under the hypothesis, the chemical nature of the massecuite influences the rheological properties and therefore the massecuite boiling conditions. Due to the nature of HTB samples being unpredictable and determined by environmental conditions and period of deterioration, the chemical constituents are not easily mimicable. This led the research toward using samples that were predetermined by factories as being HTB based off the experience and knowledge of the operators.

$$\textbf{Massecuite boiling} \propto \left[\begin{matrix} \text{Vacuum pressure} \\ \text{Boiling temperature} \\ \textbf{Rheological and chemical properties} \end{matrix} \right]$$

Based off the modelling done by MISG previously discussed, the viscoelastic properties of massecuite determines the boiling and therefore, the crystallisation capabilities of the syrup. This must be tested and documented to the best of the rheometer's abilities.

After many tests with different samples of varying viscosities, a rheometer's motor may begin to run outside of the normally acceptable range of values. This could be due to "sticking" of high viscosity samples that can cause motor to overcompensate and run at torques outside the allowable range. Rheometers require adjustment to ensure machine motor runs correctly over the course of testing. `

To do this, a motor check was required. This is a system self-check that only requires system start up and test to be administered. Generally, a motor check needs to be done every 6 months to ensure that the motor runs smoothly, and air bearings are working within the correct limits of pressure and torque. When running a motor check, it is helpful to prevent sudden air pressure changes by remaining still and shutting any doors or windows during a run.

This test is run using a standard test programmed by AntonPaar for the rig. This test runs automatically by first running a torque check that adjusts to within a specific range and then an air check to test the motors capabilities and determine if there are any leaks. Below is a normal report that is created from the motor check. This report allows the operator the chance to analyse motor check to ensure it was run and adjusted correctly.

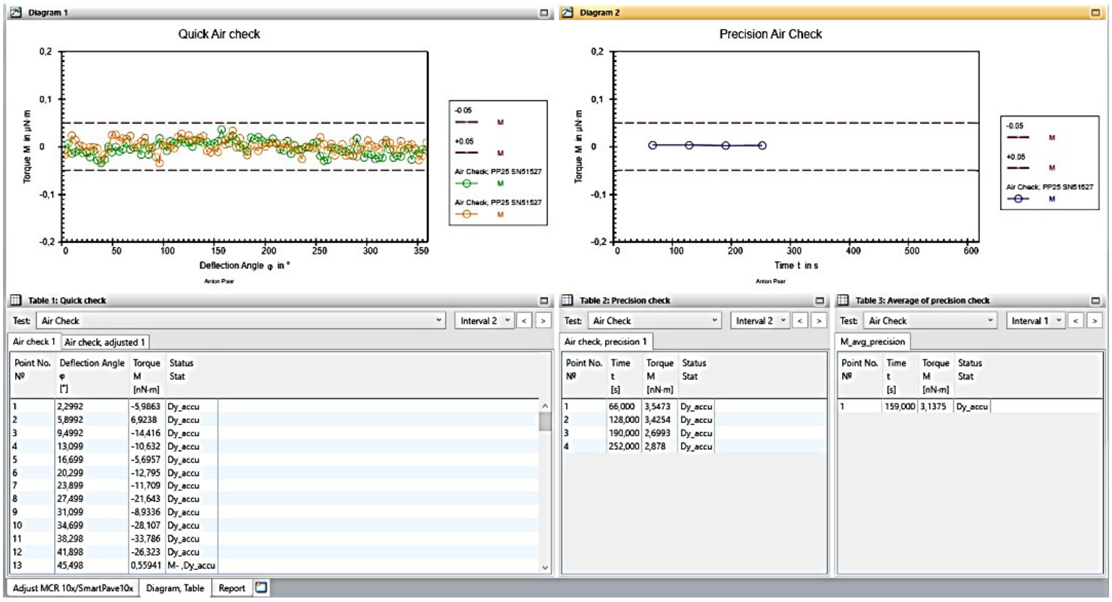

Figure 3.21: Air Check test results

Figure 3.21 depicting the air check, shows the quick initial check performed by the system where motor torque is tested against various deflection angles.. The test runs and the results compared to correct the motor movement. Initial test shows a lot of variation shown in green. After this was run, machine calculates differences and automatically corrects and this can be seen in the yellow. To test the correction done by the machine, a time vs torque test is run to look at the consistency of the torque shown on the right.

After a motor check and analysing test report, it could be assumed that the machine is running correctly. From here, it was determined if the standard tests are working correctly. The rig comes with preprogrammed tests to provide the user with a baseline of tests. These tests can be used for any sample. The test shown in figure 3.22 depicts the standard results received when a motor check is run.

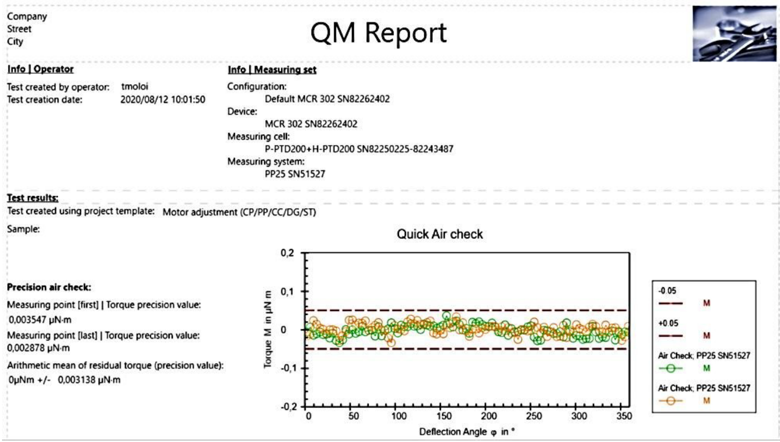

Figure 3.22: Air check report

Here the report will show various documented information such as which device was configured, when the test was completed, the operator and the results received. This allows the operator to better keep track of the machines general "health" and the normal system conditions.

To check the validity of the tests, a controlled sample is used. These are standardised samples that have ready known properties provided by the company of manufacture. For the task of calibration, a Wacker fluid was used. This is a control substance created to have a specific set of properties. This fluid provides the user with viscosity and cross over point values. When the appropriate tests are run, the results should yield these values and validate the machines capability. These tests also act as good educational samples that will help learn and understand the equipment.

Figure 3.23: Control Test Samples

Using standard flow curves, frequency sweeps and amplitude sweeps along with the Wacker substance, the machines capabilities were validated. An example of tests run for calibration is given below: a control sample listed a viscosity and cross over point as listed in the table below. To test the substance, the rheometer was run with loaded sample using a frequency sweep. When run over a wide range for angular frequency, this frequency sweep will yield a cross over point as seen in figure 3.24 below.

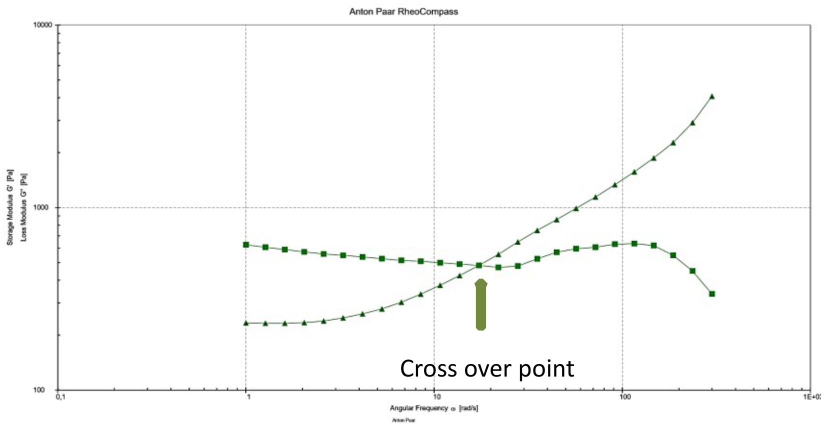

Figure 3.24: Cross over point frequency sweep

Table 3.2: Table of Cross over point values for controlled substance

Cross over point	Value
Angular Frequency	17,3 rad/s
Modulus value	482 Pa

The results using these controlled samples yielded the same results as given by the manufacturers ensuring that the soundness of tests remains constant. To ensure the best run conditions, the rheometer was also maintained by checking motors and circulators. Using the standard tests programmed onto the rheometer the operator may determine the validity of the machines results overall.

3.5 Experimental Framework

The aim of this experimentation was to **determine the characteristic and rheological changes that occur when massecuite samples have Hard-To-Boil properties.** This was done by boiling samples using the vacuum pan testing rig capable of visually documenting boiling conditions, taking samples during intervals to monitor the boiling conditions and using these samples for rheological testing to distinguish characteristics between normal and HTB samples.

It was decided that final molasses would be used to negate the crystal Brix effect. Final molasses would include the least amount crystal content while also having the highest concentration of non-sucrose solids. HTB final molasses would best exhibit the flow properties normally, due to gums. Initial stages of testing done by dosing syrups to make synthetic massecuites capable of mimicking factory massecuite. However, this was not practical and was abondoned. Naturally occurring molasses with HTB properties that have occurred naturally will be used for experimentation.

Testing has to be completed for both normal boiling and HTB samples under the same testing conditions. It was required that vacuum pan boiling be completed under constant temperature and pressure conditions such that the boiling can be visualised and reach a final Brix under no additional heating and pressure changes. During these tests, samples would be taken over time and boiling conditions documented to look at the relationship between various properties. The samples taken from these tests would be analysedrheologically at the same Brix values to document the characteristic changes between sample types.

Sample preparation required that molasses, received from factories, be diluted to the starting brix of 70Bx before testing began. To do this, dry solids balance equation is used ($m_1 b_1 = m_2 b_2$). The samples were batch prepared and refrigerated before tests to prevent any deterioration effects that could occur. Methods of testing for NIRS are omitted from this section since there is only one operating method possible that can be used. This method is documented in appendix C.

3.5.1 Vacuum pan testing procedure

In order to obtain the results correlating to the hypothesis, the vacuum pan test rig would need to be run under constant boiling conditions. The maximum vacuum pressure and corresponding temperature, determined by boiling point elevation theory, for that pressure that the rig can run at without entrainment while also using the most amount of sample that can be held without entrainment. The boiling temperature was determined by the pressure of the vacuum as well as the hydrostatic head of the tube. The values chosen for testing was determined by the maximum allowable conditions of the vacuum pan in order to prevent entrainment and/or other issues.

Table 3.3: Conditions for boiling

Condition	**Value**
Vacuum Pressure	50kPa Vacuum
Temperature of boiling	+90ºC
Hydrostatic head	+20cm on sight glass

For the experimentation within the vacuum pan, essential equipment requires warm up period. Following the standard start up, the following machines were prepped: boiler system, vacuum pump and vacuum pan. The steps for the boiler, vacuum pump and vacuum pan will not be discussed as the start-up is standard for the equipment and only requires a warmup period before boiling begins. Vacuum pan standard start up and shutdown is found in appendix C. This section looks at how samples were prepared and then tested.

3.5.1.1 Vacuum Pan Procedural Steps

1. Switch on boiler and vacuum pump using the standard start up procedures and allow to warm up

2. Connect condensers to taps and allow condensers to fill in preparation of boiling

3. Open the vacuum port that connects to the system setup

4. Open the bleed valve incrementally and adjust to 50kPa vacuum-allow the pressure to stabilise 5. Using the inlet hose, suction diluted molasses sample into the rig:

    ○ Fill sample to

        - 23cm on front pane of glass for normal samples
        - 48cm on front pane of glass for HTB samples

6. Turn on the motor for the stirrer

7. Check that all parts on the stirrer are secure
8. Open the steam valve to begin heating
9. Boiler needs to be left to bleed to allow water left in pipes from previous boiler usage, this water is a red brown colour
10. Let the steam valve bleed until water turns clear- this marks the beginning of the boiling test

    - Steam valve needs to stay open approximately an eighth ($1/8$) to achieve boiling temperature at 95ºC

11. During boiling, maintain vacuum pressure at set 50kPa vacuum pressure
12. Steam should not be altered
13. Should vacuum increase or decrease, alter the bleed valve accordingly to maintain the pressure
14. At 15-minute intervals the following must be done

    - Document the pressure at the given time ○ Document the temperature at the given time ○ Retrieve sample from vacuum pan

        - Open the sample port two times and dump the collected portion
        - Open the sample port three times to collect 100grams of sample ○ Document the mass of condensate on the steam side ○ Document the mass of condensate on the syrup side ○ Photograph boiling

Boiling time is determined by the time taken for evaporation rate to plateau-monitor condensate on syrup side- when condensate does not change for 15 minutes (time until next documentation period) then begin system shut down

For the samples, it was required that two main things be kept constant, that was the steam inlet flow rate as well as the vacuum pressure. By employing a constant pressure, this ensures that a constant boiling temperature would be reached.

3.5.2 Rheometer

For rheological testing the following objectives needed to be met:

- Determination of the changes in viscosity effects due to HTB phenomenon

- Finding the viscoelasticity of the mixture and the tendency of the samples to be more viscoelastic

For the experimentation required, samples were collected over set intervals from the vacuum pan at differing Brixes. These samples were tested using NIRS to determine basic properties, focusing on Brix. Final molasses Brixes at starting, middle and end points of both normal and HTB samples were tested with rheometer to form comparable series of curves at the same Brixes to compare results.

To test the required objectives, the viscosity and viscoelasticity of the samples needed to be tested. Flow curves, a rotational form of testing, are used to determine the shear viscosity of a sample to determine the zero viscosity of the samples at rest. For viscoelasticity of samples, the testing focuses on oscillatory tests and specifically amplitude and frequency sweeps.

Table 3.4: Rheological tests, uses and results received

Type of Rheology Test	**What kind of information can be obtained**	**What graphs are obtained**
Flow Curve	Determining the viscoelastic properties of the mixture Used for QC profiling and benchmarking from flow curves, able to determine the yield point of the sample. Able to determine the flowability of the sample to find out how to properly transport it	-Viscosity vs shear rate -Shear stress vs shear rate
Amplitude sweeps	Determines the LVER- relationship between stress and strain at any given time Able to determine the yield stress of the sample able to determine the sample stability, shelf life, structural strength	-Moduli vs shear strain -moduli vs shear stress

Frequency Sweeps	Able to determine a change of nature of samples at a given shear rate-determined by a cross-over point determine impact behaviour, dampening and storage stability	-Moduli vs angular frequency -complex viscosity vs angular frequency

3.5.2.1 Flow curve

Flow curves are graphic results representing the shear viscosity of the samples and changes that occur due to changing shear rates and shear stresses. The flow curves are used to determine the basic shear viscosity in order to find out the prevalent changes in properties. To test the shear viscosity, the standard flow curve test provided by RheoCompass was edited to suit the requirements of the tests. Figure 3.25 shows the testing procedure used for testing the flow curves of molasses.

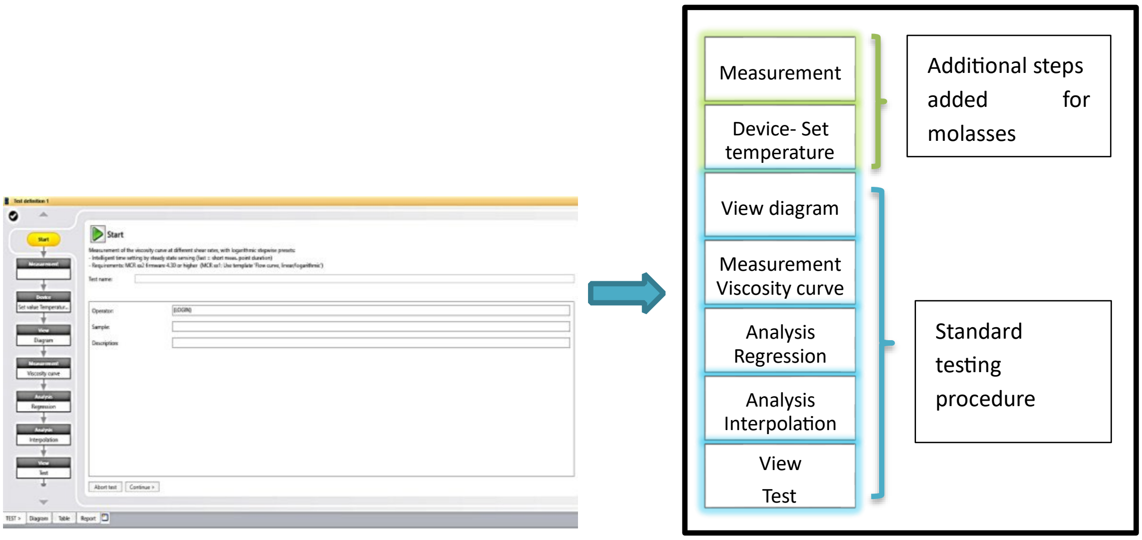

Figure 3.25: Flow curve testing procedure

Flow curve testing worked using a series of steps decided by the testing application. The test was altered to suit the purposes of the experimentation. Logically, sample will not settle immediately onto the heating plate and if air bubbles are present will affect the testing result. For this purpose, a settling period was required that acts by applying a very small shear rate that settles the sample. Then an added temperature device was added, where the rheometer would heat the sample to the designated temperature.

Thereafter the system would run the viscosity curve measurements that tests the shear strain vs shear viscosity and shear stress. Once this is completed, the system is able to run a regression curve that ultimately checks the values that are received from the measurement test to determine accuracy of results. The testing conditions applied after the settling period are the standard flow curve testing devices that apply a range of shear rates in order to determine the shear stress and viscosity. The conditions applied for testing is tabulated in table 3.5.

Table 3.5: Properties applied for flow curves

Properties	**Values/descriptions**
Number of points	50
Duration	Steady State
Timeout	30s
Shear rate application	
Profile	Ramp Logarithmic
Initial	0,01 s^{-1}
Final	100 s_{-1}

3.5.2.2 Sweeps

It was brought forward by Fowkes et al. (2018) that the HTB phenomenon occurs due to viscoelastic changes. This property type shows a complex shear modulus, G^*, that defines fluid movement of these samples and is made up of a viscous and elastic portion. The storage modulus represents the elastic portion and is represented as G’. The loss modulus represents the viscous portion and is represented as G”. These respectively describe the stored deformation energy and deformation energy lost through internal friction. If G' > G" the sample is considered a viscoelastic solid. If G" > G' the sample is considered a viscoelastic liquid. To determine these properties, an amplitude and frequency sweep is required.

The amplitude sweep tests are applied in order to determine the linear viscoelastic range (LVER) of samples. This range describes the area of testing within which the samples can be run without sample deformation. This prevents the destruction of the samples internal structure that could result in false graphs with incorrect plots leading to invalid observations. The figure shows the testing procedure that is run by the rheometer to receive this range.

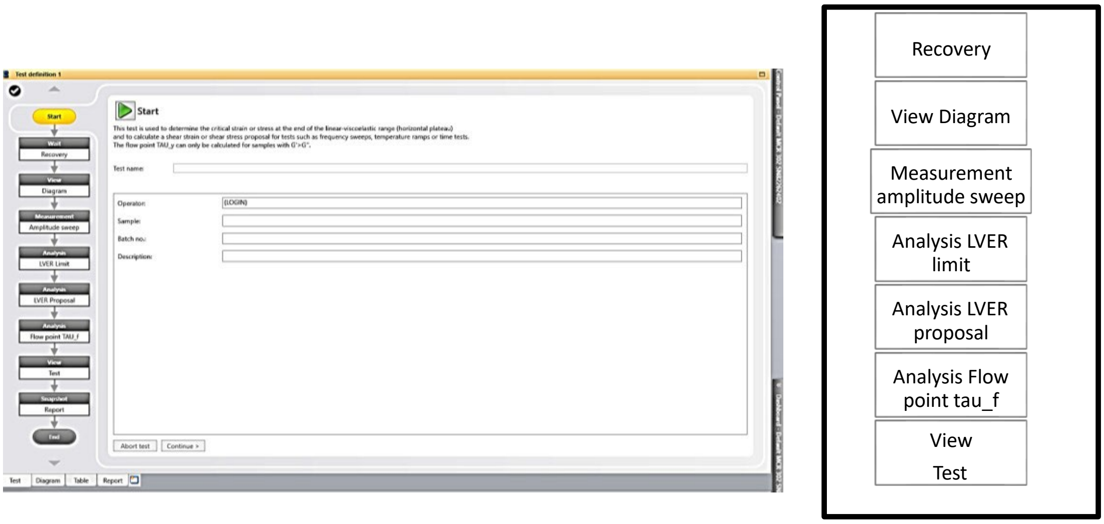

Figure 3.26: Amplitude sweep process

The measurement system in place has a recovery period to start to let the sample structure return to original properties. The measurement process for determining the amplitude sweep values is done using oscillatory tests to determine the storage and loss moduli. Storage modulus measures the total energy required to deform a sample and move it while the loss modulus measures the substances resistance to deformation and therefore the total energy lost during the testing process. These proportions represent the elastic and viscous portion of the mixture: the elastic portion being able to deform and return to its original state being the storage modulus while the liquid having the inability to expand and having a resistance to action on it represents the loss modulus. This is important in determining the viscoelasticity of the samples in relation to the hypothesis and is done by applying shear stress and strain over time to determine the samples' ability to deform and resistance to movement. The conditions for testing are tabulated in table 3.6 for easy viewing.

Table 3.6: Conditions for amplitude sweeps

Properties	**Value/description**
Number	25
Duration	Time set by machine
Shear strain (oscillating)	
Profile	Ramp Logarithmic
Initial	0,01%
final	100%

Angular Frequency	
Profile	Constant
Value	$10\ s^{-1}$

The frequency sweep is used to determine the time-dependent properties of a substance that is run in a non-destructive deformation range. This non-deformation range is achieved by first testing using an amplitude sweep for each sample to determine the LVER where the sample can be run safely. The frequency sweep test is also applied in order to determine the effect of shear stress on the storage and loss moduli.

This test was necessary in helping create the link of viscoelasticity to the properties noted during vacuum pan boiling. It is possible to determine the changes in viscous and elastic properties over a changing angular frequency. Frequency sweep are done using an oscillatory movement and so this angular frequency is representative of a shear being applied using this oscillation. The determination of the moduli will determine the predominant viscoelastic property.

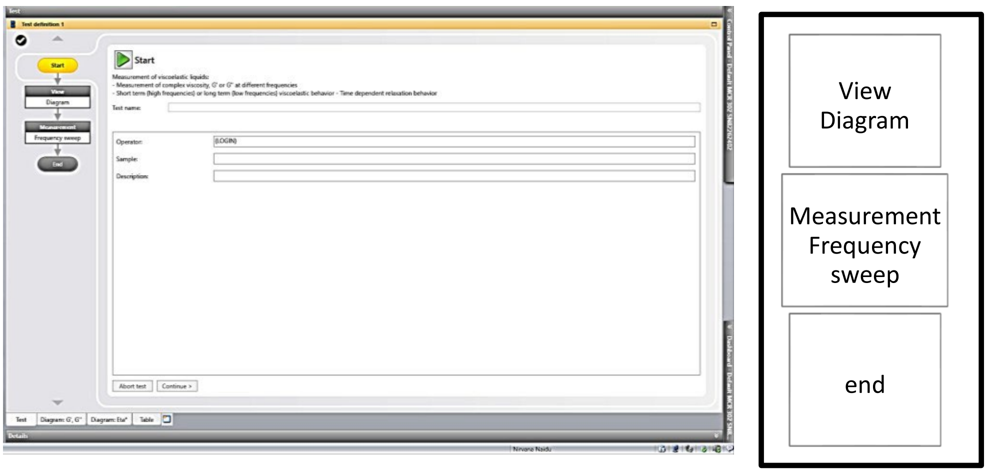

Figure 3.27: Frequency sweep test

The conditions that are chosen for the frequency sweeps is based off the amplitude sweep results that determine the range in which shear strain can be run. The conditions used for frequency sweep tests is shown below.

Table 3.7: Frequency sweep conditions

Properties	Value/description

Number	16
Duration	Time set by machine
Shear strain (oscillating)	
Profile	Ramp Logarithmic
Value	5%
Angular Frequency	
Profile	Ramp Log
Initial	100 rad/s
Final	0,1 rad/s

3.6 Conclusion

This section gives a detailed look into the various pieces of equipment that were used to obtain the experimental results of this thesis. The importance of each mechanism and their basic principles were discussed. The baseline of all tests, were to be done, in the vacuum pan test rig and samples collected from those tests were run using the NIRS and rheometer to determine substance properties in alignment with the hypothesis of this work. Rheometer would define a link between sample types, noted boiling changes. The experimental procedures required in order to complete these tests were discussed with regards to the relative equipment. The proposed experimentation and equipment setup simulated factory boiling conditions. Phase one of the experimentation design was done using the vacuum pan testing rig that would allow constant monitoring of boiling conditions and visual assessment and documentation of internal ebullition over the boiling period. Conditions for boiling would be maintained at steady state values in order to ensure same conditions being tested among sample types. Using rates of condensation on this rig, the result would theoretically yield notable changes in heat transfer between normal and HTB massecuite samples. Phase two of testing looked toward two pieces of equipment, namely the NIRS and rheometer where basic chemical constituents of samples would be tested before plotting families of curves across sample Brixes and types in order to determine the differences between HTB massecuite and normal samples. These differences would be noted by differing viscosity and deformation values.

Chapter 4

Experimental Testing & Troubleshooting

4.1 Introduction

In order to **investigate the mechanism of poor boiling characteristics due to the presence of polysaccharides**, samples of material that had similar boiling characteristics to normal and HTB massecuites were required. Over this period, there were three distinct testing phases where three different substances were tested. These substances were:

- Synthesised white sugar syrup with starch,
- Massecuite
- Molasses

As testing proceeded, difficulties arose that were not known when the research and experimentation process began. This required the changing of substances and experimentation adaptation to suit the rig capabilities. Due to this, the hypothesis and testing approach was evolved to the final experimental procedure discussed in chapter 5.

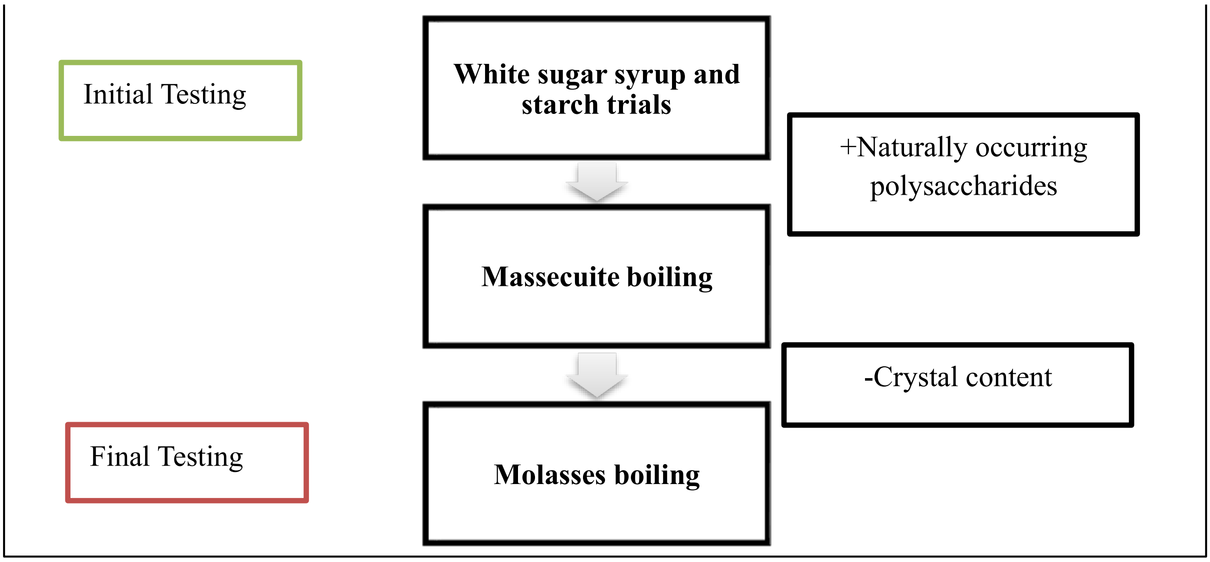

Figure 4.1: Evolution of experimentation

4.2. Methodology for testing

The theory that this work is based off is explained more in detail in Chapter 2, section 2.3., where bubble suppression and the theories surround HTB are discussed. These tests required that pan boiling be monitored visually and results documented for comparison and paired with rheological results to determine relationships between experiments and theory.

In order to monitor the substance visually, it was important to remember the mechanism being investigated. For normal samples, samples that have no HTB characteristics or influencing gums present, boiling patterns and bubbling are theorised to differ as compared to HTB sample, a sample containing influencing gums and/or shows characteristic of HTB (Fowkes *et al.*, 2017).

The assumed signs that are based on the presented theory, of differing boiling characteristics were in bubbling and boiling data collected. Theorised qualities are listed below:

- Bubbles that form appear to have reduced buoyancy
- Bubble size may:
  - be reduced substantially and smaller bubbles that form may collapse on themselves
  - have fewer large bubbles due to the increased energy required for bubble growth
- Bubble shape and flow may be irregular as energy is not enough to overcome the mixture's viscoelasticity and bubbles may tend to be slower moving as size is too small to flow quickly through the liquid to the surface
- Less condensate will be collected from boiling in HTB samples as it is difficult to remove water
- Could take a longer period for HTB samples to reach the same temperature as normal samples due to reduced circulation
- Presence of surface fouling due to decreased rate of heat transfer

The boiling was photographed, temperature and pressure readings were monitored and samples were taken over set time intervals. The experimental procedures and how they were altered to suit the substances being tested are discussed in each section.

4.3 White Sugar Syrup and Starch Trials

This section looks at the testing being done for the white sugar syrup trials done in the early stages of experimentation. Here, boiling was modelled using a synthetic syrup dosed with starch, mimicking

HTB properties. This was chosen as an initial starting point where the "synthetic massecuite" would have a clear, easy to monitor and visualise liquid with the properties found in HTB. Starch was chosen as a cheap method of introducing polysaccharides to understand the boiling and handling of the rig.

The experimentation to be completed in alignment with the hypothesis included testing with a suitably concentrated clear, sugar syrup, to which polysaccharides were added. This sugar syrup was made with first boiling sugar to increase chances of noting bubbling effects through the calandria that may not be seen in darker boiling solutions. The purity of the sugar eliminates the possibility of unknown inclusions that may alter boiling properties. The clear syrup represented the boiling molasses where the effect would be seen and negates effects of present crystals that knowingly alters fluid flow by increasing viscosity.

Based off calculations shown in appendix A1, an appropriate amount of first boiling sugar was added to water in a steam and stirrer facilitated pilot pan. To achieve saturation of all added sugar, water was kept below boiling point at 70ºC and sugar added incrementally until dissolved. This yielded a clear syrup that acted as the control substance and the basis of all testing for this section.

For the HTB properties, the syrup would be dosed with an available polysaccharide capable of:

- accurately depicting the hard-to-boil nature of HTB massecuite
- creating an increase in viscosity without completely ceasing the boiling and circulation while still inhibiting flow thus altering crystallisation capabilities of the mixture.

4.3.1 Preparation and Experimentation

The sucrose syrup manufactured for this testing was boiled within the vacuum pan rig at operating conditions standard to factories. Vacuum pressure was maintained between 80-90 kPa vacuum gauge (10-20 kPa atm abs) and heated to approximately 75 ºC over a period of half an hour.

All tests were run for the same period, with constant conditions being maintained. To mimic a massecuite, the Brix of the syrup would need to reach super-saturation, generally around 85 % to 90 % dry solids content, however this region is highly unstable during boiling and can lead to spontaneous crystallisation. Syrup was manufactured under-saturated at 65Bx, the Brix of syrup entering vacuum pan and boiled to a final set time of half an hour.

To create the effects noted in hard-to-boil substances, a common occurring polysaccharide needed to be used. After discussion, it was decided that for the preliminary stages of testing, corn starch was chosen to act as the altering polysaccharide. The chosen gum was starch as it is easily attainable with known characteristics while also being naturally occurring within the plant structure. While starch does not have the required rheological response to shear, it is able to provide insight into the apparatus operation.

A standard run for the vacuum pan required approximately 30 litres of syrup to fill above the upper sight glass and enough to create flow down the down-comer pipe. For this mass of syrup, it was determined that 150 grams of corn starch would be added into the mixture as a pre-dissolved solution to prevent clumping in syrup. Dissolving of sample is noted by the starch turning clear once temperature increases.

To achieve a pre-dissolved, pre-gelatinised starch mixture, starch was added to 5 litres of water and stirred over time in a hot water bath. Corn starch, when used in cooking, is dissolved at a temperature of 70-80°C and turns translucent. When dissolved, the solution will become more viscous.

Starch was used to act as gums within the syrup. Normally gums would be present within the massecuite before the sample is received. This could have been easily done by mixing the starch quantity in prior to the test run. This however was not ideal to do since the precise quantity required to obtain the suspected surface tension effects was unknown. The starch solution was added in one-third portions and left to boil to ensure starch dispersal through the mixture. After doing so the viscoelasticity was visually monitored and photographed for documentation purposes.

Starting the dosing to the system, 50 grams of pre-dissolved corn starch mixed with 4.8 litres of warm water and suctioned into the rig and allowed to mix. After bringing up the mixture to boiling, the boiling was visually monitored until the excess water evaporated. The boiling was monitored, and the conditions documented.

To ensure longer boiling periods that remain constant between samples, initial dissolved solids content is kept at undersaturated, and warm water periodically added to the pan. This is done in factories when vacuum boiling to prevent spontaneous crystallisation within pans. For the starch samples, this additional water was added with the starch in it to maintain boiling while also allowing smooth integration of starch molecules into the syrup.

4.3.2 Results and Discussion

The pure clear syrup tests were run twice, and the starch dosed clear syrup test run once due to limitation of sample quantity. The data results for these tests can be found in section A.1 in appendix A. The variable factors documented over the boiling period are as follows:

- The fixed time intervals within which boiling is occurring
- Dissolved solids content in the form of Brix was done and samples collected at 10-minute intervals as well as before and after each starch addition into the system for starch tests
- The pressure and temperature of the system during the run on both steam and vacuum sides
- Mass of condensate produced from steam side and syrup sides condensers weighed over time

For clear syrup tests, samples were boiled within the pan testing rig over a period of 80 minutes. Samples were taken every ten minutes to test the Brix over boiling and photographed at intervals to note the changes. Factors affecting boiling were monitored and documented in the tables found in Appendix A, section A.1.

For the good samples, the vacuum pressure was maintained in the 80-90 kPa gauge zone in order to reduce boiling temperature. Sample initially started with a Brix content of 65Bx and was boiled up to 90% Brix. Between the two samples, the total condensate collected, measured as a cumulative value, was 10 litres over the boiling period from the syrup side. Steam side condensate yielded an average of 7 to 8 litres of water produced every ten minutes.

Bubbles formed at the heat transfer surface and slowly rose, gaining momentum and joining with other bubbles to grow larger. Once the bubbles reached the top, they would burst, and this would be noted by rapid liquid movement at the upper surface of the pan. The rate of heating due to convection within the mixture was high and heat passed through the liquid quickly forming lots of bubbles. Bubbles were seen to move quite rapidly through the mixture and movement was not uniform once boiling temperature was reached.

Figure 4.2 shows the bubbling pattern becoming more turbulent once the boiling temperature was reached. Erratic bubble movement was most likely due to the presence of cold spots as cooler syrup came forward to the heating area under natural convection causing irregular circulation. The red arrows on the sides depict the rising heated current while the centre irregular shaped arrow depicts uneven flow.

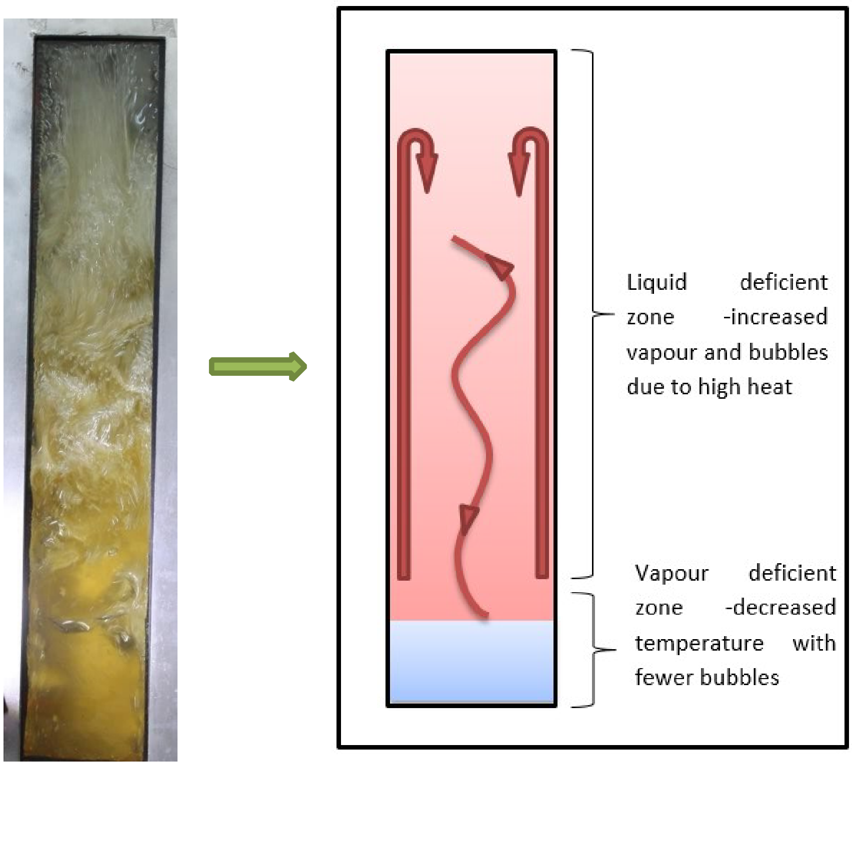

Figure 4.2: Syrup boiling without starch

The good samples were uniform with the boiling. Difficulties arose in maintaining the vacuum pressure between the two tests as this then affected the speed and intensity of boiling. Under the standard energy laws, the total amount of steam condensate used should be approximately equal to the amount of water boiled off on the syrup side. This however is not the case for these tests as the condensate collection on either side is approximately 1:6.

This could be due to several reasons. It is possible that the condenser on the syrup side was not able to condense the vapour and uncondensed vapour may have been sucked into the vacuum pump instead of joining the total mass in the vapour storage tank. It was important to note that while this energy law applies to ideal state samples, in this real test, one must account for general properties of the boiling liquid, losses of heat to the environment and insufficiency of equipment. While energy laws say condensate produced should be equal theoretically, one must account for the liquid properties and experimental procedures. Syrup was made to be 65% dissolved solids of which the dissolved solids is sucrose. This sucrose accounts for 65% of the mixture while the other 35% is the total water. With increasing Brix, it became harder to remove the water in the mixture, as the immediate boiling point of water was not enough to overcome the elastic and viscous properties of the mother liquid. This resulted is a requirement for more heat to be added to the system.

It was also important to note that usage of water to prevent spontaneous crystallisation during the boiling period. By maintaining the Brix of the solution over the boiling period, it is possible to extend the testing period. This attributed to decreases in temperature during boiling which could correspond to reduced condensate formed.

The addition of corn starch to the syrup was used to understand flow property conditions of the testing rig. Corn starch was suctioned into the system in thirds of the initial quantity before further diluting with 5 litres of water to prevent clumping and uneven mixing.

The syrup before doping had a boiling pattern as theorised and tested previously. Small bubbles formed at the heat transfer interface before gaining momentum and rising and circulating in the pan. At the bottom of the calandria there was the vapour deficient zone as temperature in this area is lower than the rest of the tube while the upper area was liquid deficient as bubbles filled the mass of this area decreasing the overall hydrostatic head. Bubbles flowed turbulently as they rose, easily moving through the system, unhindered by any additional effects due to the lack of impurities. Under these effects it was possible to assume the heating through the calandria was even.

After 20 minutes of boiling, the first quantity of starch was added. This dose of gums immediately turned the mixture cloudy and reduced the boiling zone. This could have been due to the addition of water entering the system cooling the overall temperature within the pan or due to the starch that was moving through the syrup. Figure 4.3 shows the boiling that occurs once starch has been added. The area at which bubbles form is reduced, bubble formation at the heating surface was occurring from a smaller area and general heated area is decreased in size.

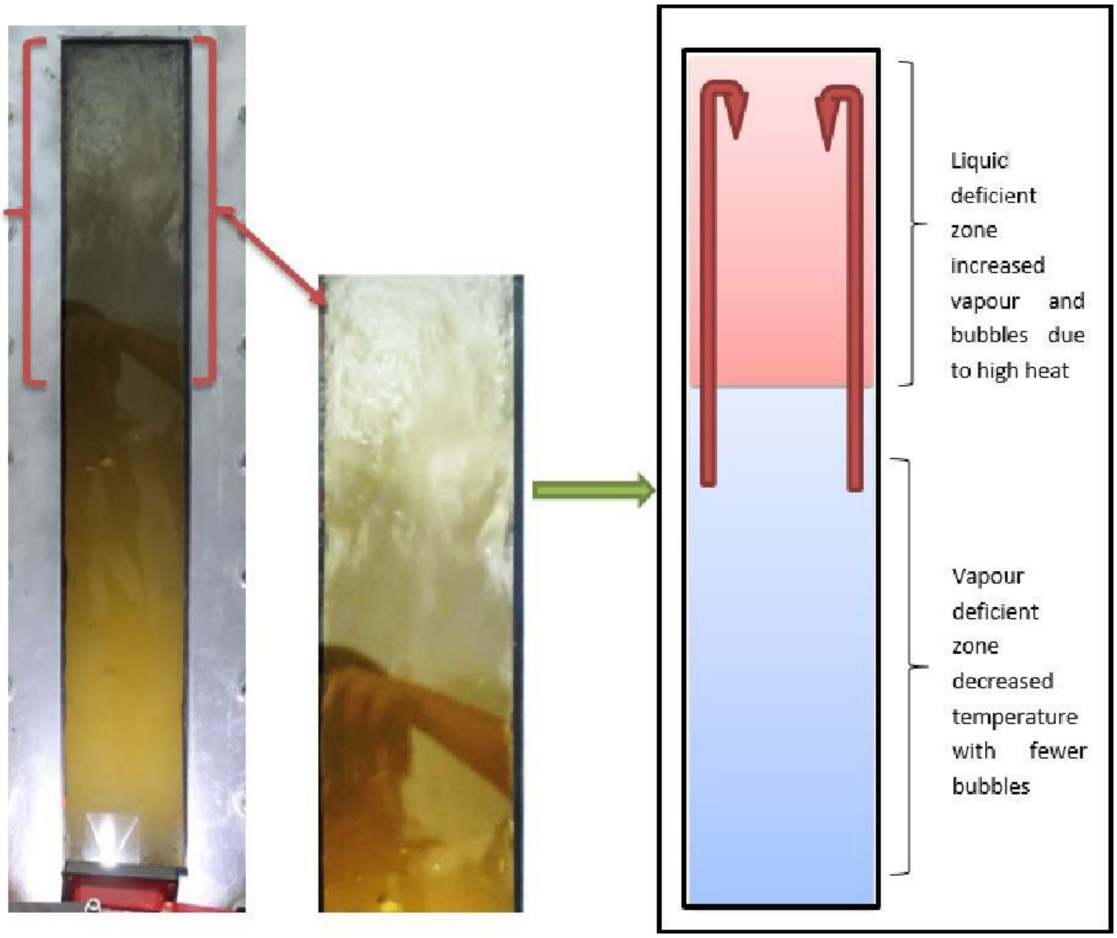

Figure 4.3: First starch addition

When starch was first added to the system, Brix returned to the starting value. Bubble growth was visibly lessened and contained to the upper portion of the tube. The samples received at this point were thicker than samples taken previously. Circulation and boiling was slowed over this time. Bubbling was different compared to the tests without starch. Smaller bubbles at the heat transfer surface were still present however total number of bubbles was reduced. Bubbles were characterised by fewer, larger bubbles and many small bubbles. Rate of evaporation was reduced over this time.

For the second starch addition, the same method was applied where sample was suctioned into the already boiling system as starch diluted in excess of 5 litres of water that would be boiled off over the boiling period. Figure 4.4 depicts the noted effects.

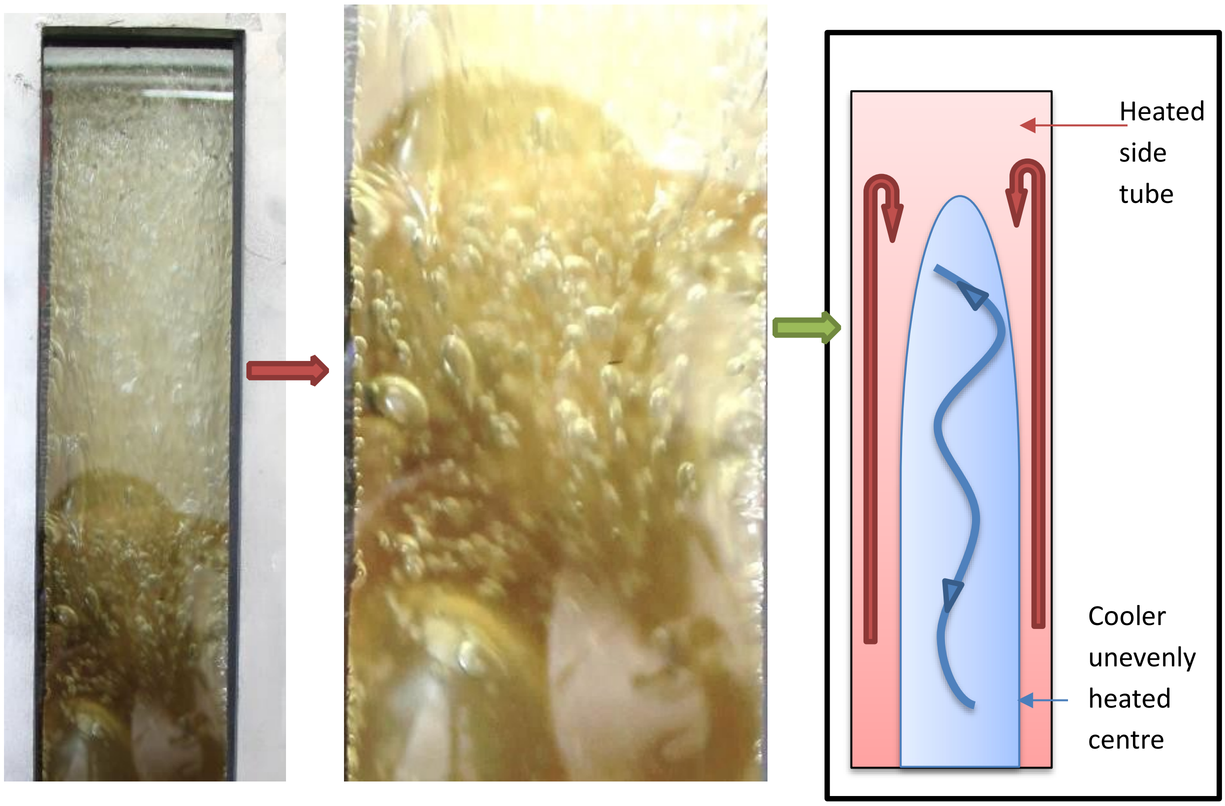

Figure 4.4: Second starch addition

The bubbling found after second starch addition was photographed to note the changes. This image shows the bubbling when boiling first began. The tube has no clear bubbling regions and bubbles of all sizes and shapes were noted through the mixture. At the top of the tube where bubbling is most prevalent, and vapour normally takes up the total visual area, there was less turbulence and bubbles moved slower compared to the rapid movement seen in the clean sample.

Larger bubbles were seen to stretch as they moved through the mixture indicating a possible increased viscoelasticity. Many smaller bubbles were also noted to stretch as movement was difficult through the liquid. Pattern of movement through the calandria was less uniform and on the lower end of the tube bubbles began descending as buoyancy was not enough to overcome the liquid surface effects to move through the liquid. Bubbles formed during this stage would both grow and rise slowly to the upper surface of the liquid, or collapse on itself.

The bubble movement could be attributed to more cold spots as the altered rheology would cause less heat transfer and particularly away from the heat transfer surface. Central section of the boiling tube having different temperatures yielded an irregular boiling pattern as bubbles move within the currents formed.

Once the boiling was stopped and the mixture cooled, spontaneous crystallisation within the testing rig occurred and the dosed syrup solidified forming large irregularly shaped crystals against the surfaces of the pan. The surfaces became areas on which the sucrose began to deposit due to the saturation level being so high. The pan after crystallisation can be seen below. To remove this, the system needed to be flushed excessively with water to rapidly remove these crystals.

In the rough sense, corn starch increased the apparent flow properties of the mixture and this was visually noted due to the changes in bubble formation and liquid movement through the front tube. After starch addition it took far longer to evaporate the same amount of water from a pure sample. However, in the broader scope of the work, it was not possible to determine the rheological property changes as samples, once cooled, would crystallise. These samples could not be rheologically tested as the crystals formed large irregular shapes and left no liquid that could be tested for viscoelastic properties. This leaves the work to make assumptions for these tests based only off the visual boiling aspect of testing.

One of the issues with working with starch was the property effects it created. While it was able to alter the properties of the liquid by "thickening" the mixture, the properties created did not represent the properties experienced within a factory setting. Starch allowed for understanding property changes but not the required qualities. The conditions being experienced by cane stalks determine the polysaccharides and impurities that, when combined, cause the HTB effect. In order to recreate a HTB synthetic massecuite, there would require an in depth analysis and trial-and-error combination of different compounds to replicate conditions.

The results for this section only come in the form of vacuum pan boiling. Samples were collected for rheological testing however, once cooled, would spontaneously crystallise due to the high Brix of the samples. Samples of this variety would require to be tested immediately or kept in a hot water bath for this reason.

The results of the vacuum boiling are not accurate as the testing pressure was taken from a gauge later found to not be working correctly. Due to this, the pressure values received become irrelevant.

There were no signs of burning onto the heat transfer surface. Once boiling was completed and steam addition ceased, the sample began to spontaneous crystallise onto surfaces, glass and stirrer due to high Brix making it difficult to remove from the boiling pan.

It was decided that other tests run hereafter would not be boiled for a set period of time, but rather leaving the end point as a final Brix. This final Brix became a constant among samples in order to adequately compare the properties when rheologically tested. The varying time taken to reach the final Brix was used as an indicator of property change as HTB samples will have increased boiling time for the same final Brix.

The samples to follow were ones that were categorised by factories as HTB rather than using dosed samples. This study was not meant to investigate attempting to define the chemical makeup of HTB samples but rather in the effect that the causative compounds would have on heat transfer and ebullition.

The next step in experimentation looked at testing with massecuites received from factories. The determination of HTB substances was based off the effects that the factory noted during periods of extended bad weather and classified by their own tests to determine impurity values. The samples for proceeding testing were C-massecuites, the final phase of boiling, where impurities would be concentrated to the highest and HTB effects are at the worst. The samples obtained from the factory would have constituents that would produce the effect that is being tested.

Photographic evidence was also limited due to inexperience with photography. Photos were refined to ensure there were no reflections and the quality would be made better in order to analyse the boiling better.

4.4. Massecuite and HTB massecuite samples

Massecuite samples were used to properly mimic impurity and dissolved solids as would be experienced in factories. These samples, while darker, would express more accurate characteristics in order to test the theories of this research, i.e. testing the theories of altered rheological properties and their effects on vacuum pan boiling.

4.4.1 Preparation and Experimentation

Massecuite was diluted to an initial Brix like the syrup entering a vacuum pan. This was done using dry solids. This used the mass and Brix of the current sample to find the mass of the same sample at an increased or decreased Brix. By calculating the change in mass, the dilution mass can be calculated.

$$m_1 b_1 = m_2 b_2$$

C-massecuite received from Noodsberg sugar mill was used. The total sample received was four portions of 25 litres. These samples were weighed and the Brixes were tested in order to calculate the proportion of water required to dilute sample. Once water was added, massecuite was mechanically stirred until water was all incorporated.

Figure 4.5: Dilution technique for massecuite samples: weighing samples (L) stirring samples (R)

Massecuite was removed from its storage container and heated carefully to achieve a target dry solids concentration. To obtain the dry solids concentration required, a calculated amount of water was added and heated together. Due to the high viscosity of the massecuite, mixing of water evenly was difficult and may have led to dissolution of crystal. While this is a problem, when combined with the fact that samples were different, each requiring difficult and long preparation times, means that samples may not have been accurately replicated. The crystal content and Brix would not be constant between samples.

It was deemed at this point that sample preparation for massecuites was impractical due to the heating process required to do it. The time taken to dilute samples was impractical as increased time required for the preparation of one sample, would lead to the deterioration of the next. Massecuites were found to be very unstable with regards to shelf life and chemical deterioration occurred over short periods of time. This led to samples undergoing Maillard reactions that affected the boiling processes.

For rheological testing, at this point it was advised that the mixture be tested on the rheometer under pan conditions where the temperature would mimic the boiling temperature of a C-pan and the conditions being replicated under shear be representative. As such the tests were run at boiling temperatures (90°C) and under a low range of shear and torque.

4.4.2 Results and Discussion

Massecuite was boiled from a set initial Brix, 70%, to a set final Brix, 85%. Diluted samples were boiled under vacuum to Brix up samples such that the boiling periods and boiling effects could be compared at set intervals. The results of this section can be found in appendix A, section A.2. This section looks both at the vacuum pan testing as well as the rheological tests run using the vacuum pan.

4.4.2.1 Vacuum Pan Boiling Tests

When boiling massecuite, it was first noted that massecuite aerates upon addition to the system. Massecuite immediately formed a two-phase froth that filled calandria tube when vacuum was applied. This occurred before any heat was applied to the system noting a possible need for degassing of samples.

The formation of this aerated foam and bubbles caused colour change within the samples, noted in Figure 4.6. Massecuite entering a cold vacuum pan was a caramel light brown that is not transparent. As heat is added to the system and convection and circulation passes heat through the system, the colour begins to change and becomes the better known darker brown colour normally noted by massecuites.

Colour change was attributed to release of trapped gas due to addition of heat however the level remains very high due to aerating effect. Increased viscosity of massecuite means at temperature lower than boiling, bubbles will form however they would not have energy high enough to escape the mixture. These bubbles can remain trapped within the gas and will cause the level to rise.

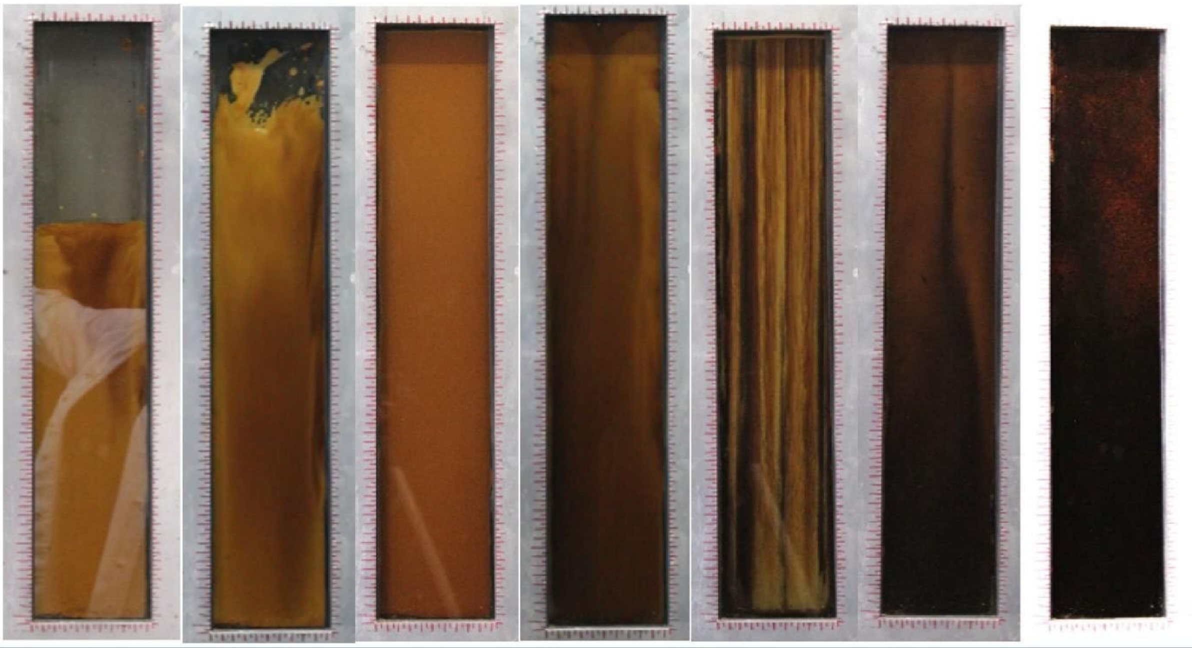

Figure 4.6: Aeration of samples

The general opacity of massecuite was too high to see deep into the mixture. Visualisation of the boiling process could only be done at the viewing glass surface where heating is not present. While this is not ideal, the sample choice being a real massecuite is important in accuracy of chemical and rheological properties. The boiling seen in Figure 4.7 was documented during the massecuite testing phase. The circulation within the images is better depicted in the illustration alongside. It was possible to distinguish the upper bubbling region (liquid deficient zone) and the lower liquid region (vapour deficient zone). Bubbles can only be seen at the surface of the glass where boiling would be occurring slowest due to the lack of heating at the glass interface.

It was unclear as to the exact flow within the boiling tube. Bubbles could be seen forming at the heated sides and moving up in a dense layer. The circulation pattern showed bubbles forming at the heating surface, rising and gaining momentum to reach the upper liquid surface as more bubbles collected. At the glass interface it could be seen that the centre of the pipe would facilitate a downward flow. This was probably due to a naturally established convection due to the central portion of the pipe having a lower temperature than the heat transfer surface.

Figure 4.7 (R) showed the general heating and circulation conditions that were experienced in the pan. The lower portion of the calandria tube is depicted in blue as it is the zone where heating is lowest and bubble formation does not occur as often. The upper tube portion, shown in red, shows the zone where temperature was highest, and most bubbles are found. Here the bubbles escaped the mixture, releasing gas and contributing to heat transfer and evaporation. The heated area of the tube was larger than the cooler area showing good circulation as heat spreads evenly through the mixture.

The arrows are shown as red and blue with red representing rising bubbles that carry heat upward toward the upper surface and blue showing bubbles that descend through the middle due to decreased temperature. The bubble flow that moved down the middle could also be made up of a stream of bubbles that do not have the energy to rise to the topmost surface. At the bottom of the bubbling area, the bubbles move toward the back of the tube where visualisation is no longer possible.

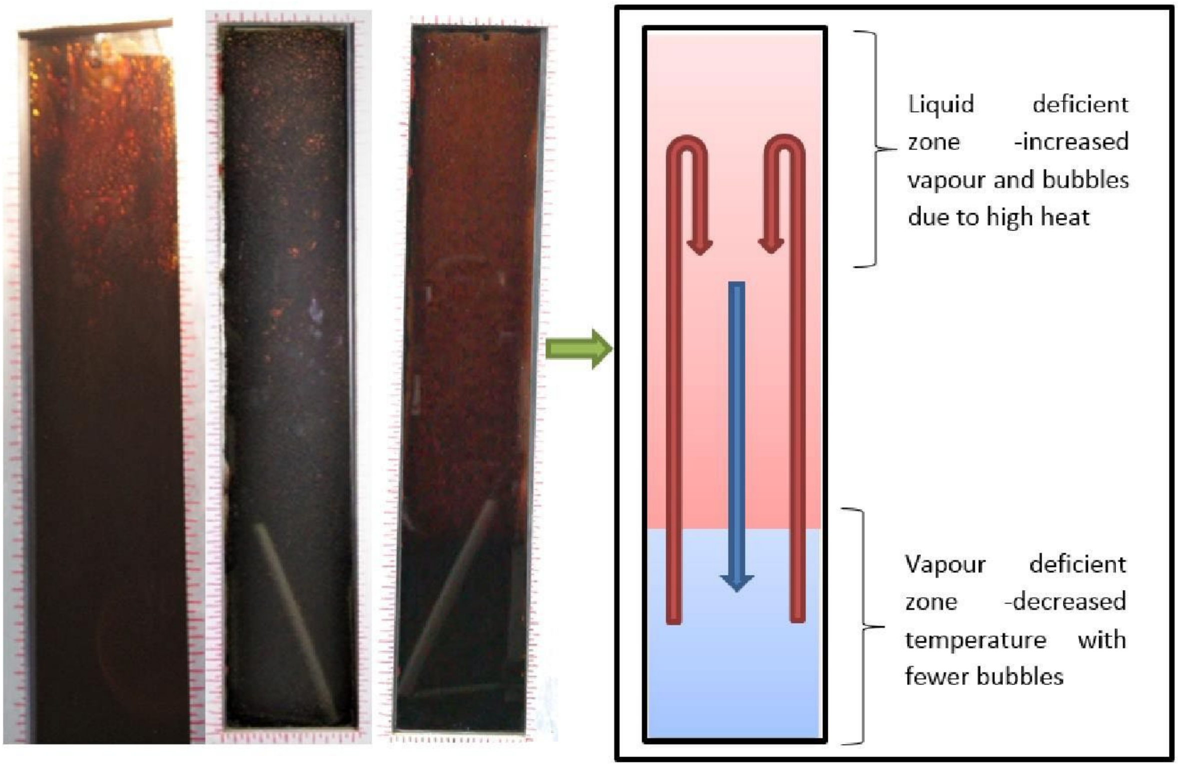

Figure 4.7: Boiling within calandria (L) and circulation within tube (R)

The surface effects of a good massecuite tends to foam and rise in levels when boiling begins. Factories will use antifoam to prevent the excessive foaming and rising of massecuites level as the strong vacuum pressure. Excessive foaming is depicted in Figure 4.8. The use of antifoam in testing was determined counterproductive to the hypothesis as antifoam works as a surface effect modifier that alters the rheological flow properties of the mixture.

Figure 4.8: Foam formation within vacuum pan boiling at the upper viewing pane (L) and in calandria (R)

When entrainment occurred, depending on the severity of the entrainment, the test had to be cancelled. Large quantities of entrainment required immediate and quick system shutdown before system was cleaned out. If the signs of possible entrainment were caught before the actual process occurred, the system would be adjusted accordingly to ensure little to no entrainment occurred. Due to the entrainment possibilities, the testing had to run at constantly changing conditions. Under the aim of these experiments, the pan conditions needed to mimic the conditions in a factory in order to characterise the differences one would expect under boiling theory of bubble growth inhibition. When the vacuum pressure and temperature was kept at factory conditions, definite entrainment would occur. Once the signs of entrainment were learnt, it was possible to adjust and alter the conditions to prevent this from happening. However, this meant that every time boiling was reached, the pressure and steam would be cut off and then allowed to rise again. This left little time for actual visual documentation and data collection. The results of the tests are not consistent, however through this process, more knowledge of system handling was gained.

Problems with testing with massecuites were linked to the instability of the samples. While massecuite was the ideal liquid in terms of accurately testing qualities, the general handling of this product was difficult, even without the added impurities. Massecuites contain a large quantity of dissolved gases due to the general boiling process and circulation within the pan. Massecuite having increased viscosity also tends to hold gas well and when diluted and stirred, dissolves more gas within it. This gas can be released during boiling and cause entrainment.

It was at this point that the system limitations were brought to light. The system was not adequately built to handle the samples it needs to run. With an increasing vacuum pressure, the level within the tank would rise too high and entrain as upper liquid deficient portion of tank is very light. Antifoam cannot be used due to possible alteration of surface effects. The disengagement space designed for the vacuum pan cannot handle the excessive frothing that occurs in massecuites run at the ideal conditions standard to vacuum pans.

The general temperature and pressure was also difficult to control. Boiler working on cyclic loads having an inconsistent steam application to the system paired with the difficult to handle vacuum pressure that fluctuated throughout the testing made testing conditions inconsistent. Due to the instability of boiling requiring overhandling of system where pressure and temperature had to be constantly changed to try to prevent entrainment and let the test run long enough to note results, it is possible that the rig never reached boiling when working with these massecuites. While it is notable that bubbles form at the heating interface, it was difficult to determine whether boiling was reached through the entire calandria. The temperature of the sump and the total condensate collected over the boiling period is significantly smaller than for the tests run with starch. It was also difficult to Brix up the samples and Brix remained almost constant over the boiling period.

Another effect to note was the general hydrostatic head change within the pan. When boiling begins and vacuum is raised, the upper portion of the tank becomes liquid deficient as majority of the contents is at boiling temperature. At boiling temperature, phase change will occur yielding bubbles that will have more energy to release vapour at the surface.

This vapour-filled zone decreased the actual hydrostatic head within the calandria, and it became difficult to know whether there was circulation in the downtake. To prevent entrainment during testing, the system was half to two-thirds filled with liquid (approximately 15-20 litres). This means that sample was not filled high enough to allow flow to the unheated downtake. While the level of the tank may have appeared high enough such that flow and circulation would be possible, it may not have actually been enough.

It was difficult to gauge whether the pan was at the boiling temperature since the only temperature device within the pan was in the sump. It was important to be able to determine the boiling temperature in order to distinguish dissolved air bubbles and boiling bubbles. For future work, a probe measuring the boiling temperature of the front calandria needed to be in place for better analysis.

Due to the general limitations of vacuum pan that were not known prior to starting this study, the pressure of vacuum boiling cannot exceed a certain maximum as height within the boiling tube. This was required as entrainment of samples will occur at higher vacuum and affect the data required to draw conclusions about the testing.

The aeration problem does not allow for the rig to be run at the same conditions as would be experienced within a vacuum pan and would now require a weaker vacuum pressure and higher temperature to reach boiling. Normally this would be avoided in factories as this may lead to caramelisation, bitter taste or darkened colour of sucrose. In this study, these factors are not of high importance as the testing prevents sucrose crystallisation as a whole and focused rather on getting the mixture to boiling temperature to note the changes due to deterioration products.

For further testing it was deemed necessary to also look at the changes based on heat transfer coefficients. With HTB being noted to have a substantial effect on the heating process within massecuites, it was important to move toward testing that effect in correlation to the bubbling effect as they are directly linked. It was also important to be able to test this effect while keeping in mind the limitations of the apparatus.

The test results for the vacuum pan testing became problematic as there was constant vacuum fluctuations, changing temperatures and moments of entrainment that affected the general boiling and mixed into the condensate, sticking within the pipes and affecting the overall mass changes that require monitoring for successful tests.

While it made it difficult to run with a constant worry of entrainment occurring, the aeration property of massecuite became a possible indicator of liquid surface effects. It could be hypothesised that the denser HTB samples with increased viscoelasticity would aerate less while the normal sample would aerate more and rise higher. The dense mixture would reduce the formation of air bubbles and would in general be less likely to store air due to this different consistency.

During boiling, it was important to maintain the pressure and temperature to prevent entrainment as well as to keep the conditions the same as factory conditions. With the increasing difficulties due to the equipment limitations, difficult system handling and lack of appropriate samples, HTB samples were not run. The inability to control the system well at this stage lead the project to rather move forward and look to working with a different substance as well as working under different conditions. Due to the constantly changing vacuum pressures and temperatures, the experiments were not able to be replicated. This required that the experimental method be re-examined such that the testing could be replicable while still being representative of the hypothesis.

For future tests, the crystal content would be removed to reduce the viscosity effect it causes (Shah, 2017). The part of the mixture where boiling occurs is within the molasses (mother liquor). The molasses contains all dissolved solids, sucrose or otherwise, and will show the best results when sucrose has been removed. The chosen molasses is final molasses wherein there would be the highest concentration of non-sucrose solids.

4.4.2.2 Rheology

While it was not possible to run HTB samples using the vacuum pan test rig due to limited amount of sample and absence of proper boiling technique capable of handling massecuites, HTB sample was still tested rheologically.

Massecuites in general were previously tested on the rheometer to learn how to handle the system as well as for development of experimental method. For samples run previously it was observed that large crystals affected the results. The crystals would first prevent the spindle from reaching the optimal gap position set by the rig and would break when spindle spun, causing the spindle to suddenly lower and results to go askew. This led to the determination that all rheology samples need to have sucrose crystals removed.

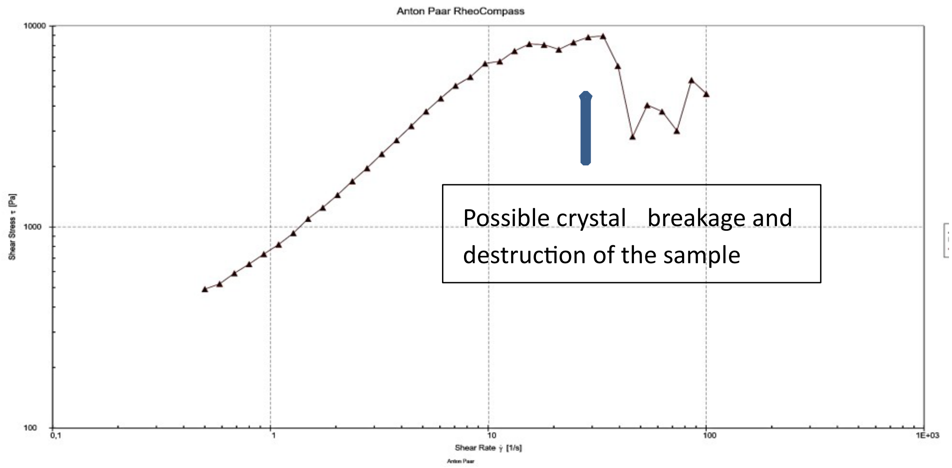

Figure 4.9: Flow curve problems due to crystal presence

For rheology, the HTB sample was filtered using a nutsch filter. This means the sample had its larger crystal content removed by filtering the massecuite through a fine mesh under pressure. This yields molasses that does not contain large crystal particles known for altering flow properties. Once the sample was nutsched, it was compared to normal massecuite samples.

The testing method at the time was still not finalised and testing conditions were recommended values from literature. While it was important to attempt to run samples at the temperature experienced in the vacuum pan, samples are too small to do this. Sample size was approximately 2-3 grams of liquid that was further reduced under the spindle and can easily dry and burn due to increasingly high temperature.

The recommended temperature and shear conditions applied (refer to table 4.1) to the system was taken from the dissertation titled “An investigation into the viscosity of C-massecuite using a pipeline viscometer (Shah, 2017).

Table 4.1: Rheometer tests

Properties	**Values**
Test run	Flow curve
Rheometer temperature	30ºC
Shear rate range	0,1-20 and 0,1-100 s^{-1}
Graphs obtained	Viscosity vs Shear rate Shear rate vs Shear stress

Logic dictates that massecuites do not experience excessive shear forces during the boiling process. The general speed of circulation and velocity of syrup through calandria is extremely low and the only shearing motion within the mixture would be based off mechanical stirrers which also do not circulate at high velocities.

The shear rate applied to samples looked at a low and high shear rate to investigate the zone where massecuite flow would normally fall into while also looking at the extreme effects of deformation in order to determine the changes in properties that may be faced under an increase shear rate. This low and high shear rate range fell from 0,1-20 1/s and 0,1-100 1/s. The results of the lower shear run are depicted in the graph where high shear rate is since the ranges coincide. Both graphs and results can be found in appendix A.2 in full, however in this section, only graphs for the low shear will be shown as it more accurately depicts the properties that massecuites face.

The test that was used to compare samples is the most basic, rotational viscosity test namely the flow curve. Flow curves are quick and easy tests generally used to plot viscosity relationships and can be used for many different samples to yield basic viscosity results. The graphs that are obtained from this test are viscosity vs shear rate and shear stress vs shear rate. Graph of shear stress vs shear rate plots the changing viscosity over the test period due to shearing effect and can classify liquid properties based off this graph shape.

Samples were run in triplicate and the average of the values plotted. Extensive results are found in section A.2 where the results tables and other graphs can be found. The figures below show the graphs of shear rate bs shear stress (Figure 4.10) and graphs of viscosity vs shear rate (Figure 4.11) for the massecuites.

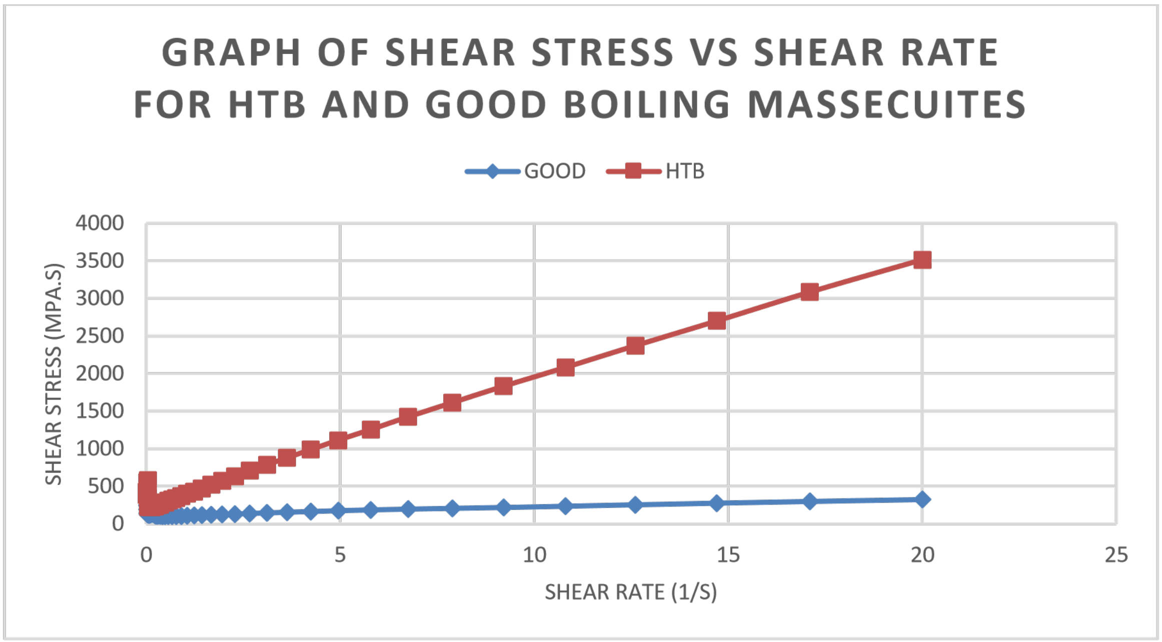

Figure 4.10: Graph of Shear rate vs Shear stress for normal and HTB samples

For these tests, samples were taken at their initial Brixes, this being the Brix of the samples when they were received for testing. The sample Brixes being 79,4% for the good sample and 85,7% for the HTB. Both samples were nutsched to stop the effects of large crystals on viscosity. Both graphs are used for basic property determination as the shape of these graphs will be able to determine the general viscosity of the mixture as well as the fluid type.

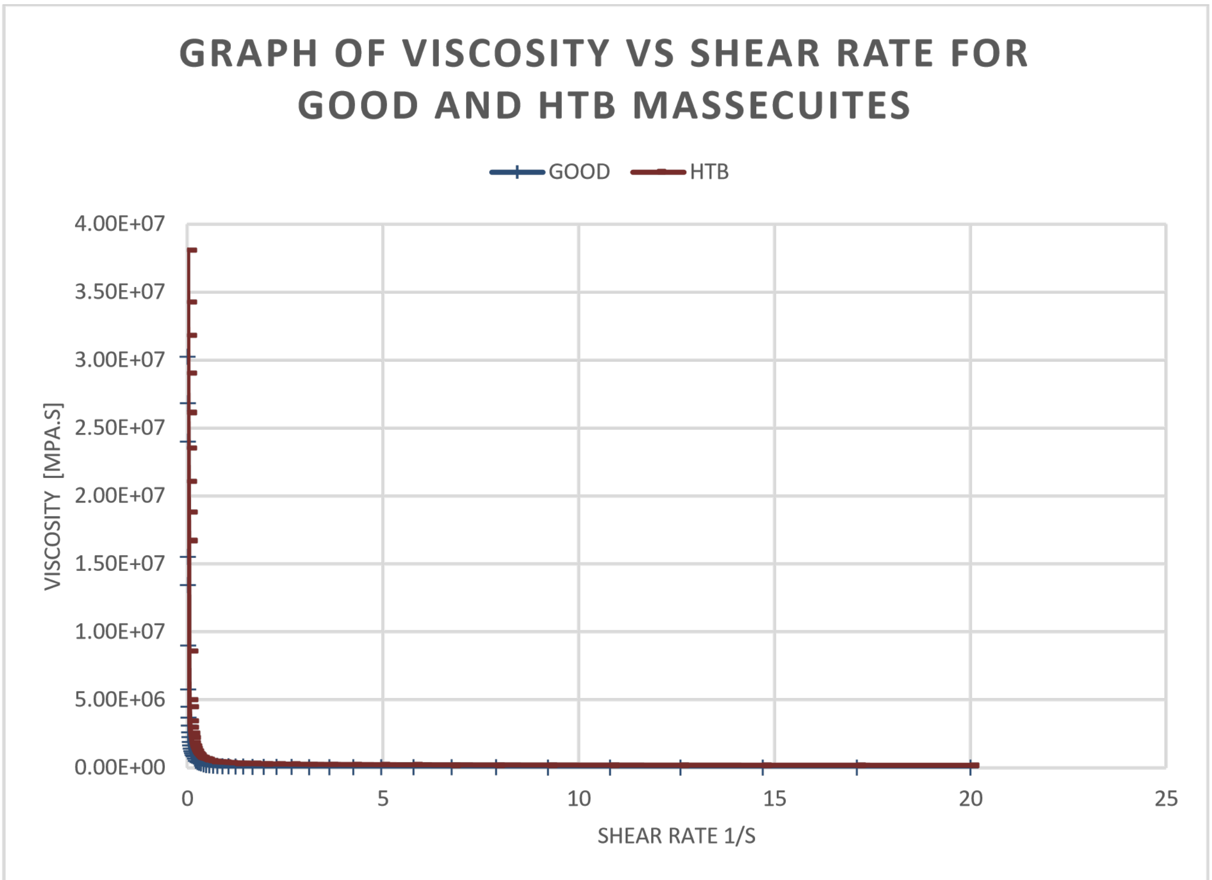

Figure 4.11: Graph of Viscosity vs shear rate for normal and HTB samples

Based on the shapes seen by the graphs, showing a shear drop with a flattened curve, the results show shear thinning depicted by a reducing viscosity with an increasing shear rate. Compared to the graph represented in figure 2.5, the shapes are approximately the same. Graph of shear stress vs shear rate represents the viscosity of the sample. It is difficult to see the difference in the graphed results to determine the viscosity differences. The graph scale is altered for better analysis. This is shown below in Figure 4.12.

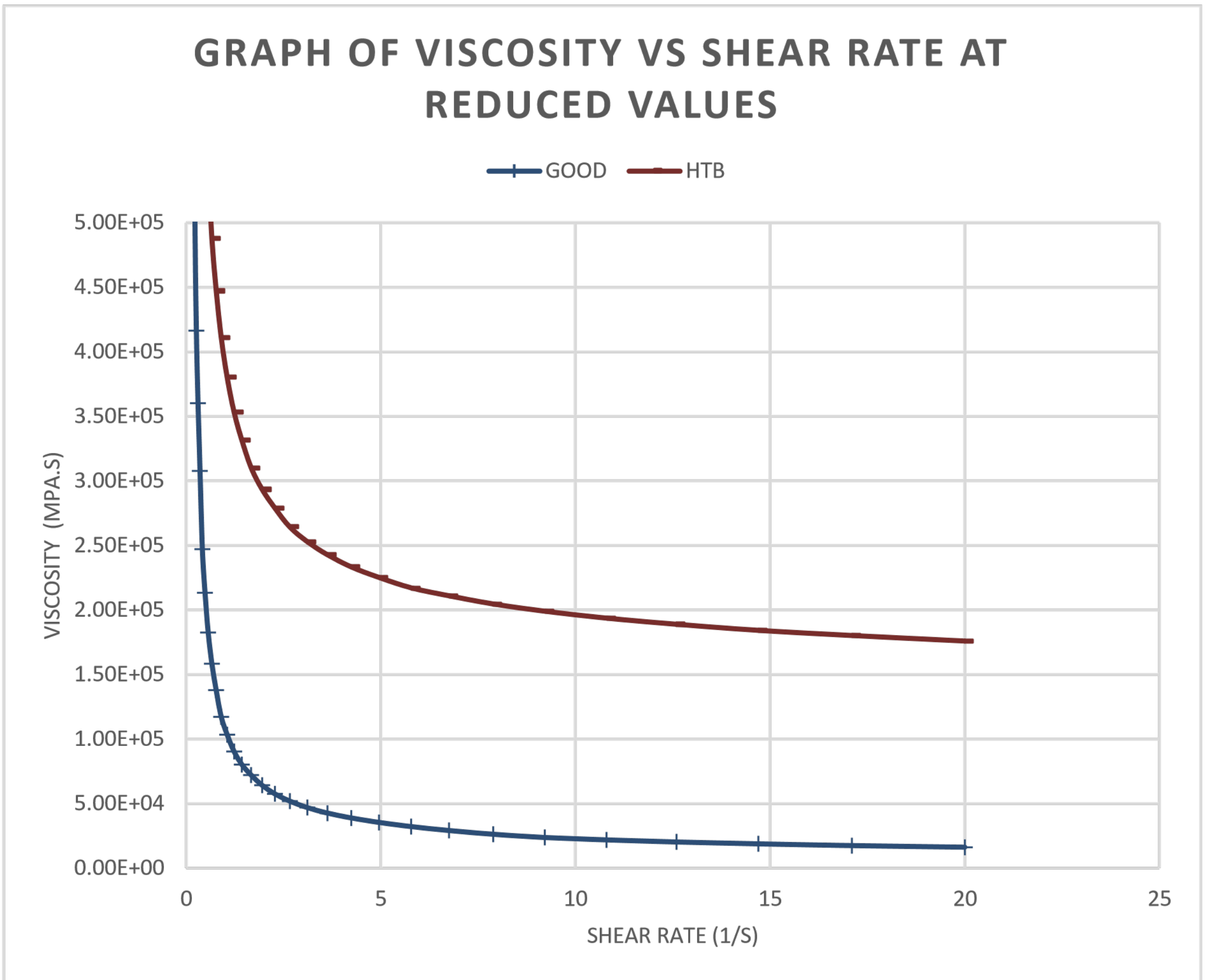

Figure 4.12: Scaled version of graph in Figure 4.11

In Figure 4.12, the different viscosities can be clearly seen. The viscosity at which the graph plateaus is taken as the viscosity of the mixture under shear. For good and HTB samples, the viscosities are 1573816302 mPa.s and 171630-178740 mPa.s. Issues lie in the different Brix values of samples. The good sample had a much lower Brix than the HTB sample. While these values are not representative of all HTB samples, in this case it helped to understand better the differences one would see between samples.

The error in these values lie in the Brix of samples. The HTB sample was at a higher Brix than the normal sample and would have always had a different viscoelasticity value than the normal sample. It became important for future work that any samples compared be at the same Brixes in order to prevent this error from happening.

In the research done by Shah (2017), it was concluded that the effect of Brix on viscosity while important to account for, is not as hugely impactful as the temperature that is used during testing. The given temperature of the sample may also not accurately represent that would be experienced in the pan. While this was true it was also important to remember that the pan would be boiling under lower temperature due to vacuum and under the rheometer, the sample has no account for vacuum. The sample size was also too small to work with increased temperatures. Tests previously used for mock trials tested the effects at elevated heat however these samples would burn and caramelise, jamming the machine and destroying the sample and test. Results gained from testing at high temperatures are not adequate and thus samples are run under lab standard temperatures used by the SMRI when testing massecuites on a viscometer.

With increased temperature, massecuite results would yield a shear thickening property due to the removal of sample water over the boiling period. This is inaccurate as many other work topics that have tested the flow properties of massecuites have discerned that the liquid is of the pseudoplastic variety i.e. shear thinning (Shah, 2017).

While it was adequate to use the flow curve graphs to model the massecuite differences quickly, it was not the most accurate test for samples of increased viscosity. Flow curves are rotational tests generally used for liquids of a freer flowing consistency. While this was fine for the normal samples, the HTB samples where increased viscoelasticity would be expected, require testing using oscillatory tests.

Oscillatory tests are better suited to thicker liquid consistencies and yield more accurate results. The oscillatory tests corresponding to flow curves, that yield results for determining sample viscoelasticity, is the amplitude and frequency sweep. These tests will be done with the flow curves to ensure the results cover a range of tests and yield most accurate results.

It was also noted that tests done at this point were only completed on one Brix for each type of sample. For future tests, families of curves were formed to display the various changes at different Brixes in order to distinguish a clear relationship between all values and types of samples.

The rheology results received here paved the way for future tests and were used when modelling tests for final experimentation required of this dissertation. The test procedures are expanded upon in subsequent chapters.

4.5. Conclusion

The experimental process was done with dosed synthetic syrup and factory grade massecuites. This produced an essential learning opportunity. The results of the white sugar syrup allowed for basic boiling visualisation and changed the sample type to massecuite to remove the need for dosing as well as ensuring samples do not require too much chemical testing and rather the focus of the work remained on the boiling visualisation and rheology.

The massecuite tests help us to understand the sample type more as well as determining limitations of the testing apparatus that required the process to change. Preparation of samples was difficult to do and impractical to heat. Samples deteriorated due to the time it takes to prepare each sample. Difficulties with controlling the boiling conditions yielded unusable results however it expanded the testing and helped find better means of testing the liquids without requiring new machinery. The massecuite tests also looked at removing the effects of Brix on the samples and thus moved toward testing with molasses. Rheological tests were also expanded on and would look at using flow curve, amplitude and frequency sweep tests to ensure the best results.

The tests utilizing molasses are the proceeding results in chapter 5 and 6. These tests were run using the knowledge obtained from previous tests as well as the work done by other researchers in the field of massecuite rheology.

Chapter 5

Vacuum Boiling Results

5.1 Introduction

This section discusses the tests run using the vacuum pan boiling apparatus. Due to limitations of the testing equipment and quantity of samples that could be tested, the final tests were limited to two repeatable tests. The following section looks at the **results from the vacuum pan testing portion of the research**. The expanded experimental results are found in appendix B.

5.2 Experimental methodology

For the vacuum pan portion of testing, it was necessary to test the boiling hypothesis. In Fowkes et al., the theory discussed bubble suppression due to altered rheological properties of massecuites in the form of increased viscoelasticity. This was said to result in bubble suppression due to the bubble energy requirement increase, where the energy of the phase change must be high enough to overcome the combined surface and elastic effects of the mixture, when gums are present. Bubble suppression reduces evaporation, circulation and convection, leading to difficulties in boiling, noted best by an increased viscoelastic property of the massecuite, and elongated boiling periods.

The testing for this section looks at working with molasses, the liquid portion of the massecuite, where boiling would occur, eliminating the effects of Brix on the flow properties. This would ensure viscous properties were linked to impurity content rather than the Brix.

The molasses samples were diluted to 70% Brix, stirred and introduced to the system where boiling would be completed. For dilution of the samples, samples were poured into 25 litre buckets at the same volume level and diluted to the correct °Brix. It was interesting to note that for the same volumes of sample, there was a difference in weight; good boiling samples were 27kg while HTB samples were 31.56-32.26kg. This shows a difference in the density of the samples.

The tests were run using the experimental procedure described in chapter 3. Briefly explained, the tests were run under constant steam addition and vacuum pressure, in order to determine the boiling point elevation (BPE) of the samples. Under these conditions it is theorised that for samples with excessive gum content, rate of evaporation would be lower than for normal samples. This would be noted by reduced condensate formation on the boiling side for the constant boiling conditions.

Logically speaking, BPE of the sample requires that, for an increasing Brix, there requires an increasing vacuum pressure and increasing steam input that also depends on the hydrostatic head of the calandria.

If the steam and pressure remain constant, at a given point of time, boiling would reach an end and sample will no longer be able to increase the Brix levels. For the HTB samples where the heat transfer is said to be difficult and evaporation reduced drastically, samples would reach this at a lower evaporation rate and Brix.

In order to test this theory, the samples were boiled at constant vacuum pressure and steam inlet also kept constant in order to maintain these conditions. The vacuum pressure was lower (i.e. absolute pressure was higher) than what would be run in a standard pan due to the limitations of the testing rig. Pressure was kept at 50kPa vacuum and when boiling picked up, would be adjusted accordingly to prevent sudden changes due to phase change in the condenser that contributes to the vacuum pressure. Steam into the pan was left open such that the steam introduced into the system was kept constant over the boiling period.

Under the theory of bubble suppression, it was assumed that bubble appearance, number of bubbles formed, and flow patterns would change due to the liquid consistency. Samples that were HTB were said to have reduced bubble growth, size and movement under the increased viscoelasticity, according to the hypothesis. To note these effects, the boiling would be documented photographically and compared between sample types.

The following results are documented over 15 minutes intervals for the period specific to the sample type:

- Vacuum pressure in kPa as well as absolute
- Temperature measured using the probe
- Temperature measured using the probe in the pan sump in ^{0}C
- Mass of condensate formed on the syrup side in kg
- Mass of condensate formed on the steam side in kg
- Brix of the samples measured by the Brixmeter during testing as a percentage (%)
- Brix of the samples measured by the NIRS after testing as a percentage (%)

Within the results, all vacuum pressures were converted to absolute for easier understanding, full results of all experiments can be found in this chapter. These final tests were run under the apparent BPE hypothesis where constant steam and vacuum was introduced into the system. Imaging and boiling documentation was done at the 15-minute intervals and will be discussed here.

5.3 Results and experimental discussion

The results of this section are presented here as well in appendix B. In appendix B the tabulated results of conditions over the boiling period can be found and will be investigated and analysed in the form of graphs. These graphs will depict the Brix vs boiling temperature for both the Brixmeter Brix and NIRS

Brix. It is noted that the NIRS measuring method was more reliable than with the Brixmeter as per the discussion in section 3.4.1.

The documentation of results required periods of stabilisation. The temperature probe within the boiling calandria reached the middle of the boiling pipe, nearer to the front surface in order to measure temperature at the area where visualisation is possible. With temperature, the changing of values was likely due to bubbles passing over the probe, circulating the liquid at different temperatures and causing fluctuating results. Pressure, as discussed previously, may fluctuate due to the phase change within the condenser that contributes to vacuum pressure. For the temperature, it was required that the temperature be allowed to even out before the value was taken, this would take a few seconds. Vacuum pressure needed to be increased or reduced to deal with the fluctuations as the changing pressure may invalidate the boiling results.

For the good boiling sample, the system was required to be filled partially; i.e. measured against the glass reference measurement, volumes were filled to 23-24cm from the bottom of the viewing glass for good boiling sample and 46-48cm for the HTB samples, with masses of 27kg and 19,82-26,52kg respectively and volumes used being 10,27litres for good samples and 13.20-13.46 litres for HTB . This was as a result of aeration and foaming of samples. The lowered level prevented the chances of entrainment. At this height level, hydrostatic head will be reduced as well as affecting the boiling point elevation. For the HTB samples, it was noted that there was less aeration and foaming and so more sample was required to fill the tube for these tests.

The graph of Brix vs temperature looks at the changing Brix over the boiling period. This represents the changing boiling occurring as increasing temperature describes the rate of heating and Brix represents the rate of evaporation.

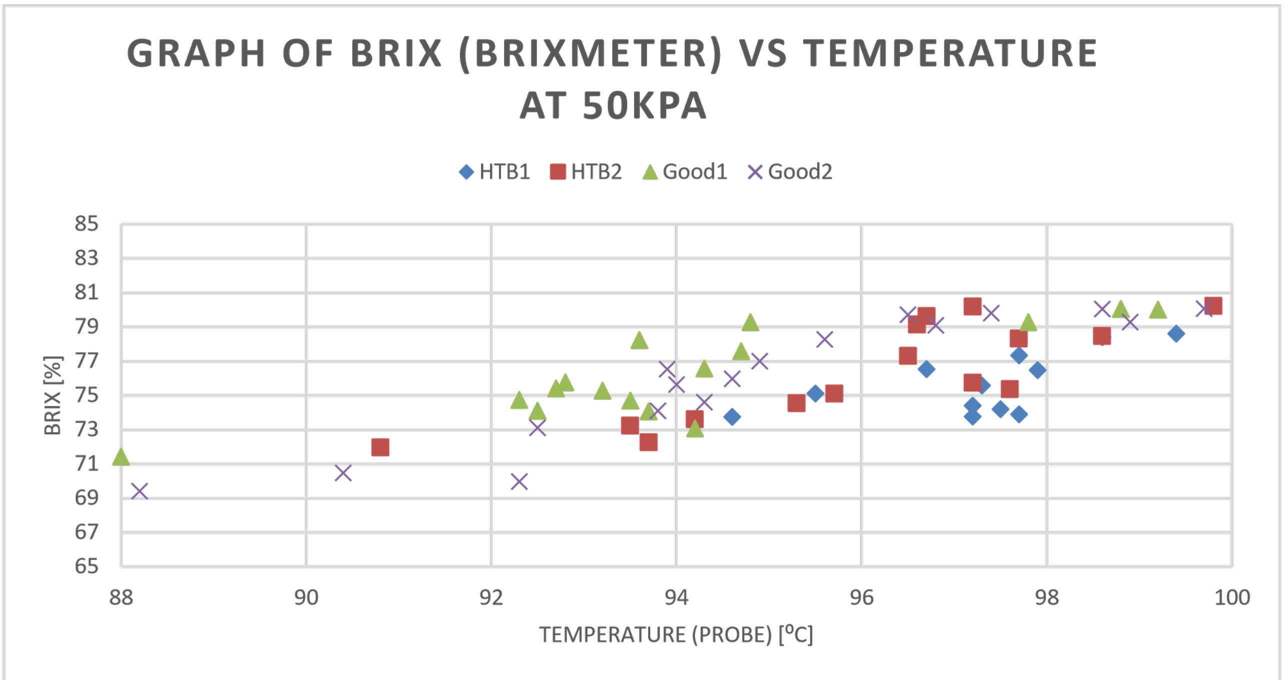

Figure 5.1: Graph of Brix (Brixmeter) vs boiling temperature

Figure 5.1 above looks at the Brix vs temperature at 50kPa vacuum over the boiling period. The Brixmeter had varying Brix results that did not correspond to the NIRS results. It is important to note that all results were taken in triplicates and averaged out to gain the most accurate results possible. Figure 5.2 looks at the graphed values for NIRS Brix vs temperature.

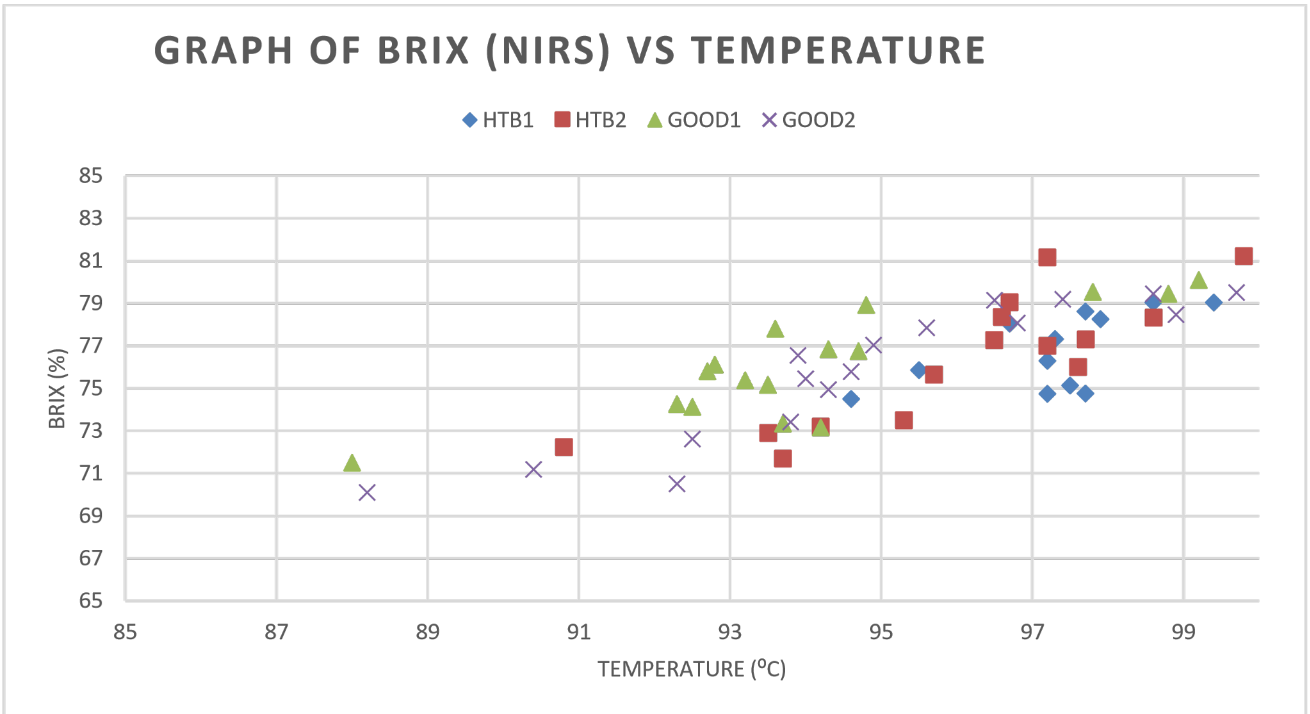

Figure 5.2: Graph of NIRS Brix vs boiling temperature

Looking at the distribution of the scatter, the good samples looked to have more uniform scatter that increased with the increasing temperature. Points have an increased density at the range of 92-95 ºC and even out and plateau at higher temperatures. For HTB samples, the increased density occurs around 96,5-98,5ºC. HTB samples would probably have had a plateauing affect like the good boiling samples if boiling had continued further.

While there wasn't a large difference between sample types in figure 5.2, there was still a difference that could be noted. The possible reasons for the lack of differences is most likely as a result of the sample amount difference. Good samples used less molasses than the HTB samples. This was due to the aeration affect that occurs during boiling and vacuum addition. The HTB sample did not aerate as much and required a lot more sample to ensure the sample could fill the boiling tube. This could be linked to an increase of density of the HTB sample that requires more energy to aerate than the good boiling.

Another important set of results is the evaporation occurring over time. The evaporation rate can be calculated from the Brix of the rig but is also indicated by the rate of condensation formed on the boiling side and stored within the storage tank. The condensate mass was plotted against temperature in order to look at the evaporation occurring over time. To better analyse the results, initial points where mass of condensate was 0 kgs was removed.

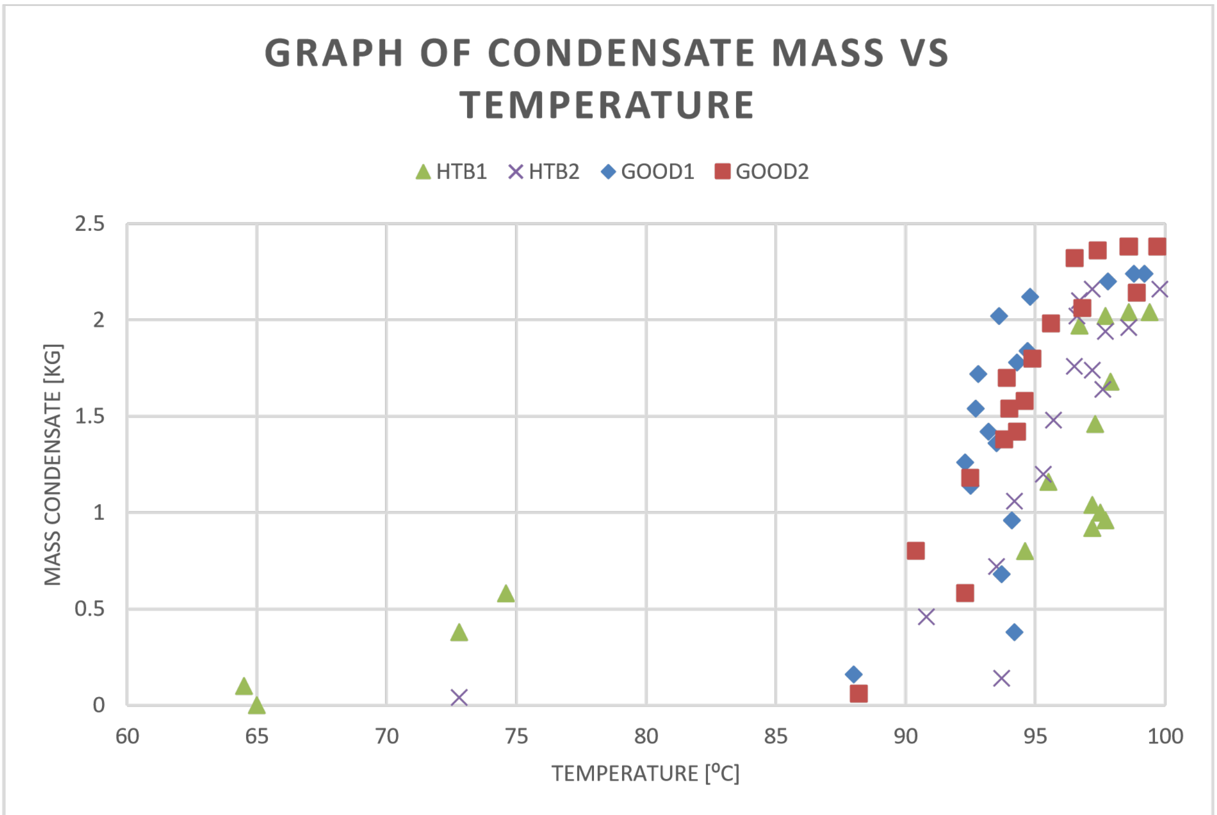

Figure 5.3: Graph of Condensate mass vs temperature

The graph of condensate vs temperature could be seen to have the following differences:

- HTB samples were seen to start producing condensate at lower temperature (65-75 ^{0}C) likely due to boiling only occurring at the heated interface-while the probe reads low temperature, evaporation is still occurring implying boiling only at heat transfer surface
- Good samples started producing condensate at higher temperatures (86-87^{0}C) since the molasses reached boiling the temperature faster, as the central area of tube reached a high temperature 15 minutes after boiling began
- It was important however to look at the total mass of condensate produced for samples between good and HTB samples. Good samples produced 2,02-2,38 kgs of condensate while the HTB samples produced 2,16-2,4 kgs of samples. Under the theorised results, it was expected that HTB sample would not only evaporate less but would also have a decreased temperature. For these tests however, one must look at the boiling conditions.

Using the values obtained it was possible to calculate the theoretical condensate to be formed. This was done using the following formulae:

$$Bx = \frac{DS}{DS + W}$$

Where : Bx=Fraction of Brix on sample

W=Water content

DS= Mass of dry solids

By determining the dry solids fraction and finding the change in water content between intervals, it was possible to calculate the condensate formed theoretically to yield the Brix received. Thereafter the cumulative mass of condensate formed theoretically was calculated. This can be found within Appendix B, Section B.1. The cumulative masses were plotted in figure 5.4 below.

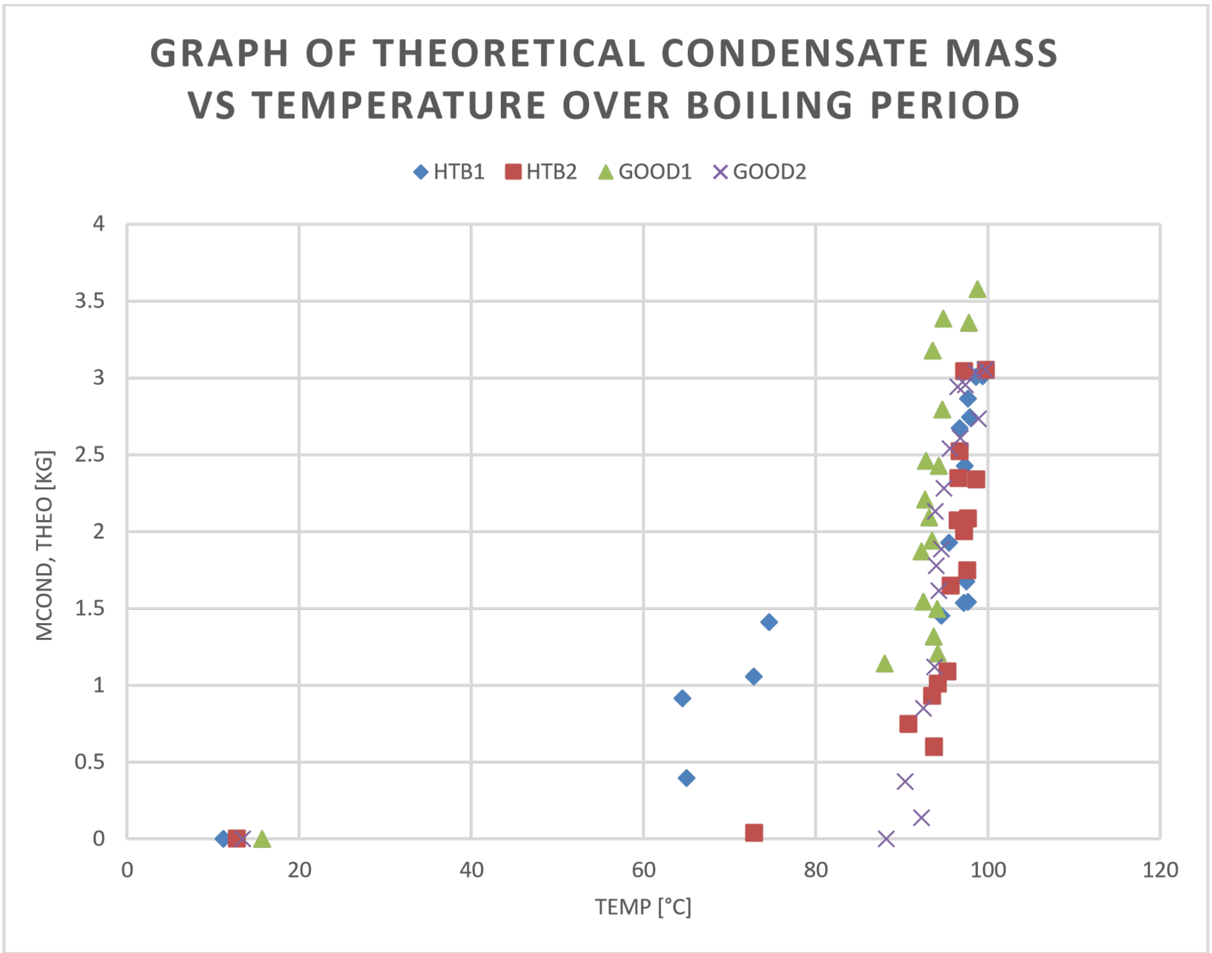

Figure 5.4: Graph of theoretical condensate mass vs actual condensate mass collected over boiling period

Both graphs displayed a steady increase in the condensate collected when the temperature of the system reached roughly 80°C. However, the actual condensate showed a temperature delay where the spike in condensate mainly occurred at 95°C. This was likely due to the heat transfer limits of the testing apparatus. The theoretical mass condensate reaches approximately 3-3.5kg whereas the actual mass condensate reached approximately 2-2.38kgs. These values were irrespective of HTB or good boiling. There is a notable loss between the actual and theoretical and this was likely a result of condensate being lost to the vacuum pump.

As previously stated, to prevent entrainment but allow for circulation, the pan was filled as high as possible. With Good boiling samples, the molasses had a higher amount of frothing than HTB. This was linked to the viscosity and density effects, caused by deterioration in HTB, and resulting with an increasing level as boiling continued. This can be determined by looking at the volumes and masses of each sample being used. This meant that volume of good boiling samples was less than HTB. HTB samples needed to be filled higher because of their lack of frothing and level rise under vacuum. The

HTB sample had to have higher level in order to allow for circulation as well as filling the tube entirely to allow visualisation.

This disproportionality between sample amounts lead to the effects noted above. It is most likely that if the good sample were increased to the same amount as the HTB sample, then condensate produced would have been more. As analysed in the third point of the condensate analyses, the samples produced roughly the same condensate. When the difference in the initial volume is considered, the lower condensate formed from HTB samples is highlighted further.

There were several limitations of the vacuum pan that lead to errors in the results obtained. The rig limitations that were not previously known and had to be overcome in order to properly analyse the work. These limitations led to:

- Having had reduced fill levels to prevent entrainment due to inadequate disengagement space
- Having had to reduce the vacuum pressure (increase absolute pressure) to prevent entrainment due to inadequate disengagement height
- Increasing the boiling temperature in correspondence with the decreased vacuum pressure

The boiling temperature needed to be increased in response to the low vacuum. Steam enters the system at a minimum temperature of 100 ºC and boiling is required to be above 90ºC, in order to achieve boiling. This leads to a large heat loss coefficient, due to the similar temperatures. Latent heat transfer is higher when the change in temperature between two areas is greater. With the surrounding environment being cooler than the boiling pan, it is most likely that heat loss to the environment contributes to the imbalance of the condensate produced.

The sump temperature of the pan indicates circulation effects. Good circulation would imply heating of the downcomer pipe relative to the front pipe. The sump temperature probe measures the temperature of the downcomer and sump that will heat as circulation causes hot liquid and vapour to rise out of the front boiling tube and move backward to pass to the downtake. Cool liquid would be pulled out of the sump and enter the boiling tube as the cycle continues. The sump temperature values were lower for the HTB samples than the good boiling ones showing a reduced circulation within the HTB sample than the good sample.

Based off the results of these tests, with Good boiling samples, the temperature of the downtake increased faster when compared to HTB samples. The Good molasses boiling increased to 80ºC over 30 minutes while the HTB samples reached 80 ºC after 60 minutes. This was linked to the viscoelasticity effect that assumes that gum presence produces a viscoelastic increase and circulation within the molasses was reduced.

It would have been of interest to look at repeating these conditions for multiple samples. However, the shear lack of samples, due to unavailability at the given time, led to only two tests being run per sample type. Extremely hot weather caused deterioration of some samples in storage leading to even fewer testing opportunities. The possibility of dilution and re-boiling of samples already used was discussed. However, the heating footprint on the sample could alter the characteristics. The temperature history of the sample could increase the rate of the Maillard reaction and alter the properties of impurities.

It was also important to note that while the tests are being run to test deterioration effects on the boiling. Using samples that are deteriorated after processing will invalidate the results. The deteriorative effects that were required should be based on deterioration that occurs during the harvesting and initial processing phases. After production deterioration does not accurately depict these properties and it is not well known how this will affect good boiling.

5.4 Visual discussion of boiling

For the visual aspect of testing, the boiling process was photographed for both good and HTB samples, to determine if there was a clear difference in the bubble growth and size for samples. It was vital that imaging be taken such that bubble effects could be noted easily and visualisation was clear. Pictures were taken of each portion of the boiling tube to best look at the heating zones. The good boiling sample was looked at first.

General properties of molasses are noted to froth as a result of viscosity and dissolved air. This frothing effect was noted within the testing rig.. This froth formed when boiling temperature was reached and vacuum temperature was high. Due to the limited disengagement height of the vacuum pan, it was required that the vacuum pressure be reduced, and the corresponding heat addition increased.

5.4.1 Good/Normal Sample Boiling

Good boiling samples were filled to 23-24 cm from the bottom of the front pane of glass, due to the increased ability of these samples to froth and rise under vacuum pressure. When the vacuum and heat was applied to the system, the level rose to fill the entire front tube.

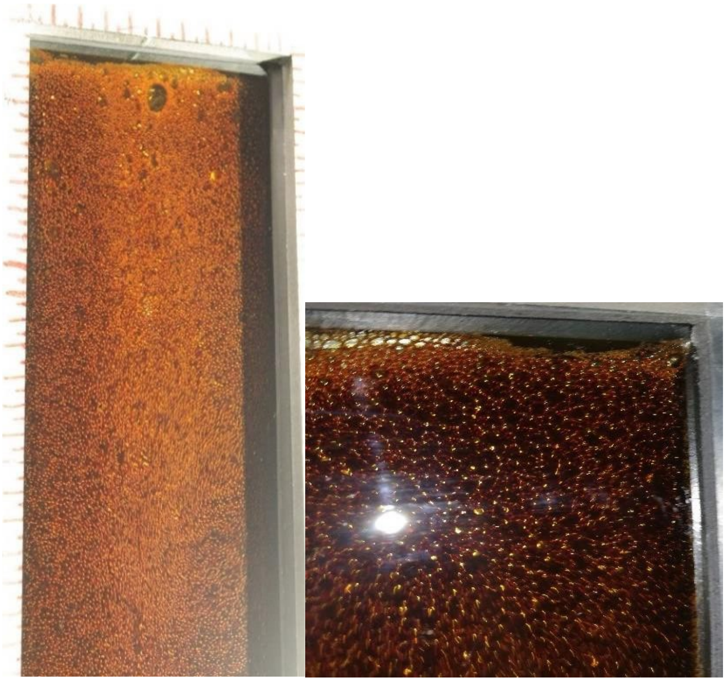

Figure 5.5: Good boiling sample; upper to middle portion (L), zoomed upper portion (R)

Boiling with good samples was filled with bubbles. These bubbles are formed at the front of the boiling tube where there were many small bubbles that formed against the glass. The bubble size goes from very small, dot like, bubbles in the lower part of the calandria to more uniform, larger, bubbles that fill up the entire space of the upper area.

This can be seen in figure 5.5 where the left image shows the full extent of the dense bubble wall with the right image showing a close view of these bubbles. Figure 5.6 shows the bottom section of the pipe, and the right image shows the bottom area of the calandria, where the bubbles are smaller and sparse. In the lower portion of the heating tube there can be seen a clear distinction in the vapour abundant layer and liquid abundant layer due to temperature gradient within the tube.

Figure 5.6: Bottom boiling section for good samples

The change in bubble size attributes to the bubble growth. A temperature increase with an increasing height on the boiling tube will allow for better bubble growth. More bubbles form with randomly scattered large bubbles. The sample colour difference between HTB and good samples was due to the frothing effect. Frothing in the good samples was a lot higher than the HTB samples. The more liquid deficient sample allowed more light refraction through the sample, making the colour look lighter in photographs.

In previous testing with white sugar syrup, it was possible to clearly note the flow patterns and behaviours of syrup during boiling. For the molasses sample, it was difficult to see past the bubble wall that formed against the front pane of glass. Higher in the tube, liquid deficient boiling was present, and this lack of liquid clearly increased the visibility of the bubbles. Deeper into the calandria could not be seen.

The bubble movement was cyclic in a different way than with the white syrup tests. White syrup tests showed a circulation that moved from the heated wall down the centre of the tube. With the molasses tests, there was circulation in the opposing plane. When samples were boiled, the bubbles could be seen descending and moving backward into the tube. It's assumed that since the front pane of glass is not heated, this is the coldest area within the boiling tube. Here due to natural circulation, the front face of the pan showed a descending motion of liquid where bubbles move backward into the liquid.

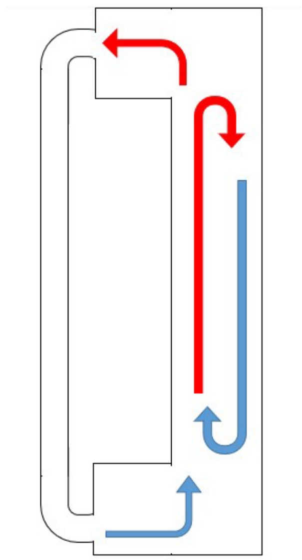

Figure 5.7: Side view of vacuum pan and theorised circulation schematic

Figure 5.7 depicts this flow. Circulation occurred through the front calandria where boiling was monitored. Circulation occurred in one cycle within the boiling tube as well as through another cycle through the downcomer.

The bubble velocity was compared by looking at the videos taken of boiling. Videos taken at the early stages of boiling, where the brix is low, and videos taken at the ending stages of boiling, where brix is high, were compared. This was done by analysing the video and searching for similar sized bubbles between the videos and determining the distance travelled over time.

Bubbles of approximately 1cm were compared at these initial and ending stages of boiling. Velocities were seen to be approximately 3.25cm/s at the initial boiling stage and ending off at 2.5cm/s. Bubble sizes were difficult to note due to what is assumed to be a wall of foam at the glass with bubble sizes being less than 0.5cm at any given point. The largest bubbles formed were seen to be 1-2cm approximately.

5.4.2 HTB Sample Boiling

HTB samples were categorised by factory experiences and were noted during periods of excessive bad weather. The factories classified the properties as having extended boiling time and increased gum content. The HTB samples had a visibly different consistency compared to good boiling samples. The differences noted were an increased weight for the same volumes and a thicker,or rope like consistency. The samples were boiled under the same constant heat input to the system with constant vacuum pressure.

The difference between the boiling that was seen with good samples and HTB samples came in the form of bubble size and flow rate. First, it was important to recall that vacuum and frothing effect does not affect HTB samples as much as good samples. In order to fill the calandria, the HTB sample had to be filled to a higher volume (48cm above the bottom of the visualisation pane). When the good sample rose due to boiling and vacuum, the HTB sample did not rise as much. This could possibly be due to the denseness of the sample that suppresses bubbles that form that would normally aerate the sample and make it rise within the calandria.

Using the theory of bubble suppression, due to rheological changes, it was observed that bubbles were smaller in size and upper the area was liquid filled with smaller sized bubbles. There were a few larger bubbles, however the number was far less than what could be seen in the good boiling samples. The bubbling in the calandria is seen in figure 5.8 where there is an indistinguishable bubble size difference between the upper and lower area with sporadic large bubbles. Smaller bubbles can be seen collecting at the heating surface on the edges of the glass pane.

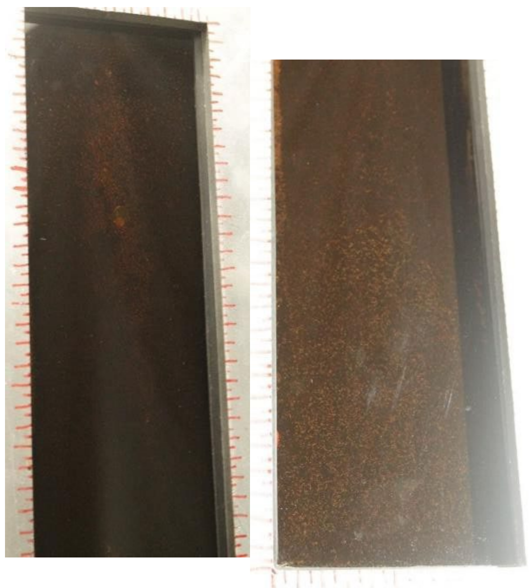

Figure 5.8: Boiling within the HTB boiling calandria upper (L) and lower (R) areas

The circulation pattern observed was the same between HTB and good molasses. The bubbles move in a downward fashion due to cooler front interface as it is unheated. Flow rate between samples were noted to change with more rapid movement in good boiling than HTB samples. This is noted with video documentation that were included for observation.

Foaming at the upper interface differed between samples. Good samples would produce unstable boiling with turbulent movement due to vapour release at the upper surface. Figure 5.8 (L) and 5.9 shows the bubbling experienced in good samples where foam was unstable, and bubbles rose to burst. The layer of foam was significantly thinner than in HTB samples. HTB showed a thick layer of stiff foam that did not move. There was no turbulence due to vapour release and the foam did not move or become entrained.

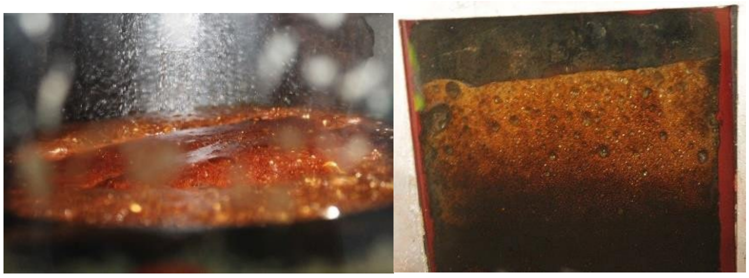

Figure 5.9: Foaming due to good (L) and HTB (R) samples

As discussed in section 5.4.1, bubbles of approximately 1cm (taken from the measurements on the glass) that formed at the bottom of the calandria, were monitored and the velocities determined. At the start of boiling, the bubble velocity was approximately 2,33 cm/s. At the end of boiling, the bubble velocity was approximately 1.33 cm/s. This shows that as more water was removed over time, the bubble velocity decreased. Bubbles were seen to disappear after travelling a short distance. This can be assumed to be due to movement away from the glass or collapsing under increased viscoelasticity. As compared to good boiling, there’s a significant difference in the velocities observed for similar sized bubbles.

The mixture was full of small bubbles looking to be approximately less than 0.25cm with sporadic larger bubbles that formed and disappeared over short periods of time. Compared to the foam bubble layer in the good boiling samples, the bubbles are smaller in comparison while still having a large number.

5.5 Conclusion

The results of this section dealt with the characteristic changes between good and HTB samples. Each substance was added to the system and tested for the required experimental method. The errors and limitations of the operation and testing rig were critically analysed in order to draw accurate conclusions from the results. Clear differences between boiling types were determined in both boiling point elevation theory as well as in bubble visualisation. These differences were:

- HTB samples are denser and heavier than the good boiling sample
- HTB tests required more total sample than the good boiling tests due to reduced aeration and foaming
- Smaller bubbles were noted for HTB tests

- HTB samples evaporated less water for the boiling period

Chapter 6

Rheology & NIRS Results

6.1 Introduction

This section covers the chemical and rheological testing of samples for both good and hard-to-boil. The samples were tested on a Near Infrared Spectrometer (NIRS) to accurately and quickly determine the Brix and other dissolved solid content, to pinpoint any changes between samples. Rheological testing is used to determine and characterise the flow properties of the molasses samples to **find the inherent characteristic changes that caused the boiling changes** noted in chapter 5. For all the results in this section, tests were run in triplicate to ensure the technique gives the same results each time samples are tested. For the graphs and values, for both NIRS and rheology, the received results are averaged out before being plotted.

6.2 NIRS Results

NIRS readings are important in determining the basic properties of the molasses samples, quickly and accurately. Each test on the vacuum pan yielded 15 samples for each good boiling sample, and 17 for each HTB boiling sample. The NIRS was used for a better and more accurate Brix measurement that is tabulated with the results of the vacuum pan boiling. Briefly, other tested properties would be analysed in this section.

The results obtained in this section are found in appendix B, section B.2. The NIRS yields results for: Brix, pol, sucrose, glucose, fructose, ash, dry solids and the colour of the sample. It is essential to note that the Brix reading from the NIRS is more reliable than the Brixmeter measurements taken during the testing to monitor boiling progression. This is due to the predetermined and calibrated procedures programmed onto the NIRS system, that is coincident with lab testing methods, to determine different properties. The theorised cause looked at an increase in gum levels within the boiling liquid, resulting in the changed rheological properties noted in vacuum pan boiling stage. Using NIRS, it was possible to find these changes without having to run in depth analytical tests for the specific gums and quantity changes that falls out of the scope of this work.

The theory states that due to effects of present gums, the purity content of molasses will increase. This was due to difficult boiling conditions that stunts boiling, by reducing the crystallisation capabilities of the solution. A lowered evaporation rate implies that water is not removed from the mixture, reducing the rate of crystallisation and resulting in less sugar being removed from the massecuite when boiling occurs.

This increased purity could be noted by an increased dissolved solids content, noted in the NIRS. For both good and HTB, the samples boiled up to the same Brix over the different testing periods. While there were comparable Brixes, the total dissolved solids content within the mixtures at the same Brixes were different. This is point of interest as the samples used for all testing was final molasses.

Final molasses was chosen as the mixture for experimentation as it represented the boiling portion of the massecuite, removing the large crystal content effects and having the greatest concentration of impurities due to completed boiling cycle. The final molasses for a good boiling sample should differ in constituents to the HTB final molasses, as the purity and general dissolved solids content within HTB samples should be higher. This would be a combination of the increased gum content as well as high overall purity at the end.

For example, the properties of the samples obtained, when boiling was completed, are tabulated in table 6.1 below. This table shows the various Brixes, sucrose contents and dry solids as a percentage of the overall mixture.

Table 6.1: Table of NIRS results for comparison

Test Sample	**Brix [%]**	**Sucrose [%]**	**Dry Solids [%]**
Good 1	79,51	30,75	76,78
Good 2	80,1	31,58	77,03
HTB 1	79,04	39,58	79,54
HTB 2	81,23	40,58	81,16

Looking at the sucrose content for the good samples, as compared to the HTB samples, there is a clear observation that there is more sucrose solids found in the HTB samples than in good samples. The percentage of dry solids content was also higher for HTB samples, than good ones. These conclusions may be drawn from the results, however, the problem with this comparison is that the Brixes between the good and HTB samples are not identical for the NIRS Brix measurements.

Looking at the first HTB sample and first good sample, the Brix percentage of the good sample is higher than the HTB sample. This should imply that the general contents of the mixture will be higher in the sample of higher Brix. At 79,5% Brix, there is 30,75% sucrose content and 76,78% dry solids. For HTB at 79,04% Brix, there is a sucrose content of 39,58% and dry solid content of 79,54%. Comparatively speaking, there is a larger percentage of solids content within the HTB samples that could support the hypothesis put forward at the start of experimentation.

6.3 Rheology Tests

Rheological testing of samples received from the vacuum pan boiling was required in order to distinguish the characteristic changes occurring to the sample's flow properties. It was theorised that the flow properties of HTB samples would tend to be more viscoelastic than that of good samples, leading to the inherent problems experienced in factories. The samples would particularly have a higher elastic portion, or storage modulus when tested, causing the effects commonly attributed to HTB.

For all tests, samples that were representative of 70, 75 and 80 Brix were analysed, in order to compare good and HTB samples, without the differences due to Brix affecting the results. To first test the basic viscoelastic changes between samples, flow curve tests will be applied. Flow curves use a machine to determine the shear strain occurring within the sample, to calculate the shear stress and viscosity. Viscosity was defined as the shear stress divided by the shear rate.

For the rheology of molasses testing, samples were collected at 15-minute intervals over the boiling period. This resulted in numerous samples that needed to be tested rheologically. The tests run will determine changes in viscosity at a constant temperature.

These results are tabulated in appendix B and are graphically represented in this section. The graph results are averaged out to create the most accurate values to represent the samples. Figure 6.1 shows the shear stress vs shear rate plotting all good and HTB samples at the various Brixes.

The standard testing procedure can be found in Appendix C, section C.3. Samples were run at 30°C to prevent burning and dehydration of the sample.

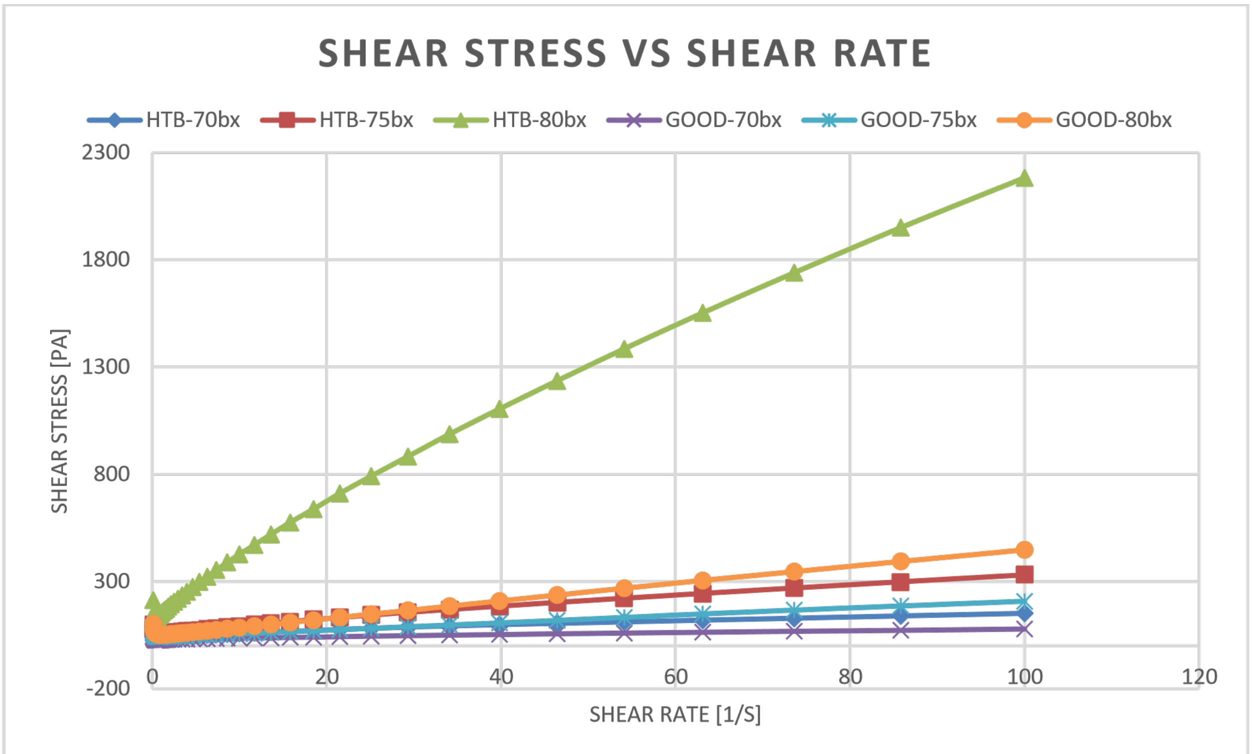

Figure 6.1: Graph of shear stress vs shear rate for all samples for good and HTB

Figure 6.2 shows the graph of viscosity vs shear rate. This graph depicts the change in viscosity due to an applied shear. On this graph, the viscosity values of lower Brix samples overlay in order to fit on the graph. This required that the graph values be looked at a smaller range for a better comparison of the overall viscosity changes for increasing shear.

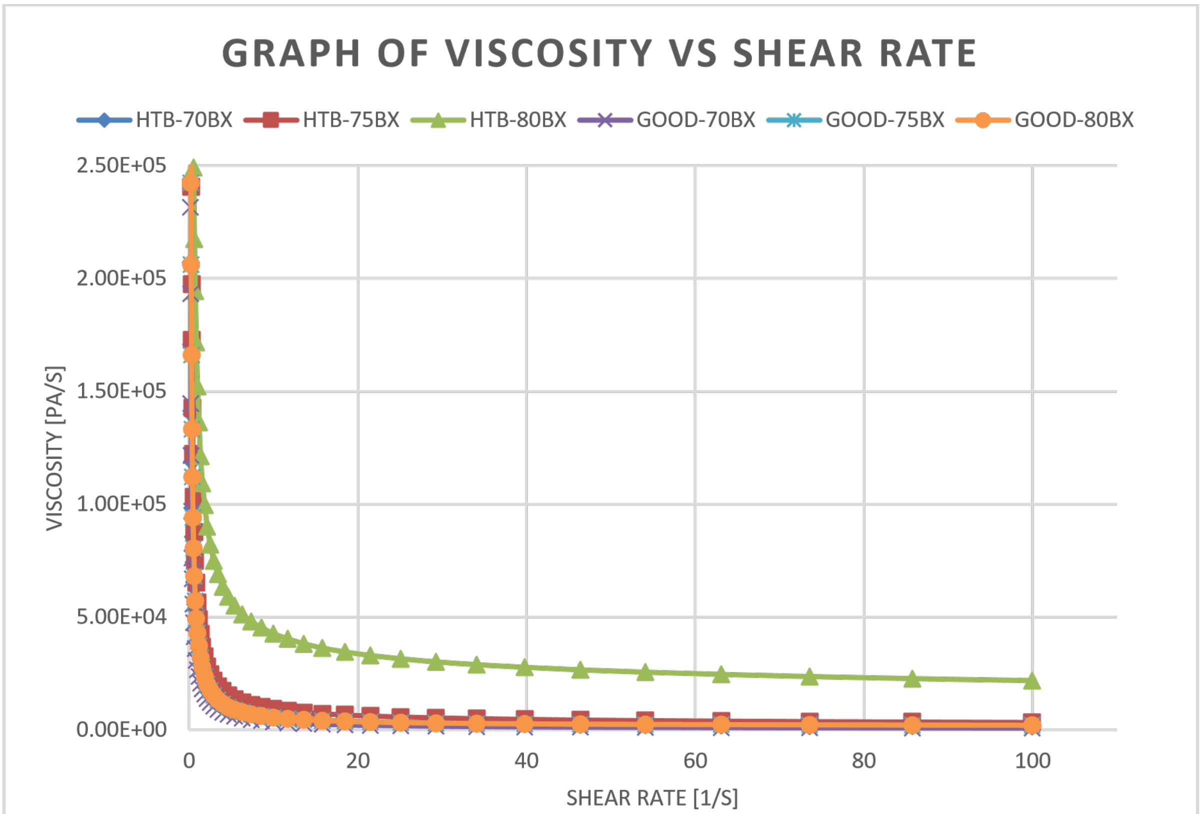

Figure 6.2: Graph of viscosity vs shear rate

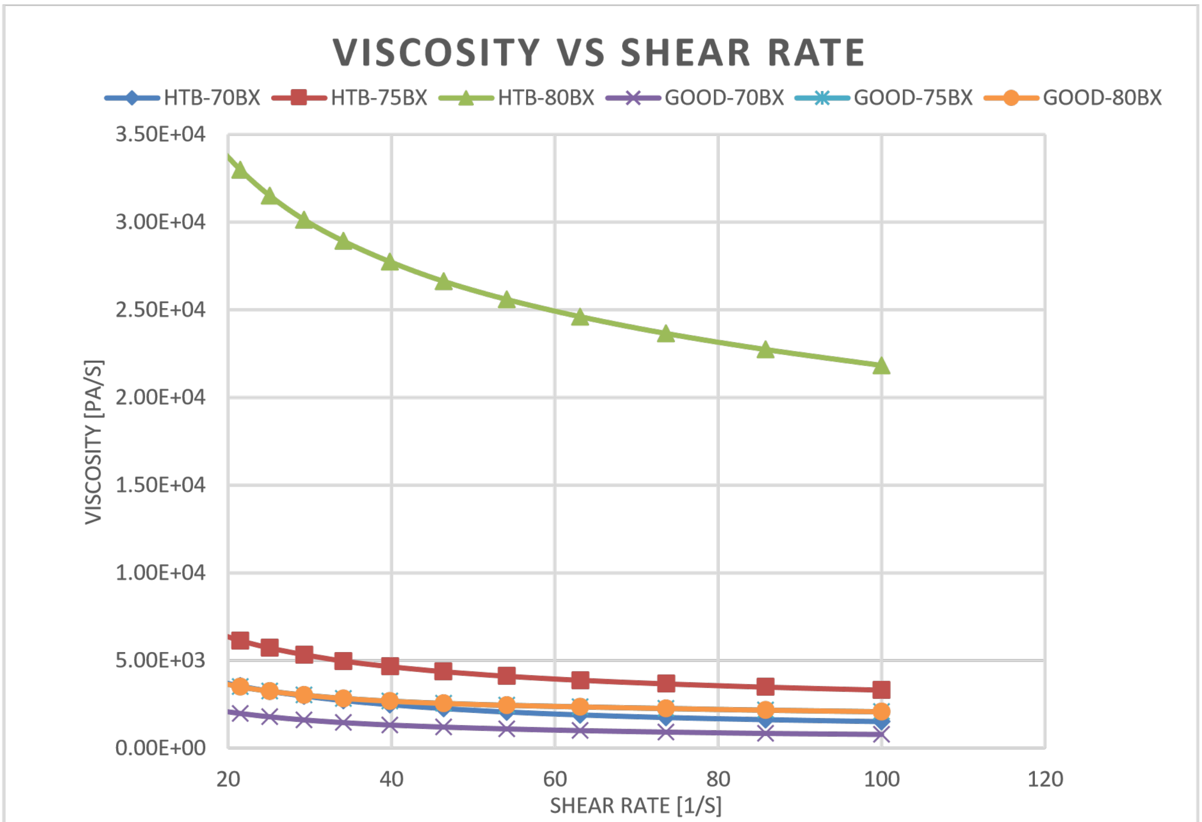

Figure 6.3: Graph of viscosity vs shear rate for all samples for both good and HTB samples

The visual representation of the results from the graphs plotted in both figures show the reducing viscosity occurring as shear rate increases being indicative of shear thinning quality of molasses. Both, good and HTB samples show shear thinning qualities. Under the influence of an increasing shear rate, there is a notable decrease in viscosity. The difference between the samples lies rather in the viscosity values.

At the same Brix and shear rate, HTB samples can be seen to have higher viscosities than the good samples. Looking solely at the graphic representation, the HTB viscosities at the various Brixes is seen to be significantly higher than good samples. At 80% Brix for the good sample, the viscosity was far lower than the HTB samples at the same Brix. Good samples at 80 Brix had a viscosity being closer to the HTB sample at 70 Brix. Comparing the zero viscosities, viscosity of the sample when at rest, the following table can be drawn.

Table 6.2: Zero viscosities of samples at different Brixes for different samples

Good boiling		**HTB boiling**	
Brix [%]	**Zero Viscosities [mPa.s]**	**Brix [%]**	**Zero Viscosities [mPa.s]**

70	576000	70	710000
75	864000	75	977000
80	1030000	80	2140000

The zero viscosities for the different samples indicate that with increasing Brix, there is an increasing viscosity for both sample types. However, for the HTB samples, there is a far higher viscosity result, which is linked to the increased gum content.

Amplitude sweep shows the storage and loss modulus, and how these values get affected under a constant shear strain. This oscillation test is run to determine the linear viscoelastic range (LVER). This testing method uses the loss modulus G" and storage modulus G', that represent the liquid viscous portion and the solid elastic portion. The LVER is used to find the safe zone for sample rheology where the samples can be tested without any destruction of the structure.

The LVER was represented graphically as the portion of the graph where the loss modulus line and shear modulus line are both parallel. The sloping shape of the graph represents the point at which sample structure has been destroyed.

The results received are plotted in graphs that can be found in appendix B, section B.3. of value from these graphs is the LVER of different samples at 70, 75 and 80 % Brix. This is tabulated in table 6.3 below. Determination of the LVER is important in order to determine the region within which the sample will not be destroyed by further testing.

Table 6.3: Linear Viscoelastic Range for samples at different Brixes for different samples

Good boiling		**HTB**	
Brix [%]	**LVER (Shear strain) [1]**	**Brix**	**LVER (Shear strain) [1]**
70	0,0001-0003	70	0,0001-0,0002
75	0,0001-0003	75	0,0001-0,0003
80	0,0001-000263	80	0,0001-0,0003

The LVER ranges determined using the amplitude sweep test is quite similar for both HTB and good samples. The HTB sample has a smaller LVER at the 70-Brix point, while the good boiling sample has a lower LVER at 80 Brix.

Using the LVER, the range of strains are chosen for the frequency sweeps that will run samples at this range to prevent sample deformation. Frequency sweeps describe the “time dependent behaviour of a sample in the non-destructive deformation range” (AntonPaar, 2020a). The oscillatory test works at the LVER to determine the sample stability and behaviour. Figures 6.4 to 6.6 show the frequency sweeps for the varying samples at 70, 75 and 80% Brix.

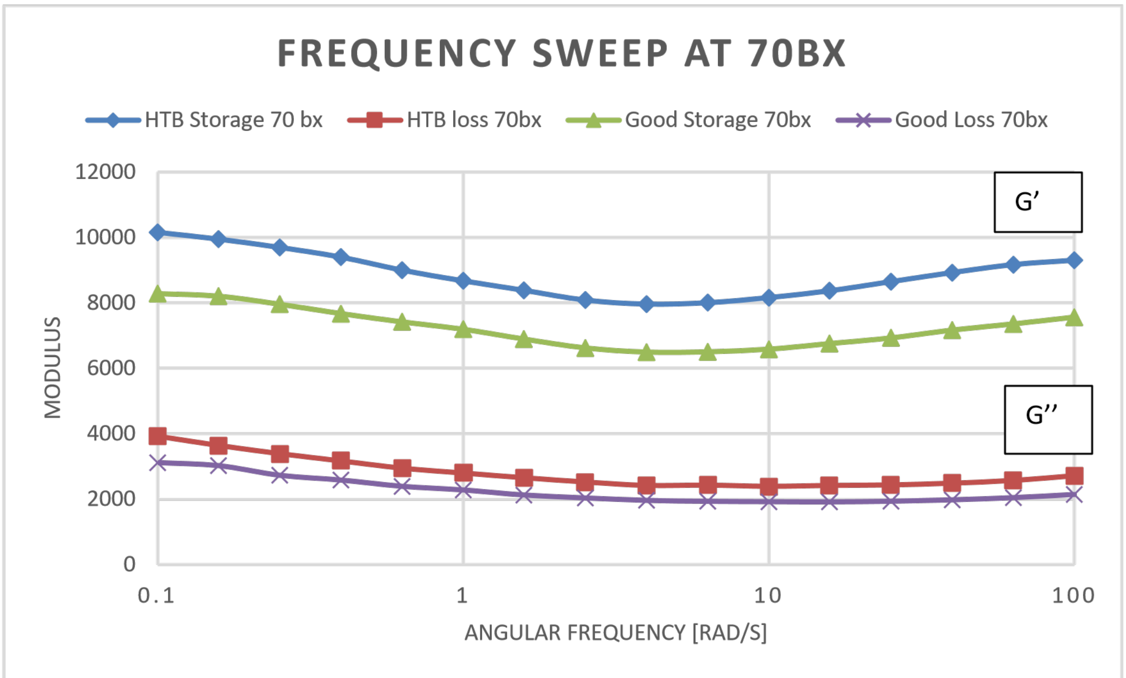

Figure 6.4: Frequency sweep of samples at 70bx

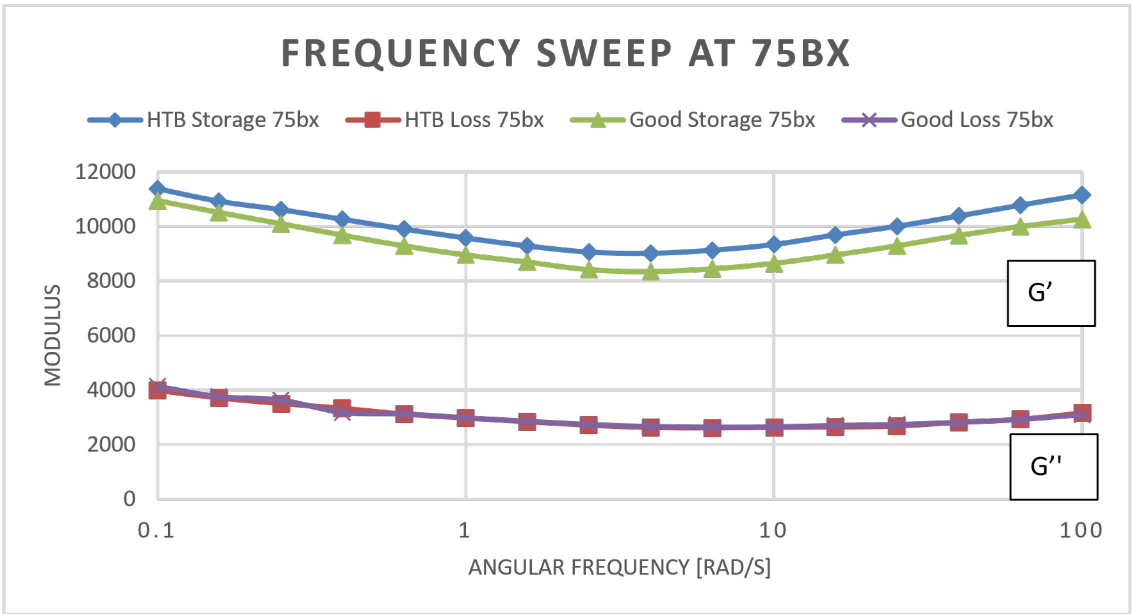

Figure 6.5: Frequency sweep of samples at 75bx

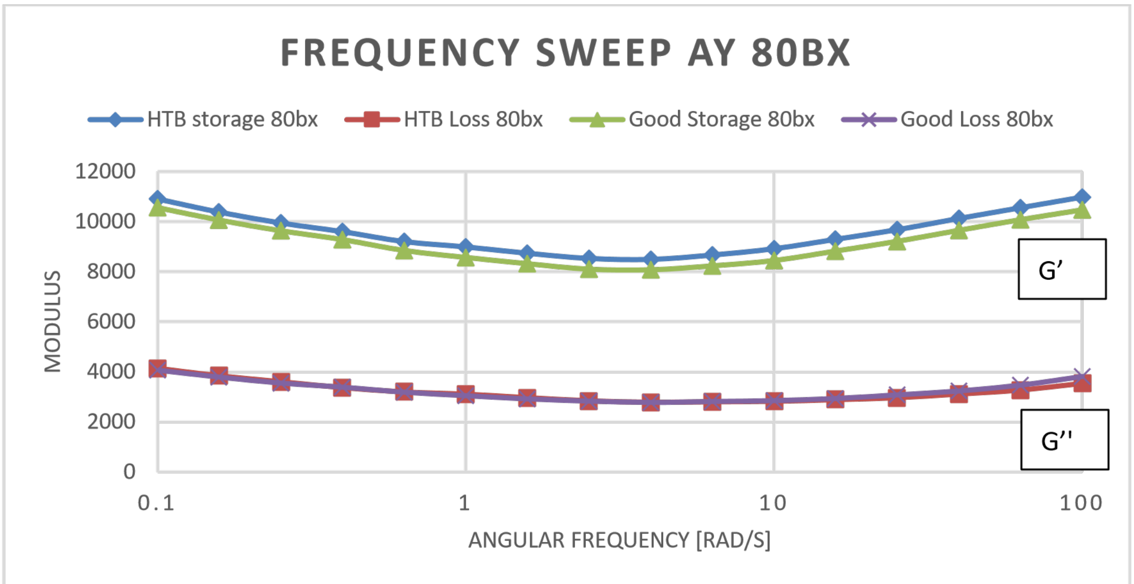

Figure 6.6: Frequency sweep of samples at 80bx

For the analysing of the graphs above, it was important to recall the use of storage and loss moduli. These moduli represent the liquids viscous and elastic properties. In the case of these tests, the angular frequency applied was ramped up over time to determine the change of these properties over an applied force. Frequency sweeps, run at the varying Brixes show the following:

- All samples showed a higher storage modulus than loss modulus implying a higher elastic property than viscous

- For all samples, the good and HTB samples had higher values for both G' and G" showing that it tends to be more of a viscoelastic solid than viscoelastic liquid with the HTB sample having a higher G' than the good sample.
- The greatest differences in the sample rheology was found at 70% Brix where there was a significant increased HTB storage property
- The storage modulus for all samples at the various Brixes are higher for the HTB samples than the good boiling implying a more elastic property in the HTB samples
- The loss modulus for the 70% Brix samples was significantly higher for the HTB sample than the good boiling, while the other Brix tests showed a closer modulus between the two. This was probably due to increased removal of water at higher Brixes while at the lower Brix, the sample held more water

An essential note are the changes of the higher storage modulus. With the storage modulus being representative of the elastic portion of the sample, any change in this parameter would contribute to the hypothesis set forward in this research topic. The HTB samples showed a higher storage modulus that could be linked to the presence of property altering gums. This supports the hypothesis that the changes in the elastic portion of the molasses can be linked to the altered boiling seen in HTB samples.

6.4 Conclusion

This section looked at the rheological and chemical testing of the samples received in order to determine a possible link between the properties and the flow properties experienced during the vacuum boiling stage.

The following points could be observed:

- Rheology shows that at the varying Brixes, there is an increased viscosity in HTB samples
- A higher elasticity within the HTB samples is also a point of interest, showing that the sample is a viscoelastic solid rather than a viscoelastic liquid

At the start of the experimentation, it was required that testing is to be linked to hypothesis that stated that an **increase in gums caused an elastic effect** changing the standard boiling expected for massecuites. The results obtained from these tests coincide with the statements put forward by the hypothesis.

Chapter 7

Discussion & Validations

7.1 Discussion

The purpose of this study was to investigate the mechanism that causes that HTB effect in refinement of sugar. The study involved researching previous ideologies surrounding the issue. This involved analysing how factories resolve the issues surrounding HTB massecuite, as well as investigating theoretical frameworks, that explain the causing mechanism of HTB. A hypothesis was then proposed in chapter 3, where the focus of the study was aimed at testing the validity of the hypothesis. Several aims and objectives were listed in chapter 1, to validify the proposed hypothesis.

The following section will describe how the aims and objectives were met in order.

- Various theories were investigated on the cause of HTB. Many examined potential chemical properties, such as the effects of polysaccharides on the mixture. The Bubbling Theory was of most interest, as it aligns the most with the mechanical nature of the study.
- The vacuum pan was altered as follows:
    - Addition of a sample port that allowed for sample taking and Brix monitoring over the boiling period
    - Addition of a secondary sight glass that allowed monitoring of the upper portion of the pan. This secondary pane was used to prevent entrainment by monitoring the level of sample during boiling
    - Addition of the steam side condenser allowed for sample collection and measurement to monitor heat being let into the system. The steam condensate monitoring was done in the final experimental method to ensure constant boiling over the testing period
    - Stirrer motor was changed to a higher power, AC motor in order to be able to handle the extreme conditions that were predicted to happen when HTB samples were boiled
- The vacuum pan was tested by using a series of different sample types, to determine its capabilities of contributing towards the proposed hypothesis. By initially using a method that required a vacuum pan testing rig to mimic the conditions of massecuite boiling in a factory, it

was possible to look at the system's limitations. Here it was determined, experimentally, that there were difficulties in handling the system at a higher vacuum pressure due to the instability of the samples. Upon heat addition, the samples began to foam and aerate within the pipe, rising in level and causing entrainment. For a factory vacuum pan, the disengagement space is adequate to prevent entrainment; however, the rig was not initially designed for this. Other methods of massecuite handling include using surfactants, like antifoam, to reduce this foaming effect; however, this could not be done because it could have on the sample's rheology. While the test rig could perform the final experiment, these limitations must be considered in the results.

- The testing rig was used to perform the final experiment on 4 main samples: 2 HTB and 2 good samples. These samples experienced a standard boiling procedure. Photographs of each sample was used to try and provide a visual representation of the boiling phenomenon. These results were then compared in terms of their boiling points, as well as their bubble formation. Another collection of data was performed on the rate of mass condensate forming, as the samples were boiled.
- The experimental method developed for the rheometer was representative of research theory and the results provided good insight to the theories of HTB. The rheology tests were run to determine the property changes that are said to be linked to the presence of gums that cause the HTB phenomenon. Using the rheometer, the following was completed:
    - Testing to determine the viscosity of both good and HTB samples by means of flow curve testing. Here, samples were run under the same conditions to compare the viscosity differences among samples. The results of this testing observed a notable difference between HTB and good viscosities with HTB samples having an increasingly higher viscosity as compared to the good boiling samples.
    - To determine the sample viscoelasticity, the samples needed to be run using an amplitude sweep to determine the linear viscoelastic range (LVER) in order to run frequency sweeps capable of determining the viscous and elastic properties. These tests look at the storage and loss moduli that represent the elastic and viscous properties of the liquid respectively. From these tests, the characteristics of HTB was determined and compared to good boiling samples. Both samples had a higher storage modulus, but HTB samples were seen to have this elastic portion having a higher value than in good samples.
    - Crystal content in viscosity was determined during the early stages of testing. Crystal content yielded graphs with problematic results. The rheometer would

not lower to the correct gap size due to the crystal size and content. These crystals prevented the rheometer from lowering and when shear was applied, the tension of the spindle as it tried to lower would increase causing the motor to overcompensate and slam down. This skewed the results and made it difficult to analyse and the testing moved to crystal free liquor

- The determination of the chemical constituents was not part of the scope of this work. The HTB samples were categorised as such based off the factory experience at the given time. The factory from which HTB samples were obtained characterised the HTB samples as being high in gums with increased viscoelasticity. When tested against the good boiling samples using NIRS, general dissolved solids content were higher for HTB and when testing rheologically, HTB samples had a higher viscosity and viscoelasticity than the good samples.

Upon completing the aims and objectives, the data collected needed to be analysed, in order to confirm the accuracy of the hypothesis developed in chapter 3.

7.2 Validation

The following section lists and discusses the initial research questions. An attempt will then be made to answer these questions, through the substantiation of the study. This will also include the results achieved in various sections.

The first question investigates whether the vacuum pan, used for this study, can mimic the results of a factory boiling pan and adequately perform based off the assumptions put forward at MISG. Standard factory vacuum pans are much larger than the test rig used in this study. During the design of the test rig, the dimensions were kept in proportion of that of a factory sized vacuum pan. The test rig was able to achieve a constant pressure of 85kPa vacuum throughout the experimentation, which aligns with the required pressure in factory standard pans. The test rig did have design limitations such as entrainment as a result of aeration of samples, which could interfere with the accuracy of the results. To overcome this, tests needed to be altered around the issues with the rig. With regards to the MISG modelling assumptions, the rig was able to adequately perform based off the mathematical assumptions being put forward. The experimental method maintained heat inlet to the system where latent boiling occurred and water condensate was removed. Uniform boiling without burning and deposition onto the heating surface was experienced within the rig. Overall, the test rig was able to simply replicate the boiling process as if they occurred in a standard factory, however future work may need alterations to disengagement space to prevent sample intake to the condensate collection side.

The second question investigates whether the vacuum pan can provide a good visual presentation of the boiling process occurring. While the various samples were boiling, there was a noticeable visual difference between HTB samples, and standard samples. One was clearly able to see the bubble formation and the bubble flow, as well as the differences in them during the boiling process. The photographs, shown in this dissertation, show a glare on the front panel. This occurs due to the lighting in the laboratory. For maximum viewing to occur, the experimentation must be performed in a better lit scenario.

The third question investigates whether the test rig can handle the harsh effects of boiling HTB samples. Even with the lack of samples, it was possible to run HTB samples on the vacuum pan testing rig. It was assumed that there may be issues where the altered viscoelastic properties would cause the issues described within the literature review (refer to page 12). This was not seen to be a problem and, while it did take longer to get HTB samples to the same °Brix as good boiling samples, it was still completed using the planned experimental procedure. It was possible to remove water from HTB samples at the same conditions used for good boiling. This however was not part of the problems with the testing rig. Aeration and entrainment was a problem with both kinds of samples that would require equipment upgrades should further testing be pursued. However, with regards to the question being analysed, the system was able to handle HTB samples in terms of the applied experimental procedure.

The fourth question investigates the differences in the rheology and NIRS results between the standard and HTB samples. For the rheology study, the samples were monitored according to various Brix levels: 70, 75 and 80. This eliminated the possibility of Brix levels affecting the final results, as it was kept constant among the samples. The samples were brix tested in 15 minute intervals, throughout the boiling process. The process was repeated thrice to provide a more accurate result. With respect to the NIRS readings, there was a higher reading of sucrose present in the HTB samples. This coincides with the theorem that a higher gum level will retain sucrose. The dry solids percentage in HTB was also found to be higher, representing a higher concentration of impurities. The rheology results produced a viscosity comparison between the samples. At 80 Brix, the HTB samples showed a significant spike in viscosity, when compared to standard samples. While these differences seem large, they occur at a microscopic scale. This is most likely a result of the severity of the HTB samples being too low to create large scale visual problems.

The fifth question deals with rheological changes in massecuites impacting the boiling and bubbling regime experienced within the vacuum pan. Rheologically speaking, the differences between viscosity readings was on the lower end as mentioned before. Visually, the differences between the two samples was nothugely different but still notably different among the samples. Between good boiling and HTB, bubble difference was not great. Good boiling had bubbles of varying sizes while HTB had many small bubbles. Where boiling differed dealt with aeration as HTB samples did not aerate when boiling as much as good boiling samples. This was likely linked to density differences of the sample. Visualisation of boiling was noted using the samples received and however, a greater difference would likely be prominent ina worse-case of HTB sample be tested in future work.

The last question investigates the issues found with the testing rig. To effectively process sugar, a constant vacuum pressure is required to be maintained. This results in less heat being required for the system, which can result in the caramelisation of the sample before boiling. The testing rig could not hold an effective vacuum pressure, therefore all the results produced are not truly representative of a vacuum pan. The calandria was required to be filled completely with massecuite. When massecuite boils, it produces a foam, which is countered by a defoamer. A defoamer was not used in this study, as it would have altered the surface-tension properties of the substance. As a result, the calandria was not filled to the correct head. This resulted in entrainment occurring. Due to the possibility of entrainment occurring, the steam inlet must be manipulated during the boiling process. Boiling required a constant steam inlet. This produced the random scatter graph produced.

7.3 Hypothesis Validation

The following section is going to investigate the validity of the hypothesis. The layout will follow the same overview order of the hypothesis framework in chapter 3.

The hypothesis states that an increase in viscoelasticity, which is found in HTB samples, will lead to a difficulty in ebullition, as well as a higher boiling temperature requirement. As stated in the previous discussion, the rheology results ,from testing with the rheometer, showed that HTB samples possess a higher viscoelasticity, when compared to standard samples. This was especially noticeable at high Brix levels. This characteristic was crucial to the hypothesis, and any further statements will assume that the HTB samples have a higher viscoelasticity.

The hypothesis then examines the ebullition in both substances. During the visual boiling experiment in chapter 5, there were differences in the bubble formation. Good samples produced uniform bubbles that circulated well within the calandria and rose to the top. HTB samples formed smaller bubbles that had difficulty circulating at higher Brix levels. The amount of condensate collected from the standard samples were higher than HTB samples, even with HTB tests had a higher volume of molasses. This concludes the removal of water through evaporation was far easier to achieve in standard samples. Evaporation occurs effectively when a steady rate of bubbles form and rise to the surface of the mixture. The bubbles begin to grow until the surface tension of the fluid is overcome, and they burst. A higher viscoelasticity will result in a higher surface tension of the fluid. According to the hypothesis, this directly correlates with the statement of HTB samples producing less condensate, due to the higher viscoelastic property.

The boiling points between the samples were analysed at the previously mentioned Brix levels 70, 75, and 80. The results were taken from the experiment where the pressure of the system was maintained at 50 kPa absolute. This was the highest pressure that could be maintained before entrainment occurred. At all 3 Brix levels, the HTB samples achieved a boiling point elevation of roughly 1,5 °C. This agrees with the hypothesis, which states that HTB samples will require a higher boiling point. This difference is most present at 80 Brix, where the dissolved solids contents are highest and water is lowest. This suggests that the causing mechanism of this phenomenon is most likely the viscoelasticity.

The work was able to support the hypothesis, however, the limitations of the experimental procedures cannot be ignored. While the hypothesis does show a strong sense of validity, further experimentation is required to further substantiate the statement

Chapter 8

Conclusion

8.1 Discussion

This research study was able to provide further insight into the HTB phenomenon and the effects that it has on vacuum pan boiling. By first testing dosing of synthetic white sugar syrup, and factory grade massecuite, it was possible to determine the boiling limitations of the testing apparatus. The initial substance testing phases allowed for the finalisation of the experimental methods, for both the vacuum pan and rheological testing. When boiling the molasses, it was possible to mimic the boiling portion of massecuite. The dark colour limited the visual monitoring of the boiling process, however, the view into the pan was adequate in observing the boiling differences linked to the HTB affect. The rig limitations led to the evolution of the topic that combined the BPE study to the bubbling study. These studies are found to work hand in hand when analysing the viscoelastic effect. By using this method, it was possible to determine key characteristic differences between samples, however, it was still difficult to overcome the problems experienced with maintaining the system boiling parameters required, specifically with vacuum pressure. Using the photographed boiling differences and the changes in evaporation between samples, it was possible to determine differences in ebullition, BPE and viscoelasticity that have been linked to the ones noted within factories. These results were able to support the hypothesis, but it was important to remember the errors due to the many testing issues that had to be overcome, like the foaming effects that led to different sample amounts, and limited sample quantities that yielded fewer tests that would be optimal. Even with these problems, it was still possible to see these key differences in the visual ebullition effect and BPE differences of samples. Looking at the rheology and NIRS readings, it was also possible to see a difference in the viscoelastic properties between the samples that were described by the hypothesis. The core idea of the study was achieved with difficulty, and the changes occurring between HTB and good boiling massecuites were notable. However human error, machine errors and limitations were also considered to contribute to errors in the results, and should be considered for future research into this topic.

8.2 Summary of Contributions

This research study contributed to the sugar boiling industry by providing more information into the topic of the HTB phenomenon. The contributions to the field of sugar manufacturing is in the form of the testing that was completed and the results that were noted. The tests and methods used act as a first phase example of using the research put forward by MISG to test the theory of bubble suppression as the mechanism linked to the HTB effect. The work in this dissertation lays down the foundation for future testing in this field of study. The hypothesis and experimental method created to test the theory of bubble suppression are correct in modelling the tests around the apparent boiling point elevation between samples. This method can be used for further research into the topic.

The limitations of the designed rig can be found throughout the dissertation. Looking at the design and the problems that occurred when using it, it is possible to create a better testing rig that would allow for the visualisation of boiling within a calandria under vacuum. This rig, taking into account the limitations that were experienced in the rig used for this experimentation, could be better equipped to test the hypothesis of this work.

Using the vacuum pan boiling rig, it was possible to look into the boiling regime occurring within the calandria tube. These tests were completed with both good boiling molasses as well as ones displaying HTB properties. The characteristic changes that were noted between the samples can be retested and used for further research into how these characteristics can be linked to the HTB effect. The errors and problems that were experienced act as guidelines to prevent further mistakes.

The method used for experimental testing of molasses using the rheometer can be used to create a better method of testing for sugar substances. The knowledge received from testing with massecuites can also be used for further expansion of rheology testing of massecuites using a rheometer to determine a quick method that would be capable of acting as an indicator of HTB in a sample.

The NIRS results received from testing both the good and HTB samples were completed using the standard method was developed for the system. The numerical results gained that show the composite differences between samples can be used for further research into how the changes in these components come into play with regards to the characterisation of HTB substances. The results, found in appendix B, can be used to determine the range of acceptable component percentage that would be used to classify a HTB sample.

Using the experimental procedures, as well as the results, limitations of the tests and testing apparatus, it is possible to determine ways to recreate the testing rig and experimental method to accommodate pan boiling conditions and retest this hypothesis.

8.3 Suggestions for Further Research

Through experimental testing it was possible to look at the differences occurring when testing HTB substances against good boiling samples. Many limitations were experienced when running these experiments and thus the possibility of future research were identified.

The following limitations can lead to possible future work:

- The testing rig was limited due to disengagement height and large sample volume leading to entrainment. For future testing it would be important to consider the redesign of a vacuum pan test rig that has a larger disengagement space capable of dealing with the foaming effect or allowing for smaller sample mass.
- Limitations in rig control came about due to manual controlling of system- limited budget. This meant that the work was kept to being manual. A good recommendation would be adding digital controls to decrease the variability and errors on results
- Looking more into the chemical indicators of HTB and how they affect the boiling regime. It may also be of interest to research the constituents of the condenate formed from boiling.
- Looking into the determination of the causative compounds that create the HTB viscoelastic effects
- The development and formation of a standard rheological testing procedure for molasses and massecuites capable of dealing with the crystal content effect and also with high temperature that would not cause caramelisation and burning
- Testing on the vacuum pan to be completed in tandem with rheological testing in order to determine at which point in boiling there would be a deviation to the viscosity and the dependence on the water content of the mixture.
- Testing of the samples before and after boiling in order to the changes that occur as a result of boiling.

References

Anton-Paar (2020) *AntonPaar-Modular Compact Rheometer 102/302/502*. Available at: https://www.anton-paar.com/za-en/products/details/rheometer-mcr-102-302-502/ (Accessed: 21 May 2020).

Anton Paar (2020) *Anton Paar: Basics of Rheology*, *Anton Paar Wiki*.

AntonPaar (2020a) *Anton Paar-Frequency sweeps*, *https://wiki.anton-paar.com/za-en/frequencysweeps/*. Available at: https://wiki.anton-paar.com/za-en/frequency-sweeps/.

AntonPaar (2020b) 'Temperature Control for MCR Rheometers'.

Atago (2022) *Atago Products*. Available at: https://www.atago.net/en/products-pal-top.php#pal-spec.

Boyer, H. (2001) *Sugar Batch Vacuum Pan*, *Research Gate*. Available at: https://www.researchgate.net/figure/Sugar-batch-vacuum-pan_fig1_223021398.

Broadfoot, R., Miller, K. F. and McLaughlin, R. L. (1998) 'Rheology of high grade massecuites', *Proceedings of Australian Society of Sugar Cane Technologists*, 20, pp. 388–397.

Bukhari, M. M. *et al.* (2015) 'Investigations of the influence of dextran on sugar cane quality and sugar cane processing in Kenana sugar factory', *Journal of Chemical and Pharmaceutical Research*, 7(4), pp. 381–392. Available at:

https://www.researchgate.net/publication/301633455_Investigations_of_the_influence_of_dextran_on_sugar_cane_quality_and_sugarcane_processing_in_kenana_sugar_factory.

Chhabra, R. and Richardson, J. (2008) *Non-Newtonian Flow and Applied Rheology: Engineering Applications*.

Du Clou, H. *et al.* (2015) 'Quantifying Pan Boiling Behaviour', in *Proc S Afr Sug Technol Ass (2015)*, p. 88:288.

Du Clou, H. and Walford, S. N. (2012) 'Analytical study of gums found in final molasses from six South African mills for the 2011/2012 milling season', *Proc S Afr Sug Technol Ass*, 85, pp. 295–311.

Duffaut, E. and Godshall, M. A. (2004) 'MOLECULAR PROBES FOR ASSESSING BOILING DIFFICULTIES', *Sugar Processing Research Institute-Conference on Sugar Processing Research*, 3156, pp. 403–416.

Eccheverri, L. F. and Rein, P. W. (2005) 'Numerical and experimental study of the flow in vacuum pans', *Proceedings of the International Socierty of Sugar Cane Technologists*, 25, pp. 212–222.

Eccheverri, L. F., Rein, P. W. and Acharya, S. (2007) 'Measurements and CFD Simulation of the flow in vacuum pans', *Proceedings of the International Socierty of Sugar Cane Technologists*, 26, pp. 1341–1353.

Eggleston, G., Côté, G. and Santee, C. (2011) 'New insights on the hard-to-boil massecuite phenomenon in raw sugar manufacture', *Food Chemistry*. Elsevier Ltd, 126(1), pp. 21–30. doi: 10.1016/j.foodchem.2010.10.038.

Eggleston, G., Morel du Boil, P. and Walford, S. (2008) 'A review of sugarcane deterioration in the United States and South Africa', *South African Sugar Technologist Association Conference*, pp. 72–85.

Fowkes, N. *et al.* (2017) 'Hard to boil massecuite', *Proceedings MISGSA*, pp. 30–53. Available at: https://www.wits.ac.za/media/wits-university/ conferences/misgsa/documents/Hard to Boil Massecuite.pdf Accessed: 18 February 2019. 24 pp. %0A.

Gounden, T. and Walthew, D. (2018) 'Nirs As a Tool for Improved Process Monitoring', *Proceedings of South African Sugar Technologists Association*, 91, pp. 350–356.

Hugot, E. (1986) *Handbook of Cane Sugar Engineering- Third, Completely Revised Edition*.

Jaywant, S. A., Singh, H. and Arif, K. M. (2022) 'Sensors and Instruments for Brix Measurement: A Review', *Sensors*, 22(6), pp. 1–20. doi: 10.3390/s22062290.

Kadwa, M. (2018) *Cane payment in the SA Sugar Industry explained*, *Shukela*. Available at: https://shukela.co.za/2018/09/05/cane-payment-in-the-sa-sugar-industry-explained/.

Koster, K. C. (CG S. S. L. *et al.* (1992) 'Some Notes on Abnormal Processing Difficulties', *Proceedings of South African Sugar Technologists Association*, (June), pp. 127–130.

Lionnet, G. R. E. and Reid, J. (1993) 'Pilot plant processing of cane stalks into sugar', *Proceedings of the South African Sugar Technologists Association*, (June).

MacGillivray, A. W. and Matic, M. (1970) 'Composition of South African final molasses', *Proceedings of the South African Sugar Technologist Association*, (June), pp. 81–87.

Madho, S. (Sugar M. R. I. (2009) *Technical Note No. 14/09- Evaporation rates of South African refractory molasses*.

Mafunga, W. P. (2014) *AN OVERVIEW OF SUGARCANE PAYMENT SYSTEMS , ECONOMICS AND THEIR INFLUENCES ON THE LENGTH OF THE MILLING SEASON*.

Martin, L. A. (2008) *Biochemical and Microbiological Changes in Sugarcane Stalks During a Simulated Harvest-to-Crush Delay*.

Meade, G. P. and Chen, J. C. P. (1977) *Cane Sugar Handbook: A manual for Cane Sugar Manufacturers and Their Chemists*.

Mezger, T. G. (2006) *The Rheology Handbook*. 2nd edn, *The Rheology Handbook*. 2nd edn. Vincentz Network GmbH & Co. doi: 10.1515/9783748600367-009.

Morel Du Boil, P. G. (Sugar M. R. I. (2020) 'An overview of the impact of poly- and oligosaccharides on sugar quality', *Raw SUgar Quality Workshop*, pp. 1–16.

Naidu, N. *et al.* (2017) *Massecuite Boiling Visualisation*. University of KwaZulu-Natal.

Nel, S. (2014) 'Microbial Diversity Profiling in Sugarcane Processing : What , Why and How ?', *Proceedings of the South African Sugar Technologists Association*, 87, pp. 246–254. Available at: https://sasta.co.za/?mdocs-file=5525.

Nel, S. (2018) 'Understanding Dextrans: a presentation on the basics of gums and dextrans', in *SASTA 2018- Sugar Processing*, pp. 1–28. doi: 10.1245/s10434-019-07207-z.

Ravno, A. B. and Purchase, B. S. (2005) '2005_Ravno_Dealing With Dextran in the .Pdf', *Proc S Afr Sug Technol Ass*, 79, pp. 28–47.

Rein, P. W. (2007) *Cane Sugar Engineering*.

Rein, P. W., Acharya, S. and Echeverri, L. F. (2004) *Circulation in Vacuum Pan*. Louisiana.

Rouillard, E. E. A. (1985a) *A study of boiling parameters under conditions of laminar non-newtonian flow with reference to massecuite boiling*. Durban, South Africa.

Rouillard, E. E. A. (1985b) 'Massecuite Boiling', *Proceedings of The South African Sugar Technologisys Association*, (June).

Sahadeo, P. (1998) 'The effect of some impurities on molasses exhaustion', *Proceedings of South African Sugar Technologists Association*, 72, pp. 285–289.

Saska, M. (2002) 'Boiling Point Elevation of Technical Sugarcane Solutions and its use in Automatic Pan boiling', *International Sugar Journal*, 104(1247), pp. 500–507.

Saska, M. (2003) 'Heat Transfer Rates in Boiling of Cane Syrups and Molasses and the Phenomenon of "Hard-to-Boil" Massecuites'.

Saska, M. (2005) 'Boiling rate, heat transfer and viscosity of technical sugarcane liquors', *Proceedings og ISSCT*, 25, pp. 51–61.

Schoonees, B. M. and Pillay, V. (2004) 'A new filtration system for gum analysis in raw sugar and molasses', *Proc S Afr Sug Technol Ass*, 78, pp. 565–568.

Shah, S. (2017) *An investigation into the viscosity of C-massecuite using a pipeline viscometer, University of Natal, Durban*.

Shah, S., Lokhat, D. and Peacock, S. D. (2017) 'An investigation into the viscosity of C-massecuite using a pipeline viscometer', *International Sugar Journal*, 119(1428).

Simpson, R. and Naidoo, Y. (2010) 'Progress in Improving Laboratory Efficiencies Using Near Infrared Spectroscopy (Nirs)', *Africa*, 27, pp. 1–9.

South African Sugar Association (2020) *The Sugar Industry at a Glance*, *SASA*. Available at: https://sasa.org.za/the-sugar-industry-at-a-glance/.

Appendix A

Section A.1

Results that were received during the evolution and troubleshooting phase. In order to create the pure syrup solution used in the white sugar syrup phase of testing, the SMRI TachyX method of determining the total sugar and water required to reach a supersaturated sugar syrup was used. This calculates using the equations presented by Smith 1992 and Charles, 1960. The following equations are used to calculate the masses of water required to receive a solution at a specific supersaturation Brix:

Smith (1992) for syrup density:

$$Syrup\ Density = \left(1 + Bx_{syrup}\left(\frac{Bx_{syrup} + 200}{54000}\right)\right)\left(1 - \left(0{,}036\frac{T_{syrup} - 20}{160 - T_{syrup}}\right)\right)$$

$$m_{solution} = V_{syrup} \times Density_{solution}$$

$$m_{sugar} = V_{syrup} \times Density_{sugar}$$

$$m_{water} = m_{solution} - m_{sugar}$$

Charles (1960) for saturation Brix:

$$Bx_{sat} = 64{,}397 + (0{,}07251T_{syrup}) + (0{,}002057T_s^2) - (0{,}000009035T_s^3)$$

$$SSC = \frac{\frac{w_s}{w_w}}{\left(\frac{w_s}{w_w}\right)_{at\ saturation}}$$

Where SSC= supersaturation coefficient, w_s= mass of sugar in the solution, w_w= mass of water in the solution. After further derivation, the following equation can be used:

$$SSC = \frac{\frac{Bx_{syrup}}{100 - Bx_{syrup}}}{\frac{Bx_{sat}}{100 - Bx_{sat}}}$$

Table A.1.1: Preparation of pure syrup solution calculation

Preparation of TachyX pure syrup solution		
Variable	**Units**	**Value**
Syrup volume	L	30
Syrup Brix	%	67,0
Syrup temperature (T)	°C	25
Syrup density	kg/L	1,330
Mass of solution	kg	39,89
Mass of sugar	kg	26,72
Mass of water	kg	13,16
Saturation Brix at T	°Bx	67,4
Supersaturation coefficient	SSC	0,984064205

White Sugar syrup and starch tests

These results were yielded for the tests run with white sugar syrup and starch tests.

Test date	10 April 2018		Sample	Synthetic syrup (Mock massecuite)	
Boiling Duration	80 minutes				
Total Sample volume	30 litres	**Volume used**	25 litres	**Brix**	65,1 %

Table A.1.2: Synthetic syrup test 1 (mock massecuite) boiling (no starch)

Time [min]	**Pvac [kPa]**	**Pvac,abs [kPa]**	**Tsump [^{0}C]**	**Tcond,steam [^{0}C]**	**Mcond [kg]**	**Msteam [kg]**	**Bx [%]**
0	65	37,5	65	0	0,2	0	65,1
10	75	26,2	73	63	1,72	6,8	66,4
20	80	24,6	73	68	3,16	7,8	78,9
30	80	24,6	75	70	5,34	7,5	81,3
40	80	24,6	74	67	6,34	8,3	83,2
50	80	24,6	75	65	7,34	8	85,6
60	80	24,6	75	75	8,78	7,8	85,9
70	80	24,6	74	70	9,06	8	87
80	80	24,6	75	68	9,94	8,4	89

Total test time was 80 minutes for first white sugar test and on each interval, samples were taken. These samples however could not be brix or rheometrically tested due to instantaneous crystallisation. Refer to chapter 4, section 4.3 for the information on testing.

Test date	11 April 2020	Sample	Synthetic syrup (mock massecuite)

Boiling Duration	80 minutes				
Total Sample volume	30 litres	**Volume used**	25 litres	**Brix**	65,4 %

Table A.1.3: Synthetic syrup test 2 (mock massecuite) boiling (no starch)

Time [min]	**Pvac [kPa]**	**Pvac,abs [kPa]**	**Tsump [°C]**	**Tcond,steam [°C]**	**Mcond [kg]**	**Msteam [kg]**	**Bx [%]**
0	68	29	75	0	0,2	0	65,1
10	65	30,2	71	63	1,8	7,80	69,8
20	95	5,3	70	68	3,32	7,10	80,6
30	90	9,38	69	70	5,24	6,80	82,1
40	85	13,6	73	67	6,68	8,00	85,4
50	88	12	74	65	7,4	8,20	87,0
60	89	10,8	73	75	8,82	8,30	87,0
70	89	10,8	73	70	9,10	8,20	88,0
80	89	10,8	76	68	9,96	8,10	89,5

Test date	05 June 2018		Sample	Synthetic syrup and starch addition (mock HTB)	
Boiling Duration	80 minutes				
Total Sample volume	30 litres	**Volume used**	25 litres	**Brix**	65,4 %

Table A.1.4: Doped synthetic syrup test 1 (mock massecuite) boiling (with starch)

Time [min]	Pvac [kPa]	Pvac,abs [kPa]	Tsump [⁰C]	Tcond,steam [⁰C]	Mcond [kg]	Msteam [kg]	Bx [%]
0	90	9,38	75	0	0	0	65,4
10	90	9,38	75	63	0,30	6,90	66,4
20	85	13,6	70	68	0,58	6,50	64,4
30	85	13,6	69	70	0,72	7,20	67,8
40	80	24,6	70	67	0,89	8,40	71,6
50	88	12	70	75	1,06	8,20	63,6
60	89	10,8	71	65	1,11	8,40	74,4
70	80	24,6	73	70	1,20	8,50	84,2
80	75	26,2	74	68	1,38	8,60	94,8
	Time when starch dose was added						

Section A.2

Massecuite sample tests

These results were obtained from testing with massecuites (chapter4, section 4.4). Due to the erratic boiling patterns, problems with entrainment and inconsistencies in tests, there was no sample collection to test the Brix.

Test date	September 2019		Sample	Normal Massecuite	
Boiling Duration	120 minutes				
Total Sample Volume	30 litres	**Volume used**	25 litres	**Brix**	69,9%

Table A.2.1: Massecuite test 1

Time [min]	Pvac [kPa]	Pvac,abs [kPa]	Tsump [⁰C]	Mcond [kg]	Msteam [kg]

0	80	24,6	22	0	0
15	75	26,2	25	0	8,865
30	75	26,2	30	0	11,77
45	72	27,4	42	0	9,88
60	72	27,4	60	0,6	8,66
75	65	37,5	78	0,64	4,1
30	60	40	78	0,9	4,8
105	60	40	78	1,38	10,92
120	60	40	78	--	5,59
	Entrainment occurred				

Test date	September 2019		Sample	Normal Massecuite	
Boiling Duration	135 minutes				
Total Sample Volume	30 litres	**Volume used**	25 litres	**Brix**	70,1%

Table A.2.2: Massecuite test 2

Time [min]	Pvac [kPa]	Pvac,abs [kPa]	Tsump [ºC]	Mcond [kg]	Msteam [kg]
0	70	28,12	23	0	0
15	70	28,12	26	0	10,175
30	69	28,52	41	0	8,055
45	70	28,12	50	0,01	8,24
60	58	43,79	60	0,04	10,16

75	60	40	71	0,04	10,8
90	60	40	78	0,10	8,61
105	58	43,79	80	0,52	11,26
120	60	40	82	0,52	12,77
135	56	45,35	83	--	10,73
	Entrainment occurred				

Test date	September 2019		Sample	Normal Massecuite	
Boiling Duration	150minutes				
Total Sample Volume	30 litres	**Volume used**	25 litres	**Brix**	68,8

Table A.2.1: Massecuite test 3

Time [min]	Pvac [kPa]	Pvac,abs [kPa]	Tsump [ºC]	Mcond [kg]	Msteam [kg]
0	70	28,12	25	0	0
15	68	35,29	40	0	7,74
30	60	40	69	0	8,45
45	62	38,71	75	0,52	8,51
60	65	36,92	70	0,61	9,89
75	65	36,92	72	0,78	8,14
90	61	40	75	1,44	11,35
105	59	40,68	75	1,51	10,75
120	55	43,63	74	1,71	11,25

135	62	38,71	75	2,01	11,14
150	61	40	72	2,11	11,25
	Entrainment occurred				

Appendix B

Final Results

Section B.1

Vacuum Pan Boiling results

The results that are found in this section detail the work completed under the final experimental procedure and shows both good and HTB samples.

For these experiments it is important to look at the boiling temperature that would be required at these lower hydrostatic heads and low vacuum pressure.

Table of calculated boiling points for massecuites under vacuum pressure

Submerged depth	0,2 m																	
B [°x]\P [kPa]	15	20	25	30	35	40	45	50	55	60	65	70	75	80	85	90	95	100
60	59,675694	65,176042	69,721146	73,613735	77,030127	80,082498	82,846854	85,3771999	87,7133535	89,8855568	91,9173475	93,8274227	95,630894	97,3401583	98,9655179	100,515632	101,997853	103,418477
65	60,421184	65,929718	70,484183	74,386298	77,812017	80,873382	83,646361	86,1849587	88,5290069	90,7087705	92,7478111	94,6648489	96,4750175	98,1907338	99,8223185	101,378448	102,866488	104,292751
70	61,422057	66,946557	71,516977	75,434377	78,874557	81,949564	84,735422	87,2862045	89,6418111	91,8325684	93,8820929	95,8091535	97,6289259	99,3538645	100,994322	102,559004	104,055302	105,489549
75	62,840942	68,394385	72,991726	76,933966	80,397112	83,49345	86,299224	88,8686908	91,2419047	93,4493212	95,5146644	97,4567936	99,2909612	101,029687	102,68338	104,260794	105,769363	107,215459
80	65,012257	70,618297	75,262508	79,246946	82,748494	85,88011	88,718551	91,3184748	93,7202489	95,9545797	98,045395	100,011721	101,86895	103,629718	105,304534	106,902237	108,430333	109,895259
85	68,743064	74,451112	79,183809	83,246632	86,81874	90,014672	92,912325	95,5672032	98,020323	100,302898	102,439259	104,448762	106,347068	108,147038	109,859371	111,493065	113,055767	114,554032
90	76,563735	82,503917	87,434643	91,671052	95,398296	98,734897	101,76154	104,53576	107,100105	109,48697	111,721621	113,824164	115,810875	117,695122	119,488031	121,198963	122,835873	124,405582
95	102,02197	108,75646	114,35835	119,17946	123,42702	127,23393	130,69078	133,862284	136,796317	139,52938	142,089959	144,500742	146,780106	148,943155	151,002465	152,968624	154,850633	156,656214

Submerged depth	0,4 m																	
B [°x]\P [kPa]	15	20	25	30	35	40	45	50	55	60	65	70	75	80	85	90	95	100
60	62,599688	67,56765	71,755434	75,39043	78,611677	81,510715	84,151171	86,5791557	88,8292072	90,9278984	92,8961344	94,7506728	96,5051634	98,1708799	99,7572467	101,272227	102,722612	104,114245
65	63,413054	68,379014	72,568769	76,207693	79,433876	82,338368	84,98453	87,4183175	89,6741775	91,7786287	93,7525438	95,6126615	97,3726211	99,0436911	100,635294	102,155394	103,610784	105,007311
70	64,488017	69,45883	73,656487	77,304597	80,540458	83,454737	86,1106	88,5539047	90,8190499	92,9325328	94,91522	96,7838525	98,5520769	100,231171	101,830569	103,358245	104,821004	106,224703
75	65,990425	70,977614	75,193115	78,8592	82,112649	85,043925	87,716132	90,1751234	92,4553216	94,5832591	96,5798412	98,4618478	100,242962	101,934498	103,545919	105,085229	106,559261	107,973894
80	68,261354	73,286031	77,537547	81,237649	84,5231	87,484503	90,185137	92,6710282	94,9767564	97,1289934	99,1487663	101,052961	102,855352	104,567333	106,19844	107,756737	109,249112	110,681491
85	72,124	77,230379	81,55593	85,323579	88,671143	91,690078	94,444345	96,9805172	99,333613	101,530663	103,59299	105,537727	107,378856	109,127947	110,794687	112,38727	113,912698	115,376997
90	80,15944	85,464116	89,963914	93,88745	97,376419	100,52503	103,39928	106,047251	108,505163	110,800983	112,956788	114,99033	116,916105	118,746112	120,490404	122,157487	123,75463	125,288095
95	106,18729	112,1942	117,3013	121,76242	125,73535	129,32528	132,60604	135,631504	138,442311	141,069876	143,539029	145,869747	148,078362	150,1784	152,181201	154,096368	155,932112	157,695507

Good boiling sample 1

Table B.1: Table of results for good boiling sample 1 for vacuum pan boiling

Test date	26/02/2020		Sample	Good Boiling Sample	
Total Sample mass	27 kg	**Mass used**	27 kg	**Undiluted Brix**	82,1%
Required Brix	70%	**Mass calc**	31,667kg	**H2O required**	4,667kg
Hydrostatic head in the pipe (on the glass) **Volume within vacuum pan**			24cm Approximately 10,265 litres		

Time [min]	**Pvac [kPa]**	**Pvac,abs [kPa]**	**Tprobe [^{0}C]**	**Tsump [^{0}C]**	**Mcond [kg]**	**Msteam [kg]**	**Bx [%]**	**NIRS bx [%]**	**Mcond,theo [kg]**
0	65	50,8	15,7	15	0	0	70,133	70,1	0
15	50	50,8	88	20	0,16	4,775	71,433	71,5	0,529
30	50	50,8	94,2	77	0,38	5,53	73,067	73,16	0,613
45	50	50,8	93,7	75	0,68	7,125	74,067	73,34	0,066
60	50	50,8	94,1	76	0,96	5,685	74,078	73,64	0110
75	50	50,8	92,5	73	1,14	5,655	74,100	74,13	27,000
90	50	50,8	92,3	75	1,26	5,305	74,733	74,26	0,047
105	50	50,8	93,5	75,5	1,36	6,725	74,700	75,17	0,327
120	50	50,8	93,2	75	1,42	6,205	75,267	75,37	0,072
135	50	50,8	92,7	74	1,54	5,27	75,400	75,79	0,150
150	50	50,8	92,8	75	1,72	5,5	75,767	76,12	0,117
165	50	50,8	94,3	78	1,78	5,65	76,567	76,84	0,253
180	50	50,8	94,7	78	1,84	5,05	77,567	76,74	-0,035
195	50	50,8	93,6	75	2,02	6,28	78,233	77,8	0,368

210	50	50,8	94,8	75,5	2,12	5,535	79,267	78,92	0,383
225	50	50,8	97,8	79	2,2	5,42	79,267	79,53	0,207
240	50	50,8	98,8	81	2,24	5	80,033	79,45	-0,027
255	50	50,8	99,2	82	2,24	5,35	80,000	80,1	0,219

Good Boiling Sample 2

Table B.2: Table of results for good boiling sample 2 for vacuum pan boiling

Test date	04/03/2020		Sample	Good Boiling Sample	
Total Sample mass	27 kg	**Mass used**	27 kg	**Undiluted Brix**	82,1%
Required Brix	70%	**Mass calc**	31,667kg	**H2O required**	4,667kg
Hydrostatic head in the pipe (on the glass)			24cm		
Volume within vacuum pan			Approximately 10,265 litres		

Time [min]	**Pvac [kPa]**	**Pvac,abs [kPa]**	**Tprobe [ºC]**	**Tsump [ºC]**	**Mcond [kg]**	**Msteam [kg]**	**Bx [%]**	**NIRS bx [%]**	**Mcond,theo [kg]**
0	65	50,8	13,4	13	0	0	69,4	70,1	0,000
15	50	50,8	88,2	54	0,06	8,185	69,400	70,1	0,000
30	50	50,8	92,3	76	0,58	7,515	69,967	70,5	0,138
45	50	50,8	90,4	80	0,8	5,1	70,467	71,19	0,236
60	50	50,8	92,5	83	1,18	5,58	73,1	72,61	0,477
75	50	50,8	93,8	82	1,38	5,505	74,1	73,415	0,267
90	50	50,8	94,3	84	1,42	5,615	74,6	74,94	0,496
105	50	50,8	94	83	1,54	5,495	75,633	75,443	0,163
120	50	50,8	94,6	83	1,58	5,57	75,967	75,78	0,108
135	50	50,8	93,9	82	1,7	4,485	76,533	76,55	0,245
150	50	50,8	94,9	82	1,8	6,205	77	77,025	0,150
165	50	50,8	95,6	80	1,98	4,74	78,267	77,85	0,258
180	50	50,8	96,8	80	2,06	5,635	79,087	78,07	0,069
195	50	50,8	98,9	80	2,14	5,3	79,267	78,47	0,124
210	50	50,8	96,5	82	2,32	6,045	79,7	79,15	0,209

225	50	50,8	97,4	82	2,36	5,425	79,8	79,19	0,012
240	50	50,8	98,6	82	2,38	5,325	80,033	79,45	0,080
255	50	50,8	99,7	83	2,38	5,225	80,067	79,51	0,018

Hard-to-boil sample test 1

Table B.3: Table of results for HTB sample 1 for vacuum pan boiling

Test date	24/02/2020		Sample	Hard-to-boil	
Total Sample mass	32,26kg	**Mass used**	26,52	**Undiluted Brix**	75,9%
Required Brix	70%	**Mass calc**	28,755kg	**H2O required**	2.235kg
Hydrostatic head in the pipe (on the glass)			48cm		
Volume within vacuum pan			Approximately 13,461 litres		

Time [min]	**Pvac [kPa]**	**Pvac,abs [kPa]**	**Tprobe [°C]**	**Tsump [°C]**	**Mcond [kg]**	**Msteam [kg]**	**Bx [%]**	**NIRS bx [%]**	**Mcond,theo [kg]**
0	65	50,8	11,2	9	0	0	69,967	70,5	0
15	50	50,8	65	25	0	5,65	70,033	71,57	0,396
30	50	50,8	64,5	30	0,1	5,85	70,633	72,995	0,518
45	50	50,8	72,8	48	0,38	5,825	71,967	73,39	0,143
60	50	50,8	74,6	65	0,58	5,485	73,233	74,38	0,353
75	50	50,8	94,6	69	0,8	5,585	73,733	74,5	0,043
90	50	50,8	97,2	60	0,92	5,51	73,767	74,735	0,083
105	50	50,8	97,7	60	0,96	5,7	73,900	74,75	0,005
120	50	50,8	97,5	60	1	6,5	74,200	75,13	0,134

135	50	50,8	97,2	60	1,04	5,565	74,400	76,29	0,403
150	50	50,8	95,5	63	1,16	6,435	75,100	75,86	-0,150
165	50	50,8	97,3	65	1,46	5,85	75,567	77,315	0,499
180	50	50,8	97,9	75	1,68	6,65	76,467	78,25	0,317
195	50	50,8	96,7	75	1,97	5,67	76,533	78,04	-0,071
210	50	50,8	97,7	76	2,02	6,025	77,333	78,61	0,192
225	50	50,8	98,6	79	2,04	5,56	78,400	79,03	0,141
240	50	50,8	99,4	80	2,04	5,675	78,600	79,04	0,003

Hard-to-boil sample test 2

Table B.4: Table of results for HTB sample 2 for vacuum pan boiling

Test date	27/02/2020		Sample	Hard-to-boil	
Total Sample mass	31,56 kg	**Mass used**	19,82 kg	**Undiluted Brix**	75,9%
Required Brix	70%	**Mass calc**	21,491kg	**H2O required**	1,671kg
Hydrostatic head in the pipe (on the glass)			46cm		
Volume within vacuum pan			Approximately 13,195 litres		

Time [min]	**Pvac [kPa]**	**Pvac,abs [kPa]**	**Tprobe [^{0}C]**	**Tsump [^{0}C]**	**Mcond [kg]**	**Msteam [kg]**	**Bx [%]**	**NIRS bx [%]**	**Mcond,theo [kg]**
0	50	50,8	12,7	10	0	0	70,033	69,52	0
15	50	50,8	72,8	20	0,04	4,83	70,133	69,66	0,040
30	50	50,8	93,7	46	0,14	6,225	72,267	71,69	0,561
45	50	50,8	90,8	57	0,46	6,355	71,967	72,23	0,148
60	50	50,8	93,5	75	0,72	6,445	73,233	72,9	0,182
75	50	50,8	94,2	78	1,06	5,865	73,600	73,19	0,079
90	50	50,8	95,3	79	1,2	5,85	74,533	73,49	0,081
105	50	50,8	95,7	81	1,48	5,88	75,100	75,625	0,560
120	50	50,8	97,6	79	1,64	5,85	75,367	76,005	0,099
135	50	50,8	97,2	75	1,74	5,75	75,767	76,99	0,254
150	50	50,8	96,5	75	1,76	6,805	77,300	77,26	0,069
165	50	50,8	97,7	75	1,94	5,93	78,300	77,31	0,013
180	50	50,8	98,6	75	1,96	6,85	78,467	78,31	0,253
195	50	50,8	96,6	75	2,02	5,505	79,133	78,345	0,009

210	50	50,8	96,7	77	2,1	4,65	79,633	79,04	0,174
225	50	50,8	97,2	79	2,16	5	80,2	81,170	0,520
240	50	50,8	99,8	80	2,16	5,68	80,23333	81,225	0,013

Section B.2

NIRS

Table B.1: Table of NIRS results for good boiling samples

Sample type	Brix [%]	Pol [%]	Sucrose [%]	Glucose [%]	Fructose [%]	Ash [%]	Dry Solids [%]	Colour [UI]
Good1	70,1	24,37	27,88	4,33	8,21	10,35	69,18	175916
Good1	70,1	24,37	27,88	4,33	8,21	10,35	69,18	175916
Good1	70,5	24,58	28,05	4,35	8,22	10,28	69,55	176622
Good1	71,19	25	28,61	4,4	8,25	10,01	69,85	178200
Good1	72,61	25,36	29,15	4,48	8,05	10,25	70,89	178811
Good1	73,415	24,68	29,28	4,6	8,17	10,72	72,03	181013
Good1	74,94	24,93	29,58	4,79	7,97	11,03	72,37	180759
Good1	75,443	25,21	30,14	5,15	8,18	11,31	73,78	182467
Good1	75,78	26,04	29,97	4,79	7,92	11,35	74,07	184602
Good1	76,55	25,21	30,14	5,15	8,18	11,31	73,78	182467
Good1	77,025	25,72	30,61	4,99	8,01	11,2	74,93	187165
Good1	77,85	25,94	30,585	4,885	7,9	11,375	75,1	188652
Good1	78,07	25,38	30,53	5,08	8,04	11,12	75,13	189947
Good1	78,47	25,91	30,73	5,06	7,95	11,18	75,39	193222
Good1	79,15	25,377	30,67	4,9667	7,8433	11,657	75,873	192281
Good1	79,19	25,39	30,96	4,99	7,87	10,78	75,74	177823
Good1	79,45	25,89	30,89	5,03	7,94	11,95	76,4	193642
Good1	79,51	26	30,75	5,1	8,01	12,08	76,78	199888

Sample type	Brix [%]	Pol [%]	Sucrose [%]	Glucose [%]	Fructose [%]	Ash [%]	Dry Solids [%]	Colour [UI]
Good 2	70,1	24,37	27,88	4,33	8,21	10,35	69,18	175916
Good 2	71,5	25	28,61	4,4	8,25	10,01	69,85	178200
Good 2	73,16	24,7	29,01	4,82	8,02	9	71,55	152979
Good 2	73,34	24,99	29,08	4,73	7,78	8,7	71,04	138628
Good 2	--	--	--	--	--	--	--	--
Good 2	74,13	25,17	29,63	4,62	7,96	8,99	72,31	155187
Good 2	74,26	24,93	29,49	4,63	7,92	9,23	71,94	153945
Good 2	75,17	25,63	29,83	4,8	7,85	9,53	73,14	157713
Good 2	75,37	25,83	29,87	4,46	7,68	9,16	72,94	158345
Good 2	75,79	24,99	29,81	4,67	7,77	9,56	73,02	162269
Good 2	76,12	25,04	30,12	4,59	7,66	9,67	73,13	165653
Good 2	76,84	25,57	30,3	4,86	7,8	9,38	73,85	165568
Good 2	76,74	25,2	30,18	4,83	7,69	9,76	74,43	168722
Good 2	77,8	25,35	30,51	5,01	7,79	9,89	74,83	170389
Good 2	78,92	25,36	30,85	5	7,81	10,04	75,23	174652
Good 2	79,53	25,66	31,01	5,2	7,97	10,86	76,58	196535
Good 2	79,45	25,89	30,89	5,03	7,94	11,95	76,4	193642
Good 2	80,1	26,41	31,58	5,36	8,09	12,2	77,03	197632

Table C.2: Table of NIRS results for HTB samples

Sample type	Brix [%]	Pol [%]	Sucrose [%]	Glucose [%]	Fructose [%]	Ash [%]	Dry Solids [%]	Colour [UI]
HTB 1	70,5	36,21	34,6	3,82	6,78	9,89	74,23	166895
HTB 1	71,57	36,54	35,28	3,78	6,74	10,05	74,33	167012
HTB 1	72,995	36,78	36,11	3,75	6,59	10,14	74	167398
HTB 1	73,39	37,11	37,52	3,71	6,56	10,23	74,7	167841
HTB 1	74,38	37,11	37,54	3,69	6,5	10,26	75,01	168321
HTB 1	74,5	37,26	37,89	3,68	6,48	10,35	75,39	168652
HTB 1	74,735	37,49	38	3,65	6,43	10,48	75,87	169025
HTB 1	74,75	37,5	38,17	3,64	6,36	10,59	76,54	169100
HTB 1	75,13	37,61	38,54	3,64	6,27	10,68	76,76	169452
HTB 1	76,29	37,77	38,78	3,59	6,25	10,73	76,91	169531
HTB 1	75,86	37,77	38,62	3,57	6,27	10,7	77,22	171548
HTB 1	77,315	38,42	39,21	3,56	6,13	10,71	77,4	172343
HTB 1	78,25	37,98	39,22	3,6	6,11	10,62	78,43	175959
HTB 1	78,04	37,85	39,33	3,59	6,13	10,77	78,54	176845
HTB 1	78,61	37,98	39,41	3,67	6,08	10,9	79,24	178542
HTB 1	79,03	37,97	39,56	3,79	6,04	11,35	79,49	179833
HTB 1	79,04	38,1	39,58	3,79	6,02	11,36	79,54	179846
HTB 2	69,52	36,29	36,87	3,27	6,8	9,87	73,64	164988
HTB 2	69,66	36,32	36,99	3,28	6,78	9,94	73,87	165123
HTB 2	71,69	36,76	37,19	3,31	6,66	9,98	73,99	165025
HTB 2	72,23	36,93	37,32	3,33	6,61	10,09	74,2	165985
HTB 2	72,9	37	37,46	3,65	6,59	10,18	74,53	166857
HTB 2	73,19	37,11	37,52	3,71	6,56	10,23	74,7	167841
HTB 2	73,49	37,13	37,73	3,48	6,41	10,54	74,66	166096
HTB 2	75,625	37,78	38,63	3,4	6,2	10,87	76,08	170293
HTB 2	76,005	37,17	38,64	3,65	6,36	10,73	76,39	167683
HTB 2	76,99	38,23	39,78	3,71	6,2	10,96	77,48	165508
HTB 2	77,26	37,58	39,23	3,56	6,07	10,92	77,31	173890
HTB 2	77,31	38,42	39,21	3,56	6,13	10,71	77,4	172343
HTB 2	78,31	37,99	39,24	3,7	5,94	11,2	78,31	175222
HTB 2	78,345	37,6	39,27	3,64	6,13	10,65	78,43	175959

HTB 2	79,04	38,3	39,66	3,82	6,03	11,37	79,64	179846
HTB 2	81,17	38,4	40,39	3,83	6,19	11,53	80,8	184060
HTB 2	81,225	39	40,58	3,61	6	11,49	81,16	184060

Section B.3

Rheology

Rheological Testing Results

Flow curve results

Good boiling results-flow curves

Brix	**Shear Rate**	**Shear Stress**	**Viscosity**
[%]	[1/s]	[Pa]	[mPa·s]
70 Brix	0,1	57,601	576030,000
	0,117	45,331	388826,667
	0,136	41,637	306313,333
	0,158	36,688	231493,333
	0,185	35,706	193236,667
	0,215	31,156	144613,333
	0,251	30,540	121580,000
	0,293	28,3827	96915,000
	0,341	25,992	76124,333
	0,398	26,677	67011,000
	0,464	25,899	55802,000
	0,541	25,683	47460,333
	0,631	26,0163	41235,667
	0,736	26,540	36080,000
	0,858	26,362	30736,667

	1	26,602	26603,667
	1,17	27,561	23640,000
	1,36	28,044	20631,000
	1,58	28,649	18078,000
	1,85	29,446	15936,000
	2,15	29,921	13888,667
	2,51	30,739	12238,000
	2,93	30,668	10471,667
	3,41	30,929	9058,367
	3,98	31,086	7808,733
	4,64	31,872	6866,800
	5,41	32,783	6057,967
	6,31	32,693	5181,767
	7,36	33,487	4552,333
	8,58	34,747	4051,300
	10	34,967	3496,867
	11,7	36,584	3138,00
	13,6	37,4687	2756,433
	15,8	39,302	2479,900
	18,5	40,422	2187,567
	21,5	42,690	1981,500
	25,1	44,943	1789,333

	29,3	47,184	1611,267
	34,1	49,768	1457,633
	39,8	52,569	1320,500
	46,4	55,887	1204,100
	54,1	59,386	1097,400
	63,1	63,227	1002,100
	73,6	67,592	918,850
	85,8	72,191	841,700
	100	78,362	783,630
75 Brix	0,1	86,395	863963,333
	0,117	70,895	608113,333
	0,136	68,345	502803,333
	0,158	61,420	387546,667
	0,185	55,672	301290,000
	0,215	52,194	242276,667
	0,251	51,783	206160,000
	0,293	48,649	166116,667
	0,341	45,489	133230,000
	0,398	44,631	112103,333
	0,464	43,652	94049,3333
	0,541	43,501	80388,6667

	0,631	42,977	68116,000
	0,736	42,024	57130,667
	0,858	42,349	49378,333
	1	42,999	43000,333
	1,17	43,493	37304,667
	1,36	43,600	32075,000
	1,58	44,0153	27772,667
	1,85	43,761	23683,667
	2,15	43,817	20339,333
	2,51	44,159	17581,000
	2,93	44,613	15234,333
	3,41	45,305	13268,667
	3,98	46,189	11602,333
	4,64	46,979	10121,533
	5,41	48,199	8906,667
	6,31	49,627	7865,667
	7,36	51,233	6964,733
	8,58	53,187	6201,433
	10	55,743	5574,567
	11,7	58,382	5007,533
	13,6	61,656	4535,933
	15,8	65,494	4132,500

	18,5	70,180	3798,0667
	21,5	75,394	3499,600
	25,1	81,529	3245,833
	29,3	88,664	3027,567
	34,1	96,856	2836,700
	39,8	106,740	2681,233
	46,4	118,463	2552,267
	54,1	132,360	2445,900
	63,1	148,647	2355,967
	73,6	166,457	2262,767
	85,8	185,897	2167,433
	100	207,750	2077,533
80 Brix	0,1	102,533	1025290,000
	0,117	78,306	671680,000
	0,136	76,4145	562183,333
	0,158	75,617	477130,000
	0,185	71,221	385440,000
	0,215	65,169	302490,000
	0,251	61,0767	243166,667
	0,293	60,925	208040,000
	0,341	60,111	176043,333

	0,398	56,249	141296,667
	0,464	54,180	116730,000
	0,541	55,494	102548,667
	0,631	52,663	83469,000
	0,736	51,863	70503,333
	0,858	52,225	60891,667

	1	51,922	51924,33
	1,17	51,525	44196,000
	1,36	52,150	38364,667
	1,58	52,094	32871,333
	1,85	53,220	28803,000
	2,15	54,561	25326,000
	2,51	55,421	22064,333
	2,93	57,268	19555,333
	3,41	59,169	17329,333
	3,98	60,993	15321,000
	4,64	64,248	13843,000
	5,41	67,163	12411,6667
	6,31	70,429	11163,000
	7,36	74,41	10115,600
	8,58	79,687	9291,233
	10	85,273	8527,533

	11,7	91,940	7885,900
	13,6	99,873	7347,200
	15,8	109,137	6886,333
	18,5	119,777	6482,133
	21,5	132,650	6157,267
	25,1	147,560	5874,633
	29,3	164,753	5625,833
	34,1	185,120	5421,567
	39,8	208,917	5247,900
	46,4	236,667	5098,833
	54,1	268,463	4960,967
	63,1	304,940	4833,133
	73,6	345,977	4703,167
	85,8	393,283	4585,467
	100	447,510	4475,200

HTB results-flow curves

Brix	Shear Rate	Shear Stress	Viscosity
[%]	[1/s]	[Pa]	[mPa·s]
70 Brix	0,1	70,953	709610,000
	0,117	58,864	504920,00
	0,136	55,691	409706,667
	0,158	50,224	316903,333
	0,185	46,992	254316,667
	0,215	44,611	207070,000
	0,251	42,898	170780,000
	0,293	40,968	139896,667
	0,341	40,581	118853,333
	0,398	39,160	98370,3333
	0,464	39,718	85574,000
	0,541	40,183	74254,667
	0,631	41,387	65597,000
	0,736	40,929	55641,667
	0,858	41,754	48685,000
	1	42,079	42079,333
	1,17	42,236	36227,000
	1,36	42,438	31220,667
	1,58	42,430	26772,667

	1,85	42,946	23242,333
	2,15	43,768	20316,33333
	2,51	44,7323	17809,66667
	2,93	45,490	15533,66667
	3,41	46,394	13587,66667
	3,98	46,942	11791,66667
	4,64	48,084	10360,000
	5,41	49,848	9211,567
	6,31	51,339	8137,000
	7,36	52,833	7182,100
	8,58	55,075	6421,567
	10	57,553	5755,433
	11,7	60,120	5156,667
	13,6	63,543	4674,633
	15,8	67,07	4232,033
	18,5	71,397	3863,933
	21,5	76,264	3540,033
	25,1	81,620	3249,467
	29,3	87,150	2975,867
	34,1	92,828	2718,633
	39,8	98,775	2481,133
	46,4	104,913	2260,300

	54,1	111,717	2064,400
	63,1	119,700	1897,167
	73,6	128,690	1749,333
	85,8	139,470	1626,100
	100	151,470	1514,733
75Brix	0,1	97,702	977036,667
	0,117	77,372	663680,00
	0,136	78,874	580243,333
	0,158	73,122	461386,667
	0,185	64,421	348636,667
	0,215	62,197	288703,333
	0,251	60,476	240766,667
	0,293	57,804	197380,00
	0,341	58,974	172720,00
	0,398	56,81	142703,333
	0,464	56,834	122456,667
	0,541	55,903	103305,333
	0,631	55,266	87592,667
	0,736	55,141	74960,000
	0,858	55,929	65211,000
	1	56,287	56289,667

	1,17	57,079	48958,333
	1,36	57,757	42490,667
	1,58	58,665	37016,333
	1,85	60,361	32666,67
	2,15	60,908	28271,333
	2,51	61,99167	24679,667
	2,93	63,683	21745,667
	3,41	65,742	19254,333
	3,98	68,136	17115,667
	4,64	70,867	15268,333
	5,41	73,594	13599,333
	6,31	77,178	12232,667
	7,36	81,501	11079,000
	8,58	85,922	10018,133
	10	91,373	9137,8667
	11,7	97,598	8371,3
	13,6	104,643	7698,067
	15,8	112,907	7124,067
	18,5	121,930	6598,800
	21,5	132,160	6134,667
	25,1	143,490	5712,567
	29,3	156,227	5334,633

	34,1	169,640	4968,200
	39,8	185,160	4651,167
	46,4	202,510	4363,033
	54,1	222,033	4103,033
	63,1	244,34	3872,633
	73,6	269,743	3666,833
	85,8	298,550	3480,933
	100	330,797	3308,067
80 Brix	0,1	213,560	2135400,000
	0,117	148,163	1270866,667
	0,136	139,873	1029043,333
	0,158	144,633	912596,667
	0,185	140,307	759290,000
	0,215	137,043	636100,000
	0,251	134,233	534420,000
	0,293	136,127	464816,667
	0,341	137,463	402610,000
	0,398	134,253	337256,667
	0,464	135,890	292776,667
	0,541	134,780	249060,000
	0,631	137,187	217430,000

	0,736	142,933	194303,333
	0,858	147,213	171643,333
	1	152,227	152236,667
	1,17	158,890	136283,333
	1,36	164,843	121270,000
	1,58	173,137	109243,333
	1,85	183,950	99551,667
	2,15	193,977	90040,000
	2,51	206,257	82115,000
	2,93	219,530	74962,333
	3,41	235,687	69026,333
	3,98	252,463	63418,667
	4,64	273,797	58990
	5,41	297,853	55042
	6,31	322,613	51131
	7,36	353,277	48025,667
	8,58	388,983	45354,000
	10	426,637	42665,333
	11,7	470,387	40345,667
	13,6	519,450	38215,333
	15,8	575,223	36295,000
	18,5	638,043	34529,667

	21,5	710,710	32988,333
	25,1	791,457	31509,667
	29,3	882,680	30141,000
	34,1	987,520	28921,333
	39,8	1104,530	27746,333
	46,4	1235,630	26623,000
	54,1	1385,000	25593,333
	63,1	1552,633	24609,333
	73,6	1739,933	23652,333
	85,8	1950,067	22736,667
	100	2182,733	21829,000

Amplitude sweeps

Good boiling-Amplitude sweeps

Brix	**Shear Strain**	**Shear Stress**	**Storage Modulus**	**Loss Modulus**	**Loss Factor**
[%]	[1]	[Pa]	[Pa]	[Pa]	[1]
70 Brix	0,000	0,535	5109,200	1626,733	0,321
	0,000	0,869	5669,533	1729,033	0,306
	0,000	1,389	6186,933	1849,200	0,300
	0,000	2,198	6684,467	1942,200	0,291
	0,000	3,448	7154,633	2035,933	0,286
	0,001	5,366	7596,667	2119,633	0,280
	0,001	8,302	8015,800	2205,100	0,276
	0,001	12,798	8426,567	2288,300	0,272
	0,002	19,643	8818,033	2367,700	0,269
	0,003	30,013	9184,567	2444,400	0,267
	0,005	45,723	9535,100	2527,500	0,266
	0,007	69,330	9847,267	2622,067	0,267
	0,010	102,205	9881,433	2665,233	0,270
	0,015	139,177	9166,833	2475,267	0,270
	0,022	175,657	7880,067	2135,500	0,271
	0,032	200,707	6135,433	1658,067	0,270
	0,046	131,623	2746,367	720,220	0,264

	0,068	124,153	1761,333	476,683	0,270
	0,100	79,419	758,720	238,830	0,315
	0,147	67,106	423,337	174,607	0,413
	0,215	52,071	205,960	127,083	0,617
	0,316	35,088	75,249	81,778	1,087
	0,463	24,413	22,579	47,587	2,112
	0,680	23,269	6,253	33,633	5,388
	0,998	26,570	1,021	26,594	26,955
75 Brix	0,000	0,736	7027,467	2230,867	0,318
	0,000	1,168	7610,200	2357,033	0,310
	0,000	1,828	8134,333	2456,600	0,302
	0,000	2,846	8645,133	2552,767	0,296
	0,000	4,409	9136,367	2651,367	0,290
	0,001	6,805	9619,367	2745,900	0,286
	0,001	10,450	10073,900	2834,067	0,281
	0,001	16,004	10519,667	2926,533	0,278
	0,068	124,153	1761,333	476,683	0,270
	0,100	79,419	758,720	238,830	0,315
	0,147	67,106	423,337	174,607	0,413
	0,215	52,071	205,960	127,083	0,617
	0,316	35,088	75,249	81,778	1,087

	0,463	24,413	22,579	47,587	2,112

	0,680	23,269	6,253	33,633	5,388
	0,032	231,003	7045,367	1967,467	0,279
	0,046	156,737	3250,333	929,513	0,288
	0,068	141,593	1995,000	594,257	0,297
	0,100	102,294	959,947	358,627	0,373
	0,147	84,377	517,353	252,740	0,488
	0,215	75,235	298,087	182,880	0,613
	0,316	57,773	138,280	119,850	0,867
	0,463	41,056	45,246	76,138	1,689
	0,680	37,081	12,995	52,937	4,096
	0,998	42,674	2,415	42,675	17,731
80 Brix	0,000	0,719	6719,400	2576,800	0,387
	0,000	1,162	7461,900	2682,533	0,361
	0,000	1,851	8126,100	2829,967	0,350
	0,000	2,909	8727,900	2944,500	0,338
	0,000	4,521	9265,533	3052,433	0,330
	0,001	6,995	9784,700	3158,767	0,323
	0,032	231,003	7045,367	1967,467	0,279
	0,046	156,737	3250,333	929,513	0,288
	0,068	141,593	1995,000	594,257	0,297

	0,100	102,294	959,947	358,627	0,373
	0,147	84,377	517,353	252,740	0,488
	0,215	75,235	298,087	182,880	0,613
	0,010	114,451	10937,467	3426,500	0,314
	0,015	146,447	9556,267	2916,733	0,306
	0,022	184,627	8201,267	2526,133	0,308
	0,032	227,093	6848,933	2192,667	0,320
	0,046	233,527	4788,967	1563,900	0,328
	0,068	166,097	2302,333	813,447	0,353
	0,100	111,937	1010,957	485,147	0,479
	0,147	100,862	581,650	368,323	0,634
	0,215	103,310	375,350	299,677	0,798
	0,316	101,515	230,193	224,433	0,976
	0,463	93,201	121,573	160,063	1,322
	0,680	79,453	39,790	109,777	2,775
	0,998	88,511	7,019	88,378	12,609

HTB Results- Amplitude sweeps

Brix	**Shear Strain**	**Shear Stress**	**Storage Modulus**	**Loss Modulus**	**Loss Factor**
[%]	[1]	[Pa]	[Pa]	[Pa]	[1]
70 Brix%	0,000	0,632	6032,133	1907,600	0,316
	0,000	1,013	6614,333	2005,433	0,303

	0,000	1,606	7162,567	2110,467	0,294
	0,000	2,520	7668,833	2213,100	0,289
	0,000	3,928	8154,300	2307,633	0,283
	0,001	6,086	8618,533	2397,100	0,278
	0,001	9,381	9061,633	2480,100	0,274
	0,001	14,417	9495,667	2565,967	0,270
	0,002	22,073	9912,667	2646,833	0,267
	0,003	33,659	10303,770	2728,167	0,265
	0,005	51,144	10669,000	2815,000	0,264
	0,007	77,312	10984,000	2913,733	0,265
	0,010	113,497	10974,670	2956,833	0,270
	0,015	152,800	10064,870	2715,333	0,270
	0,022	190,933	8569,700	2305,533	0,269
	0,032	171,690	5247,767	1419,233	0,274
	0,046	148,323	3084,033	853,910	0,277
	0,068	144,770	2050,600	569,510	0,277
	0,100	91,843	870,923	296,427	0,339
	0,147	75,724	472,557	209,033	0,442
	0,215	62,679	250,843	148,260	0,591
	0,316	44,161	98,888	98,920	1,000
	0,463	32,013	31,959	61,235	1,919
	0,680	28,891	8,669	41,581	4,806

75 Brix	0,000	0,620	5907,833	1933,067	0,327
	0,000	1,030	6698,533	2129,700	0,318
	0,000	1,651	7338,367	2252,100	0,307
	0,000	2,584	7838,433	2352,600	0,300
	0,000	4,019	8319,433	2446,933	0,294
	0,001	6,211	8768,267	2540,600	0,290
	0,001	9,581	9226,167	2637,033	0,286
	0,001	14,672	9633,567	2720,100	0,283
	0,002	22,420	10036,930	2804,933	0,280
	0,003	34,155	10423,000	2889,600	0,277
	0,005	51,823	10777,430	2977,833	0,276
	0,007	77,561	10985,000	3050,633	0,278
	0,010	111,993	10798,330	3030,033	0,281
	0,015	149,737	9839,500	2746,567	0,279
	0,022	190,517	8534,300	2362,100	0,277
	0,215	62,679	250,843	148,260	0,591
	0,316	44,161	98,888	98,920	1,000
	0,463	32,013	31,959	61,235	1,919
	0,680	28,891	8,669	41,581	4,806
80 Brix	0,147	88,055	537,223	268,663	0,500

	0,215	79,422	310,940	198,570	0,641
	0,316	64,455	155,487	131,807	0,858
	0,463	47,206	55,730	84,976	1,552
	0,680	40,978	16,203	57,967	3,641
	0,998	46,339	3,127	46,303	15,492
	0,000	0,685	6485,833	2235,933	0,345
	0,000	1,101	7117,333	2394,000	0,337
	0,000	1,742	7699,000	2509,233	0,326
	0,000	2,735	8248,433	2637,633	0,320
	0,000	4,263	8778,033	2744,133	0,313
	0,001	6,597	9270,600	2845,833	0,307
	0,001	10,173	9750,100	2952,433	0,303
	0,001	15,620	10210,670	3051,433	0,299
	0,002	23,912	10660,000	3148,667	0,296
	0,003	36,471	11084,670	3244,667	0,293
	0,005	55,428	11481,000	3346,900	0,292
	0,007	83,608	11792,670	3458,200	0,293
	0,010	118,703	11390,670	3398,933	0,298
	0,015	154,707	10126,770	2974,833	0,294
	0,022	194,070	8661,433	2518,900	0,291
	0,032	234,330	7103,967	2143,600	0,302
	0,046	239,250	4951,900	1456,100	0,294
	0,068	145,147	2030,600	655,617	0,324

	0,100	110,247	1015,253	434,530	0,429
	0,147	96,493	572,973	324,760	0,567
	0,215	92,720	352,767	247,867	0,703
	0,316	87,562	211,897	178,950	0,845
	0,463	69,008	91,167	117,743	1,292
	0,680	59,428	25,776	83,478	3,242
	0,998	67,731	4,519	67,692	15,007

The plotted values for amplitude sweep values at the different Brixes, for the good boiling and HTB samples are found in figure C.1, C.2, C.3.

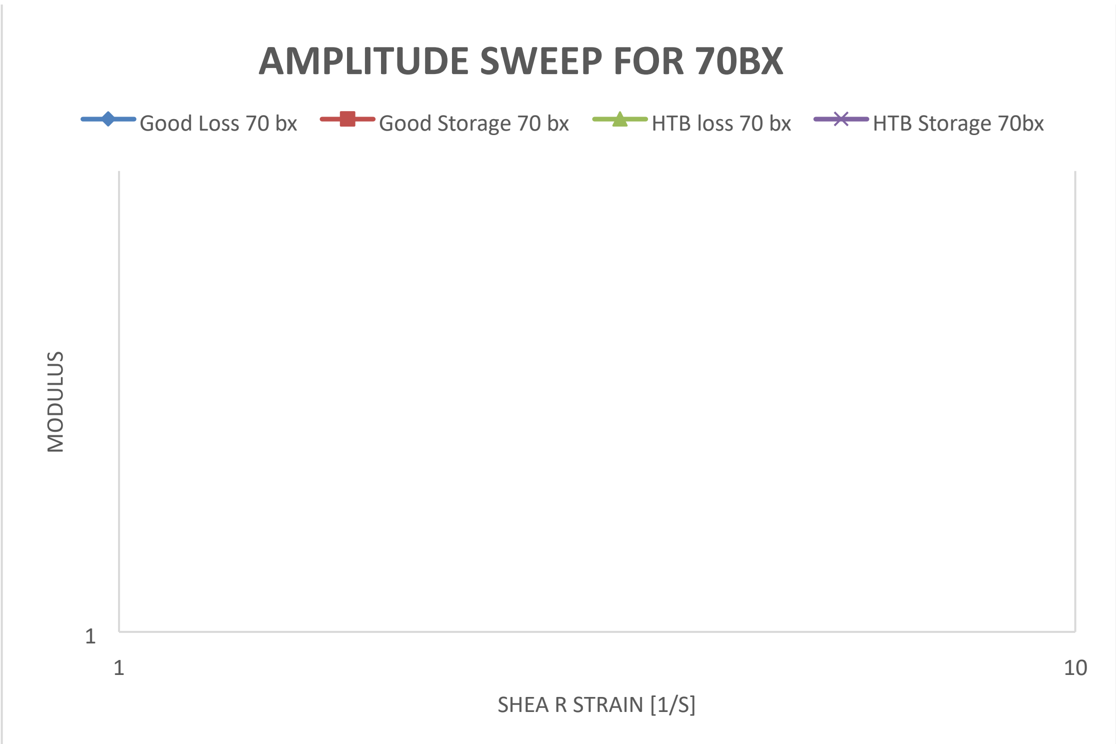

Figure C.1: Amplitude sweep at 70bx for good and HTB samples

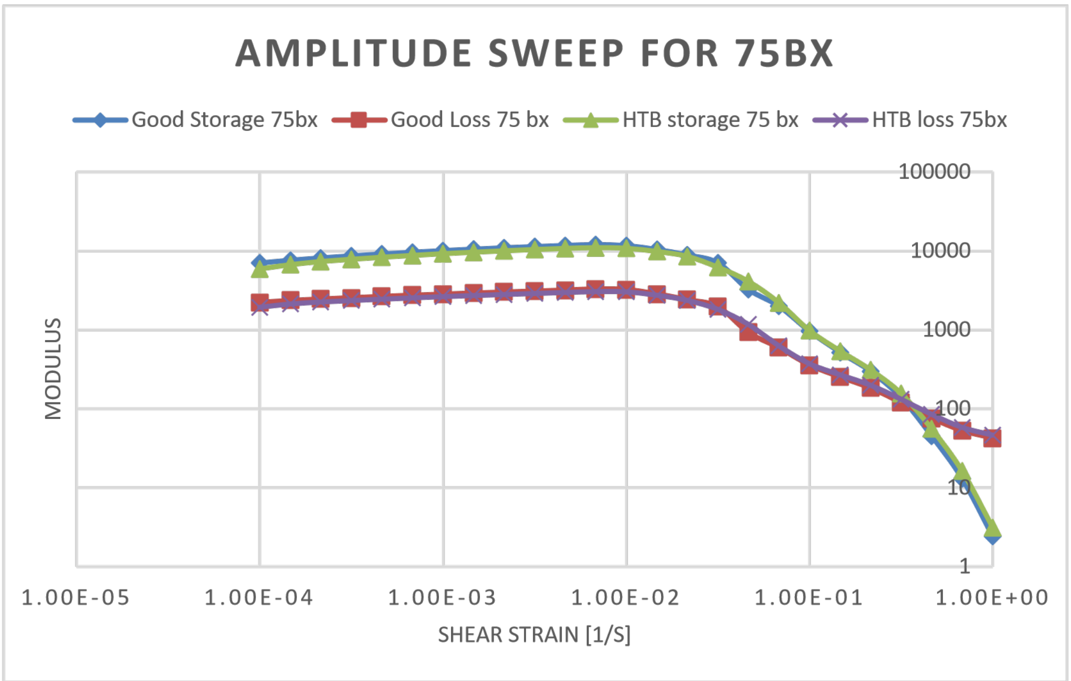

Figure C.2: Amplitude sweep at 75bx for good and HTB samples

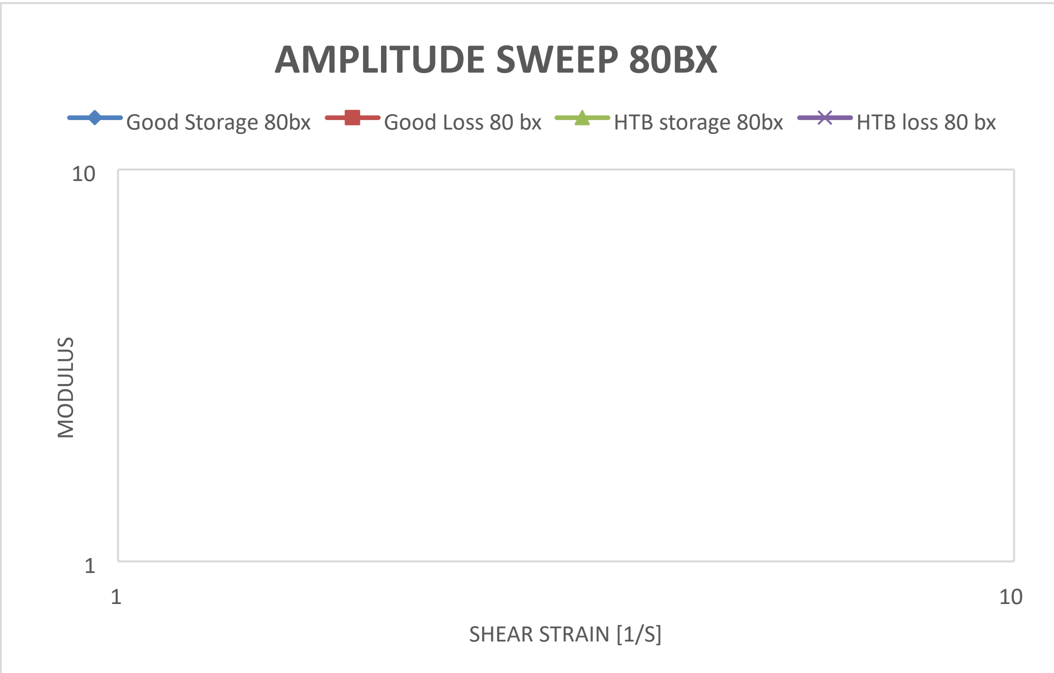

Figure C.3: Amplitude sweep at 80bx for good and HTB samples

Frequency sweeps

Good boiling- Frequency sweep

Brix	Angular Frequency	Storage Modulus	Loss Modulus	Loss Factor	Shear Strain	Shear Stress
[%]	[rad/s]	[Pa]	[Pa]	[1]	[%]	[Pa]
70%	100,000	7537,500	1917,900	0,254	0,010	0,777
	63,100	7048,600	1819,200	0,258	0,011	0,781
	39,800	6700,900	1776,200	0,265	0,012	0,802
	25,100	6481,900	1753,000	0,270	0,013	0,836
	15,800	6275,700	1714,900	0,273	0,013	0,873
	10,000	6136,400	1718,000	0,280	0,014	0,919
	6,310	6049,200	1734,900	0,287	0,016	0,976
	3,980	6075,900	1767,600	0,291	0,017	1,053
	2,510	6214,900	1842,500	0,296	0,018	1,161
	1,580	6520,200	1948,800	0,299	0,019	1,313
	1,000	6810,600	2053,500	0,302	0,021	1,486
	0,631	7047,300	2174,900	0,309	0,022	1,650
	0,398	7375,200	2328,400	0,316	0,024	1,862
	0,251	7618,900	2506,000	0,329	0,026	2,079
	0,158	7812,600	2690,200	0,344	0,028	2,306
	0,100	8047,100	2956,900	0,367	0,030	2,578
75%	100,000	9537,200	2955,600	0,310	0,010	0,998
	63,100	9256,600	2733,600	0,295	0,011	1,037

	39,800	8956,600	2622,100	0,293	0,012	1,080
	25,100	8601,900	2509,100	0,292	0,013	1,116
	15,800	8310,700	2459,100	0,296	0,013	1,163
	10,000	8074,000	2419,900	0,300	0,014	1,216
	6,310	7931,200	2436,200	0,307	0,016	1,287
	3,980	7850,600	2415,000	0,308	0,017	1,367
	2,510	7974,600	2500,000	0,313	0,018	1,497
	1,580	8224,400	2652,300	0,322	0,019	1,667
	1,000	8575,900	2701,900	0,315	0,021	1,878
	0,631	8854,600	2904,200	0,328	0,022	2,085
	0,398	9389,000	3124,100	0,333	0,024	2,383
	0,251	9693,100	3288,300	0,339	0,026	2,653
	0,158	10165,000	3485,400	0,343	0,028	2,999
	0,100	10626,000	3816,500	0,359	0,030	3,396
80%	100,000	11794,000	3966,700	0,336	0,010	1,244
	63,100	11367,000	3616,200	0,318	0,011	1,282
	39,800	10903,000	3392,500	0,311	0,012	1,322
	25,100	10422,000	3226,000	0,310	0,013	1,360
	15,800	9961,900	3133,600	0,315	0,013	1,402
	10,000	9603,000	3035,900	0,316	0,014	1,453
	6,310	9323,000	2987,300	0,320	0,016	1,518

	3,980	9173,600	3014,400	0,329	0,017	1,608
	2,510	9183,500	3067,300	0,334	0,018	1,735
	1,580	9413,900	3179,500	0,338	0,019	1,917
	1,000	9674,400	3318,500	0,343	0,021	2,137
	0,631	9959,000	3478,500	0,349	0,022	2,361
	0,398	10448,000	3725,800	0,357	0,024	2,671
	0,251	10809,000	3947,600	0,365	0,026	2,983
	0,158	11242,000	4121,900	0,367	0,028	3,341
	0,100	11724,000	4493,100	0,383	0,030	3,774

HTB values – Frequency sweeps

Brix	Angular Frequency	Storage Modulus	Loss Modulus	Loss Factor	Shear Strain	Shear Stress
[%]	[rad/s]	[Pa]	[Pa]	[1]	[%]	[Pa]
70	100,000	9306,100	2716,000	0,292	0,010	0,969
	63,100	9172,400	2572,500	0,280	0,011	1,024
	39,800	8928,400	2487,500	0,279	0,012	1,072
	25,100	8651,700	2435,300	0,281	0,013	1,120
	15,800	8371,400	2419,200	0,289	0,013	1,170
	10,000	8162,500	2391,900	0,293	0,014	1,227
	6,310	8007,600	2429,000	0,303	0,016	1,298
	3,980	7964,600	2419,500	0,304	0,017	1,386
	2,510	8086,400	2524,400	0,312	0,018	1,517
	1,580	8385,700	2654,400	0,317	0,019	1,697
	1,000	8675,500	2798,000	0,323	0,021	1,904
	0,631	9000,300	2946,500	0,327	0,022	2,120
	0,398	9400,100	3168,900	0,337	0,024	2,389
	0,251	9697,700	3390,000	0,350	0,026	2,663
	0,158	9951,600	3643,200	0,366	0,028	2,958
	0,100	10157,000	3925,800	0,387	0,030	3,272
75	63,100	10784,000	2928,500	0,272	0,011	1,201

	39,800	10386,000	2820,500	0,272	0,012	1,246
	25,100	10009,000	2684,300	0,268	0,013	1,291
	15,800	9690,600	2647,300	0,273	0,013	1,348
	10,000	9340,500	2636,100	0,282	0,014	1,400
	6,310	9128,300	2617,900	0,287	0,016	1,473
	3,980	9016,400	2630,200	0,292	0,017	1,564
	2,510	9062,000	2713,900	0,299	0,018	1,695
	1,580	9286,100	2842,800	0,306	0,019	1,874
	1,000	9578,200	2976,400	0,311	0,021	2,095
	0,631	9904,900	3117,500	0,315	0,022	2,323
	0,398	10263,000	3331,900	0,325	0,024	2,598
	0,251	10618,000	3508,400	0,330	0,026	2,898
	0,158	10924,000	3713,000	0,340	0,028	3,219
	0,100	11384,000	3986,100	0,350	0,030	3,626
80	100,000	10980,000	3540,600	0,322	0,010	1,153
	63,100	10557,000	3273,900	0,310	0,011	1,188
	39,800	10128,000	3112,200	0,307	0,012	1,226
	25,100	9678,300	2965,800	0,306	0,013	1,262
	15,800	9292,700	2888,000	0,311	0,013	1,306
	10,000	8918,400	2823,400	0,317	0,014	1,350
	6,310	8666,900	2803,300	0,323	0,016	1,413

	3,980	8493,200	2785,800	0,328	0,017	1,488
	2,510	8532,000	2844,600	0,333	0,018	1,611
	1,580	8739,300	2970,100	0,340	0,019	1,781
	1,000	8991,100	3107,800	0,346	0,021	1,988
	0,631	9203,000	3195,300	0,347	0,022	2,180
	0,398	9600,900	3369,800	0,351	0,024	2,450
	0,251	9946,700	3606,300	0,363	0,026	2,743
	0,158	10383,000	3842,800	0,370	0,028	3,091
	0,100	10906,000	4141,500	0,380	0,030	3,506

Appendix C

Standard Operating Procedures of Systems

Section C.1

Vacuum Pan Standard Operating Procedure

Sample Preparation

Samples used in this rig should be **prepared at least 24 hours prior** to test run. This rig is for molasses and massecuite boiling and is capable of vacuum boiling using vacuum provided by SMRI vacuum pump and steam provided by SMRI constant pressure boiler.

Valves Check

- When starting the equipment, ensure that the following valves/ports are **closed** ○ Exit port at the bottom of the vacuum pan ○ Inlet pipe valve ○ Vacuum breaker valve on the condenser storage tank ○ Outlet valve on condenser storage tank ○ Steam to vacuum pan inlet valve
- Vacuum to pan inlet valve should be **open**
- Check that **no other equipment has any lines open** to the vacuum pump or to the boiler

Condenser checks

- Condensate storage tank must be empty before start of experiment ○ Place bucket at condensate outlet pipe exit ○ Open outlet valve on storage tank and allow any remnant condensate to escape ○ Zero condensate scales on condenser and steam sides before starting the test

Start up

- Turn on the boiler
- Turn on cooling tower
- Turn on vacuum pump
    - **Check:** Ensure that the vacuum pressure is increasing on the pan's pressure gauge (located at the top of the primary condenser)- vacuum pressure should reach 80-90kPa and then should remain stable-vacuum pressure can be adjusted during test run

- **Sample inlet-** using the inlet hose – vacuum in the sample to be boiled ○ Amount of

  liquid required-: approximately 30-35 litres of the sample

  - Sample should reach about 5 cm on the secondary viewing pane on the top of the pan (approximately the second or third bolt height on the window) ○ Samples with higher viscosities should be preheated or diluted for ease of use

- Turn on the stirrer system ○ Check that the stirrer is plugged in to a power source ○

  Stirrer should start at low speed and can be increased as testing begins

- Air leakage and vacuum pump check:

  - Air leakages on the system- check sight glass panes, around the stirrer rod, entrance and exit ports using a soapy foamy mixture. Leakages will be seen in the form of bubbles in the pan or the soap bubbles will start to be sucked into any openings

  - Should the vacuum pan start to sound like it's beginning to over work, bleed the valve on the top of the condenser storage tank very slightly not to alter the pressures within the pan

- Water Inlet valves to condensers

  - Connect the hoses for the syrup-side and steam-side condensers to the taps found behind the pan by the drain

  - Open the taps and ensure flow into the condensers are adequate such that they are not getting hot and that there is no overflow of the open condenser (steam side condenser

- Heating up- Steam inlet

  - When the boiler has heated up, open the first valve on the steam side fully then open the second, control valve to required steam inlet

    - System should start to heat up- should take 10-15 minutes to get to 70-85ºC

    - For faster boiling- allow steam to circulate more by throttling the steam outlet valve on the back of the pan- only close it half way maximum to allow pressure build up

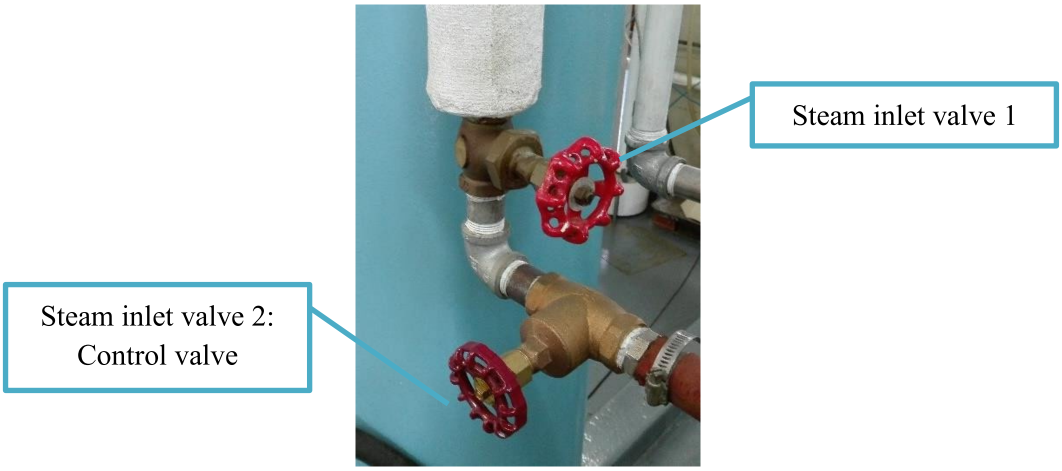

Collecting Samples

Requires several beakers and storage containers (honey jars with lids)

- Samples can be removed as the system boils using the sample port on the front of the pan, at the bottom of the viewing glass ○ Open the first valve only, keeping the second closed- sample will fill the pipe ○ Close the first valve ○ Open the second valve, keeping the first one closed- sample will drain out of the pipe
    - Collect the sample within a beaker or container-depending on the temperature of the sample, a container may not be appropriate and should then be collected in an appropriate glass beaker

Shut Down

- Close both steam to pan valves
- Turn off the vacuum pump (requires two people or one very fast one)
- Turn off the boiler
- Turn off the stirrer
- Bleed the vacuum out of the system by opening the vacuum breaker valve on the top of the condenser to reduce the pressure within the pan
- Emptying out the product-if boiling with:
    - **Water:** push the inlet hose to the back of the pan where the drain is and open it into the drain ○ **Sucrose syrup/massecuite:** empty into buckets using inlet pipe or outlet port
- Open the exit port at the bottom of the vacuum pan to remove the remnants that did not drain through the pipe
- If the system was being run with sucrose products, rinse the system out with water to ensure that remnants don't crystallise within the system ○ Rinsing out the system requires the vacuum pump to be turned on

  - If the samples were quite difficult to handle, then several rinses will need to be done and the pan may need to be boiled again to dissolve the sugar. This requires the startup steps to be done again

- When the system is clean, leave the exit ports open to allow drainage and cooling of the pan
- Empty out the condensers and condenser storage tanks into the drain either directly or using buckets

Section C.2

Standard Operating Procedure for NIRS

Near Infrared Spectroscopy (NIRS) is a means of quickly and simultaneously investigating various properties of sugar solutions. NIRS works using a refraction technique by passing light through a thin layer of sample in order to determine the properties of the mixture.

The NIRS is capable of using predetermined predictive calculations in order to test for the following properties:

- Brix
- Pol
- Sucrose
- Glucose
- Fructose
- Ash
- Dry solids
- Colour

In order to test for other components, it is possible to use the machine functions to create predictive models for determining these properties. Based off the calculations that NIRS uses to determine the liquid properties, the samples are required to be diluted. This dilution is done using calculated ratio that works best with the machine and equations. Sample preparation method:

Dilute sample in a 1:6 ratio of molasses to water

Measure 15 grams of molasses sample

Top the scale off with an additional 75grams of water

Load samples into agitator where mixing will occur

Mix sample until uniformly dissolved

Once sample was prepared, the NIRS testing can begin. NIRS testing was as follows:

Placed slide cell into the machine

Flushed the slide cell with water to ensure clean area

Sample was injected into the pipe of inlet to refraction cuvette

Opus lab was opened, sample name and other information entered before the test was initiated

Results came in the form of a table with all testable results noted

NIRS results received are used for determining the characteristic changes between samples.

Section C.3

Standard Operating Procedure Rheometer

System start up procedure:

Start-up rheometer:

Turn on water bath circulator

Turn on main switch of rheometer located on the left and back side on the chord

Ideal start up time required for rheometer is approximately 1 hour

Open AntonPaar RheoCompass

On the right-hand side of the screen, the control panel should pop up

The control panel can be expanded and reduced when clicked

Using the control panel, begin system initialisation

Once system is initialised, reset force

Attach the parallel plate attachment to the rig

Using control panel, set the zero gap

This lowers the spindle to the zero position before increasing the height to the required gap size

Gap size is set by the testing apparatus but can be altered by the user

Once the gap is set, move the sample to loading position using the arrows on the control panel

Set the temperature on the control panel to 30ºC

How samples were loaded:

Samples were mixed evenly

For the most consistent results, samples must be mixed the same amount, in the same way, among all samples

Samples were mixed for 15 seconds anticlockwise to ensure all dissolved solids that would have settled, are thoroughly dispersed through the sample

Approximately 5 grams of sample was placed on the bottom plate of the rheometer

Lower the spindle and let the sample fill the space, the rig will stop at a height slightly higher than the gap size to allow for sample trimming and accurate sample size loading

An adequate amount of sample will overflow from the area

Too little sample will not overflow and requires the system to be reloaded

Once spindle has descended, sample was trimmed to only fit beneath the spindle area before finishing the lowering method

Lower the hood of the rig to create controlled conditions

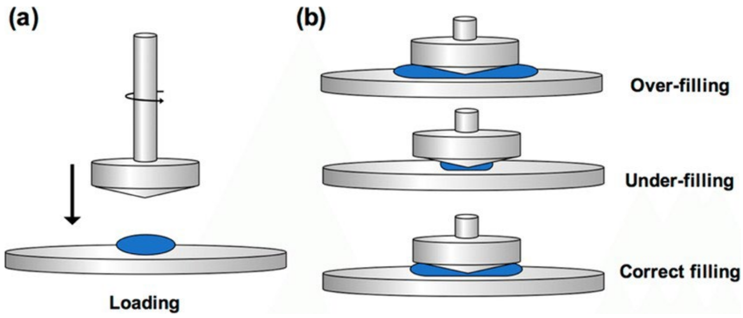

Proper sample loading

All samples were loaded, and the system initialised the same way for all tests. The tests run for the hypothesis include flow curves, amplitude sweeps and frequency sweeps.